Author:
Alghuwainem, Ghannimah Y G

Title:
Investigation of the molecular mechanisms of human mesenchymal stem cells and S. aureus interactions in osteomyelitis

Investigation of the molecular mechanisms of human mesenchymal stem cells and *S. aureus* interactions in osteomyelitis

By

Ghannimah Yousef Al-Ghuwainem

School of Cellular and Molecular Medicine

January 2023

A dissertation submitted to the University of Bristol in accordance with the requirements of the Degree of Doctor of Philosophy in the Faculty of Life Science

Word count: 32,352

Dedication

I dedicate this thesis to Dad Yousef, who is looking forward to this moment. Dad, thank you for believing in my dream and for your countless support.

I would dedicate this thesis to my lovely daughter Reem, the most beloved kid who brings the joy and passion to my life, and without your smile, I could not finish this PhD. I hope one day you will be proud of your Mum.

Covid-19 Statement

During the COVID-19 pandemic, my PhD project was interrupted due to multiple events. There was a complete lockdown, including the laboratories at the University of Bristol. The lockdown in the labs was from March 2020 to July 2020. That was followed by a new policy for lab work with very limited access and capacity to the labs and an enforced rota that made me continuously prioritise and rearrange my project design and perform the maximum work possible at the permitted time for my scholarship.

The work on human bone explant samples required the provision of samples from patients undergoing elective surgery. This type of surgery was suspended by the NHS during the pandemic leading to no provision of samples for a good period of time. The provision of samples returned later, but it remained constrained and limited. That impacted the quality of data presented in Chapter 5.

The lockdown, lack of access, and travel to see family have impacted my mental health. I am a single mother with a child in a nursery who lived in isolation from social life during the pandemic. I managed to go back home to Saudi Arabia in September 2020, which helped a little; however, due to travel restrictions, I was forced to stay a few months until allowed back into the UK with permitted immunisations.

During the pandemic, I had a challenging time with my daughter as I was the only carer for her (3-year-old now). On many occasions, I could not send my daughter to the nursery due to shortage of carers and nursery COVID-19 regulations. Moreover, I could not get additional family help due to flight restrictions during the pandemic.

Abstract

Osteomyelitis (OM) is bone inflammation that typically arises due to bacterial infection. Current treatment strategies for eradicating this condition include surgical debridement and systemic and local antibiotics. Both strategies, however, come with limitations that impact the disease outcomes. New biological approaches that can reduce the bacterial burden and help regenerate damaged bone are being sought.

The aims of this study were to identify the potential of ameliorating bone marrow mesenchymal stem cells (bmMSC) anti-inflammatory and anti-bacterial function for treating OM through modulating the Toll-like receptors (TLRs), the impact of bmMSC conditioned medium (MSC-CM) on osteogenic properties of osteoblasts and testing the therapeutic potential of MSCs in a 3D model of OM using a human *ex vivo* bone model. Stimulation of bmMSCs with TLR agonists (Pam3CK4 and PGN-SA) resulted in significant growth inhibition of *S. aureus* compared to the unstimulated control cells. Infected bmMSCs overexpressed indoleamine 2, 3-dioxygenase enzyme (IDO) after Pam3CSK4 stimulation. The inhibition correlated with *IDO* expression in response to PGN-SA but not Pam3CSk4 stimulation. The inflammatory cytokines, *IL-6* and *CCL2,* were upregulated in MSCs stimulated with Pam3CK4 and PGN-SA, respectively.

Upon administration of MSC-CM with infected osteoblasts revealed antibacterial properties of human bmMSCs on infected osteoblasts. Moreover, MSC-CM inhibited the growth of *S. aureus* using CM harvested from different cell densities of MSCs. An *ex vivo* model of OM infection was established by infecting bone explants from human femoral head with *S. aureus*.

Studies using the model revealed differential expression of bone resorption marker including cathepsin K (CTSK*),* tartrate-resistant acid phosphatase (ACP5), extracellular matrix-degrading enzymes matrix metalloproteinase 1 and 13 (MMP-1

and MMP-13), and the inflammatory cytokines *IL-6*. The expression profile suggested alignment of the *ex vivo* model with the pathological profile of OM. The addition of MSC-CM to the infection model dampened the inflammatory and resorption response. There was significant downregulation of genes responsible for osteoclastic and inflammatory activities upon culture with MSC-CM. The results may suggest that MSC-CM should be investigated further to reveal its trophic composition and derive a biological treatment for OM.

Dedication and Acknowledgements

This PhD journey was an exceptional chapter in my life, and I would like to acknowledge everyone who has played a part in completing this PhD thesis. This PhD journey wouldn't have come to an end without those people.

First and foremost, I must express profound thanks to Almighty Allah, who generously awarded me with this PhD opportunity, strength, and capability to complete this project.

I gratefully would like to thank my principal supervisor Dr Wael Kafieneh and my co-supervisor, Dr Darryl Hill, for their continuous support and advice throughout my scientific journey.

I would also like to extend my sincere thanks for the financial support provided by my sponsor, King Faisal University in Saudi Arabia and Saudi Arabian Embassy Cultural Bureau in London for their generous financial support for granting me a full scholarship.

I am deeply thankful to my colleagues. I am fortunate to be surrounded by such incredible, talented colleagues with whom I have shared lab experience for their invaluable help and continuous support during my study.

Most importantly, the enormous thanks must go to my parents (Mr Yousef and Mrs Hind), who have shared my laughs, tears, and anger over the last five years. I will always be indebted, both of you for everything you have done in my life. My father, Yousef Alghuwainem, encouraged me to complete my higher education and provided me with all I needed. My mother, Hind Alghuwainem, is the most powerful and energetic woman who gives me infinitive love and sisters and brothers.

Finally, I would like to express my gratitude to my husband, Khalid Aldossari, for his unlimited support in several ways through all the ups and downs.

Author’s Declaration

I declare that the work in this dissertation was carried out in accordance with the requirements of the University's Regulations and Code of Practice for Research Degree Programmes and that it has not been submitted for any other academic award. Except where indicated by specific references in the text, the work is the candidate's own work. Work done in collaboration with, or with the assistance of, other, is indicated as such. Any views expressed in the dissertation are those of the author.

SIGNED: **Ghannimah Alghuwainem**. DATE: **27th January 2023.**

Conference Abstracts

- Poster presentation at the 29th Annual Meeting of the European Society of Gene & Cell Therapy (ESGCT), Edinburgh, Scotland October 2022.
    - Title: The impact of TLR-2 stimulation on human mesenchymal stem cells' antimicrobial capacity
- Oral presentation at Work in Progress, CMM, University of Bristol, Bristol. November 2021.
    - Investigating the molecular mechanisms of *S. aureus* interactions with bone marrow mesenchymal stem cells (bmMSCs).

Table of contents

List of figures

List of Tables

1. Literature review

1.1. Bone biology

Bone is a supportive mineralised connective tissue characterised by its solidity, toughness, and ability to withstand compression and physical pressures (2, 3). Skeletal bones, with the assistance of cartilage and muscles, provide the body with multiple and crucial physiological functions such as structural frame, support, protection and locomotion. Bone is a reservoir of mineral substances (calcium and phosphates), growth factors, and cytokines, all of which contribute to its metabolic functions (4). Furthermore, bone contains space where hematopoietic cells (blood-forming cells) and fat (marrow cavity) are stored (5).

1.2. Bone anatomy

The long bone is divided mainly into three segments: diaphysis, metaphysis, and epiphysis. The diaphysis is a cylindrical hollow tube encompassed primarily of dense cortical bone and encompasses an inner cavity, or medullary canal, that surrounds the bone marrow-fill space (3). The diaphysis terminates with a spongy bone and a thin shell of cortical bone called the epiphysis (6). Each epiphysis end is surrounded by fibrous tissues of the articular cartilage, which aids the attachment of adjacent bones. The segment where the diaphysis joins the epiphysis is called the metaphysis (7) (Figure 1-1). Additionally, bones also have supplementary fibrous supporting connective tissues. The periosteum refers to a thin outer sheath of fibrous tissues that surrounds the superficial surface of the cortex, except the joint (8) while the endosteum denotes the delicate thinner membrane that lines the inner surface of the cortical bones, cancellous bone, and the blood vessels of the bone (Volkmann's canals). The extensive network of blood vessels is an additional supportive tissue that provides oxygen and nutrients (9)(Figure 1-1).

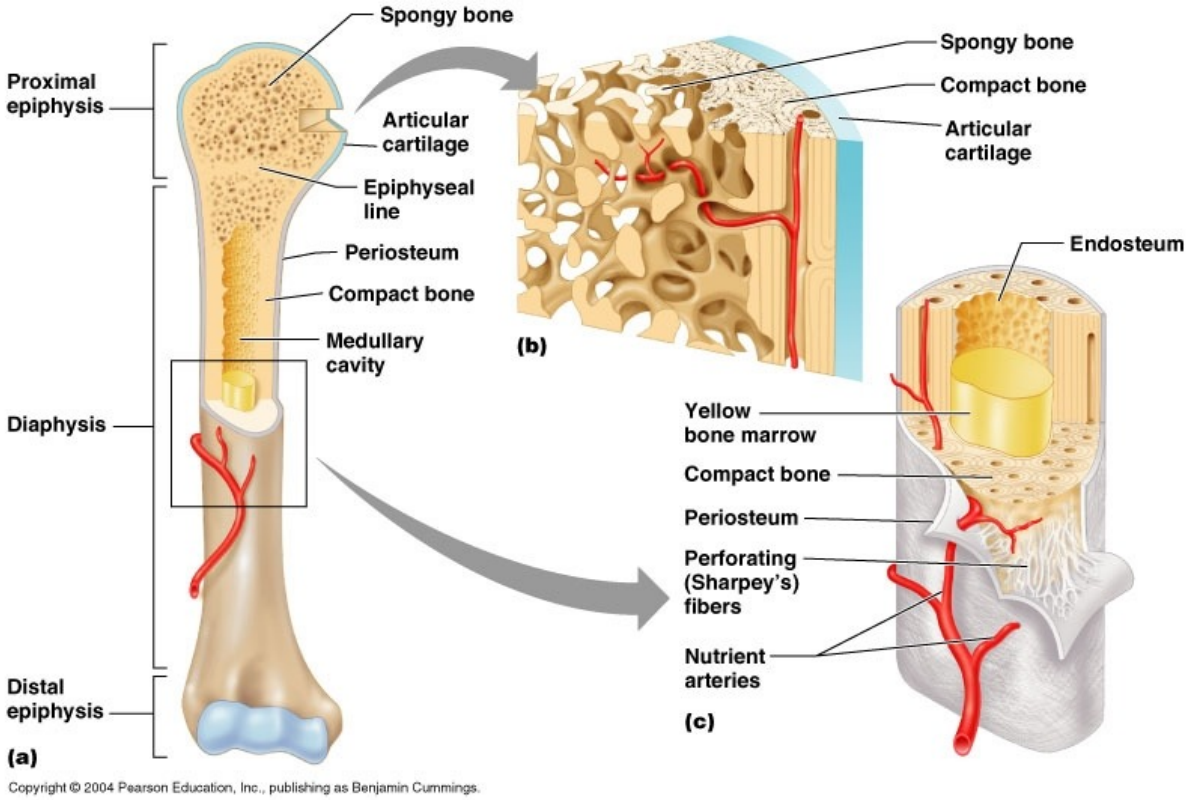

Figure 1-1 Anatomy of the long bone. This image is not original and Available from (10). [Accessed 15 January 2023].

1.3. Microscopic and macroscopic features of the bone

Bone is categorised into compact and trabecular bone (cancellous or spongy). The adult human skeleton is made of 20% trabecular bone and 80% compact bone. The compact bone, also known as cortical bone, is dense and abundant and encircles the bone marrow cavity. In contrast, cancellous bone is arranged in a honeycomb-like network of trabecular shields (11). Cancellous bone is located inside the cortex and filled with blood precursor cells and fat cells. It is metabolically active and responsible for bone remodelling and calcium exchange (11). At the microscopic level, bone is composed of different supportive cells, i.e. osteoblasts, osteocytes and osteoclasts, which are encased by an extracellular organic matrix embedded with inorganic mineral

calcium hydroxyapatite crystals (12). These apparatuses create reinforced steel- and concrete-like arrangements, which enhance the rigidity and hardness of the bone (12, 13) (Figure 1-1).

1.4. Osteoblasts

Osteoblasts are mononucleated and cuboid-like cells, located along the bone-forming surface and responsible for bone formation. Osteoblasts are originated from undifferentiated mesenchymal stem cells (osteoprogenitor cells) and represent between 4-6% of cells existing in the bone (14). Osteoblasts contribute to the deposition of bone matrix, collagen synthesis and regulate osteoclast remodelling activities (14). Osteoblasts create and induce mineralisation of the osteoid, producing the bone matrix components, including type I collagen, proteoglycans, and glycoproteins, and catalyse bone matrix calcification (15). There are three major types of osteoblasts: pre-mature osteoblast, mature osteoblasts, and osteocytes, which are trapped within the bone (16, 17) (Figure 1-2).

1.5. Osteocytes

Osteocytes are considered the terminally differentiated phase of osteogenic differentiation and account for the most abundant cells in the bone; representing approximately 90% of the total bone cell population (17). Osteocytes have a substantially longer life span, living up to 25 years, while located in the bone lacunae and matrix (14). Morphologically, osteocytes exhibit dendrite-like cytoplasmic projections, which project into the lacunar canaliculi (18). Osteocytes act as mechano-sensors, as they support gap junctions that facilitate inter-cell communication with other osteocytes and osteoblasts. They also aid in nutrient and oxygen transfer from

the surrounding vasculature system (19). Moreover, osteocytes can control osteoblasts formation and osteoclasts resorption (20) (Figure 1-2).

During the osteogenic differentiation process, pre-osteoblasts aggregate, becoming osteoblasts, the osteoblasts are entrapped within the matrix, and secrete unmineralized matrix to produce osteoid. The osteoid facilitates mineralisation, which ultimately matures the osteocytes (21). Terminal differentiation is indicated by the expression of genes which lead to the production of extracellular matrix (ECM) proteins, including osteocalcin (*bglap*) and bone sialoproteins (22).

1.6. Osteoclasts

Osteoclasts are multi-nucleated cells differentiated from bone marrow mononuclear cells of the monocyte-macrophage lineage (23). Osteoclasts play significant role in bone resorption (Figure 1-2). Osteoclasts initiate the resorption via their membrane-bound integrin receptors, which assist in linkage to the bone matrix peptides. These receptors, which are members of the β1 family, bind to collagen, laminin and fibronectin (24); however, αvβ3 integrin is the most crucial integrin receptor enabling bone resorption, which binds to osteopontin and bone sialoprotein.

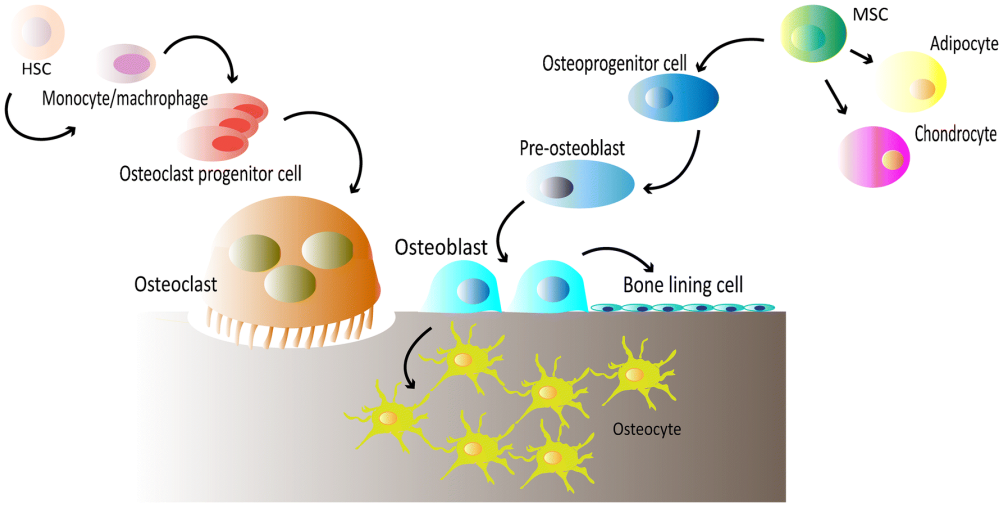

Figure 1-2 Bone progenitor cells and their differentiation into specialised bone cells. The osteoblast is the bone-forming cell differentiated from MSCs into pre-osteoblasts, mature osteoblasts, and osteocytes. The osteoclasts are drived by monocyte-macrophage lineage. This image was obtained from (25) [Accessed 30 December 2022].

1.7. Osteoclastogenesis

There are two essential molecules that regulate osteoclast differentiation: 1) macrophage colony-stimulating factor (M-CSF) and 2) the receptor activator of nuclear factor (NF-kβ) ligand (RANKL). Both of these elements are produced mainly by marrow stromal cells and osteoblasts and contribute to osteoclast formation (osteoclastogenesis) (26, 27). Besides these two molecules, an osteoblast-secreted protein called osteoprotegerin (OPG) has a role in osteoclast-genesis. OPG has high affinity to bind RANKL on osteoclasts, consequently inhibiting its ability to attach to the RANK receptor bound on osteoblasts (14).

When the osteoclast binds to the bone matrix, the become polarised and development of a ruffled border along the resorbing surface occurs in response by hydrogen ions (H^+) which produces an acidified surrounding environment. This leads to the fusion of cell membranes with acidified matrix metalloproteinase (MMPs) and cathepsin K (CTSK)-containing vesicles (14). Minerals within the matrix are dissolved by acidifying the resorption compartment, laid below the osteoclasts, by the hydrogen ions (H^+)

(14). Protein components of the matrix, which primarily consist of type I collagen, are digested by CTSK. Enzymes, including CTSK, are exocytosed from the vesicles via the action of H^+ ions and secreted from the ruffled border via both chloride channels and H^+ ATPase (28). As the osteoclast attaches to the matrix, the cytoskeleton (comprising of fibrillar actin) rearranges to form an actin ring, which initiates the development of a sealing zone around the attachment (28, 29).

During the osteoclastogenic process, M-CSF binds to receptors of osteoclast precursors (c-FMS), stimulating osteoclast formation (30, 31). Once RANKL connects with its receptor-RANK in osteoclast precursors, RANKL initiates the process of osteoclast formation (31). Moreover, osteoblasts also produce OPG, which attaches to the RANKL and prevents the interaction between RANK and RANKL from taking place (32). In turn, this prevents osteoclastogenesis. The RANKL/RANK/OPG system thus plays an important mediatory role in osteoclast formation (Figure 1-3). Additionally, the RANKL/RANK interaction facilitates expression of other osteoclastogenic factors, including the nuclear factor of activated T-cells c1 (NFATc1). NFATc1 is considered the master transcription factor of osteoclastogenesis (33). NFATc1 interacts with other transcription factors, and this regulates osteoclast-specific genes such as *ACP5* (that encodes TRAP*)* and *CTSK* (that encodes cathepsin- K), both of which play essential roles in promoting and facilitating osteoclast activity (34).

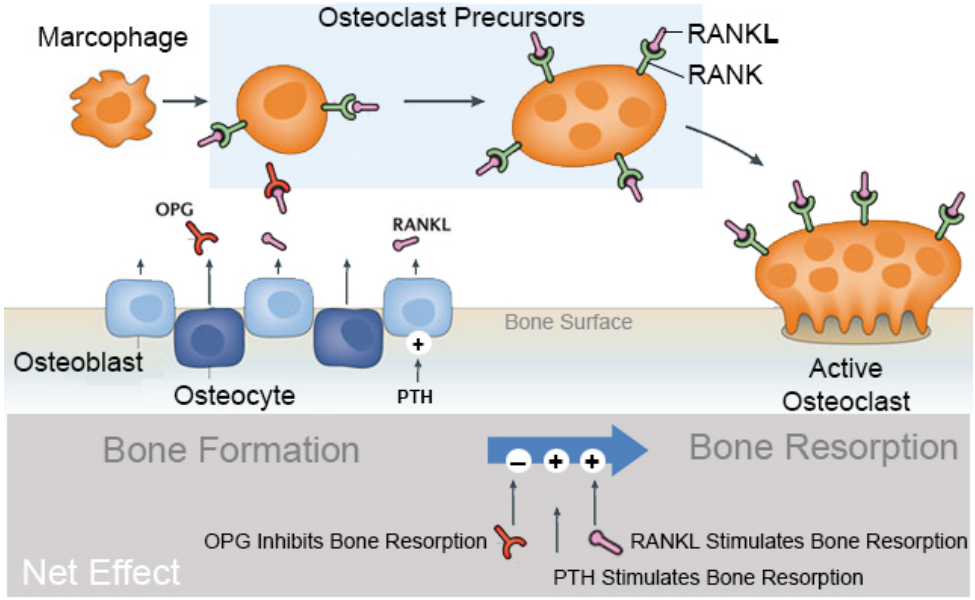

Figure 1-3 RANKL, RANK and OPG signalling. RANKL, expressed by osteoblasts, interacts with its cognate receptor RANK on the surface of preosteoclasts and mature osteoclasts. The interaction leads to osteoclast differentiation, maturation, and survival, thereby promoting bone resorption. Parathyroid hormone (PTH) stimulates bone resorption by acting directly on osteoblasts/stromal cells and then indirectly to increase differentiation and function of osteoclasts. OPG protects bone from excessive resorption by binding to RANKL and preventing it from binding to RANK. This image was obtained from https://www.orthobullets.com/basic-science/9010/bone-signaling-and-rankl (25) [Accessed 26 January 2023].

1.8. Bone ECM

Bone ECM is a non-cellular component which creates three-dimension assembly of the bones, secreted by osteoblasts into the extracellular zone which supports the integrity and flexibility of bone tissue. The bone matrix consists of organic (40%) and inorganic components (60%). ECM production is a process includes osteoblast secretion of organic matrix components (including type I collagen, bone sialoprotein, proteoglycans) and non-collagenous proteins (i.e. osteopontin, osteonectin, and osteocalcin) (35) followed by deposition of the matrix components which called mineralisation. The mineralisation process depends on both calcium and phosphate ions (36).

1.9. Physiological processes of bone biology

Three physiological processes occur during the bone lifecycle are: (i) longitudinal and radial growth, which is the formation of primary new bone that occurs at the growth plate during childhood and adolescence, (ii) modelling (reshaping), and (iii) remodeling

(bone resorption and bone re-formation). Ossification is forming new bone (osteogenesis) (14, 37). During mammalian foetal development, bones are formed by one of two approaches based on the origin of the osteoblast. Intramembranous (mesenchymal) ossification is the mechanism of bone formation, where osteoblasts originate from MSCs committed to the osteogenic cell lineage. Unlike intra-cartilaginous (endochondral) ossification denotes the process by which chondrocyte involves in bone formation by replacement of hyaline cartilage into in osteoblast precursors and continue to grow and produce bone (2, 3).

1.10. Bone modelling

Bone modelling is a process whereby bones are formed or reformed by the independent action of osteoblasts and osteoclasts in response to physiological or mechanical effects. In response to biomechanical forces, osteoblasts and osteoclasts may exert changes to bone shape and axis by adding or removing bone, respectively (14). In adults, bone modelling does not occur as often as bone remodelling. Bone modelling is often associated with clinical conditions such as hypoparathyroidism and renal osteodystrophy or in response to treatments with anabolic compounds (2, 38).

1.11. Bone remodelling

Bone remodelling is a constant process whereby old bones are removed and replaced by new synthesised bone. This process maintains bone strength and mineral balance (38, 39). This cycle ensures that micro-damaged bone is removed and not allowed to accumulate. Remodelling begins at the embryonic stage, and it is a life-long process. The unit of osteoclasts and osteoblasts which conduct the remodelling is tightly controlled to ensure the sequential nature of the process (39, 40).

Bone remodelling is a four-stage activation, resorption, reversal, and formation process. Remodelling frequently occurs randomly but is also targeted to damaged areas (38).

The activation step requires activation of circulating osteoclast precursors, detachment of endosteum lining cells from the bone, and formation of multinucleated preosteoclasts from the mononuclear cells. Then, the integrin receptors on the preosteoclast membranes bind to the bone matrix via arginine, glycine, and asparagine-containing (RGD) peptides in the bone matrix, producing sealed bone-resorbing zones below the cells (38).

The bone resorption phase of remodelling, driven by osteoclasts, occurs over 2 to 4 weeks (41). During this phase, the bone minerals are mobilised because of secretion of H^+ ions by osteoclasts and CTSK; two mediators for bone resorption (41). The H^+ ions create an acidified environment in the resorption compartment underneath the osteoclasts, which dissolve mineral components of the bone matrix. In contrast, CTSK degrades and digests type I collagen (38). The organic matrix then is digested by cytoplasmic lysosome-derived TRAP, CTSK, MMP-9, and gelatinase from the resorbing osteoclasts which results in the production of saucer-shaped How ship's lacunae trabecular bone surface, and Haversian canals are formed in cortical bone (41, 42).

The reversal stage represents the transition from resorption to the formation of bone. When resorption is complete, the resulting cavities contain many mononuclear cells, including monocytes, osteocytes released from the bone matrix, and pre-osteoblasts primed to initiate bone formation (41). Components released from the bone matrix, such as TGF-β, inhibit osteoblast production of RANKL, which subsequently slows osteoclast resorption activity (42).

The bone formation stage is completed in 4 to 6 months and requires the osteoblast synthesis of collagenous organic matrix and mineralisation regulation (35). Osteoblasts that become buried within the matrix change to osteocytes, which are inter-connected by a vast canalicular network produced by gap junction formation between the osteocyte cytoplasmic processes also connects to bone surface lining cells and osteoblasts and thus operate as a functional syncytium. Over half (up to 70%) of osteoblasts post-bone formation are subject to apoptosis, and the remainder become bone-lining or osteocytes (35). Bone lining cells operate as a blood-borne barrier, regulating the exchange of mineral ions both into and out of the bone extracellular fluid; moreover, bone lining cells are capable of differentiating into osteoblasts under certain conditions, such as mechanical force or parathyroid hormone exposure (43). In the endosteum, the lining cells help to form the specialised bone remodelling compartments before resorption by lifting from the bone surface. Every bone remodelling cycle produces a new osteon. The process is the same for both cortical and trabecular bone, with the modification of trabecular bone remodelling zones equivalent to cortical units halved longitudinally (35, 43) (Figure 1-4).

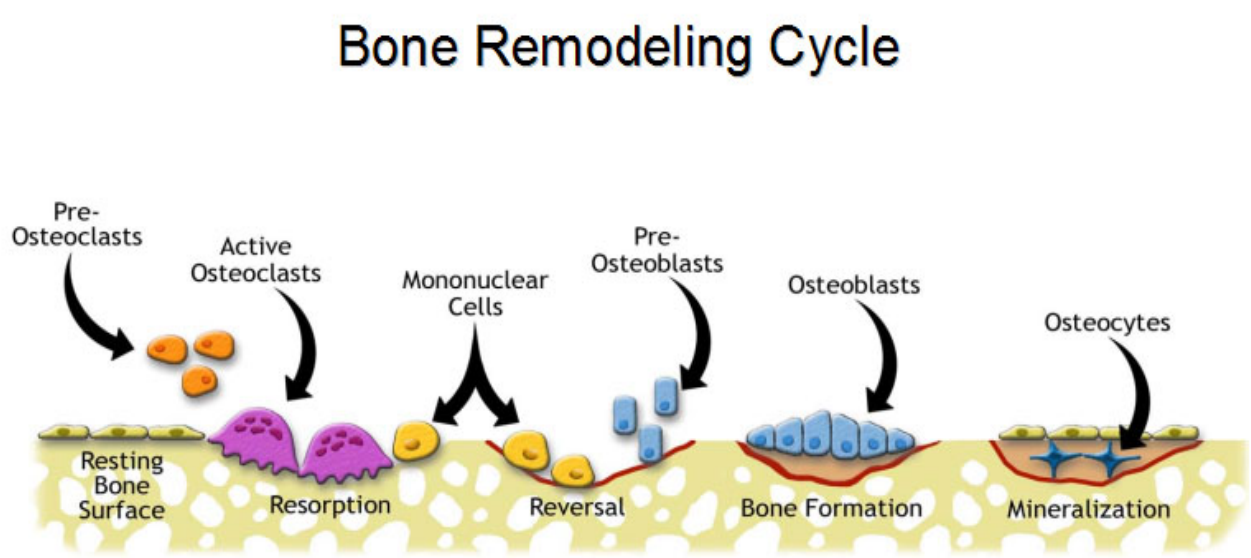

Figure 1-4 Bone remodelling cycle. Bone remodelling has 4 distinct phases.1) activation, 2) resorption and osteoclast differentiation, 3) reversal, 4) pre osteoblast recruitment and osteoblast differentiation and 5) bone formation. The original image was taken from (44). [Accessed 15 January 2023].

1.12. Regulation of osteogenesis

From the osteogenic commitment of MSCs to osteogenic differentiation toward osteocyte maturation, there are common expression patterns of bone-related genes/proteins for osteoblast differentiation. Once the osteoblast has committed to the osteoblastic lineage, bone matrix protein genes are sequentially expressed at various expression levels based on the maturity of the cells (22).

Both runt-related transcription factor 2 (RUNX2) and the core-binding factor subunit alpha-1 (CBF-alpha-1) are the master regulator which control osteogenic genes expression (45, 46). At an early stage (the prefoliation), the osteoblast progenitors express *RUNX2* and *ColIA1*, an early indicator of osteoblast commitment. Moreover, once the cells progress, they express alkaline phosphatase (ALP), this is when they become pre-osteoblasts (47). Subsequently, the pre-osteoblasts convert into mature osteoblasts during the transition phase, which is characterised by the expression of osterix (*osx*) and mineralization-associated genes such as osteopontin (*opn*), bone sialoprotein (*bsp*), and osteocalcin (*ocn*) (47).

1.13. Runt-related transcription factor 2

The multifunctional transcription factor RUNX2 regulates chondrocyte and osteoblast differentiation to control skeletal development. *RUNX2* is the main transcription gene for osteogenesis (48). Komori *et al*. demonstrated the role of *RUNX2* in a deficient transgenic model, in which no differentiated osteoblasts were identified (22). Other studies indicated that *RUNX2* downregulation can block osteoblast and chondrocyte differentiation and impairs accurate ossification (22, 49, 50). Moreover, *RUNX2* controls expression of other osteoblast-specific genes including collagen type I (*COL1A1* and *COL1A2*) and *ALP* which instructs early osteoblast differentiation (51). *RUNX2* expression was investigated in bacterial chondronecrosis osteomyelitis (BCO) models. It has been found that *RUNX2* gene is significantly more downregulated in the BCO- affected group than in the unaffected group ($P<0.05$) (52). This finding indicated that there was a significant reduction in the expression of *RUNX2* and *COL1A1* after *S. aureus* infection.

1.14. Alkaline phosphatase

ALP is a glycoprotein metalloenzyme comprises several isoenzymes. Different loci in the *ALP* gene; chromosome 2 encodes three isoenzymes for intestinal, placental, and placental-like ALP, whereas non-specific tissue loci (from the liver, bone, and kidney) are located on chromosome 1. The enzyme is highly expressed in hepatic, skeletal, and renal tissue. In clinical examination, the level of bone-specific ALP measured in the serum reflects the cellular activity of osteoblasts: a high ALP concentration indicates an increased bone turnover (53, 54).

During osteogenic differentiation, there is an increase in *ALP* expression during progression of MSC-osteogenic differentiation within the first two days of induction (55). Functionally, ALP plays a crucial role in skeletal and dental mineralisation. ALP is produced by osteoblasts. ALP is an indicator of bone metabolism and early bone formation (56). Increased ALP expression is associated with progressive differentiation of osteoblasts. It is known that the expression of *ALP* in the early stages of osteoblast differentiation, increases in mature osteoblasts and decreases when osteoblasts differentiate to osteocytes (57).

1.15. Osteocalcin

OC or bglap is the most common non-collagenous protein in the bone matrix. bglap contains a 49-amino-acid peptide and is released into the bone matrix and the blood by osteoblasts. Once synthesis by the osteoblasts, a small amount of their protein is released into the circulatory system and vast quantity of bglap is expressed in the bone. bglap is an indicator of late stage of osteogenesis and denotes osteoblast function (58). It is believed to be essential for bone mineralisation and matrix synthesis (59). The role of bglap has been investigated by Ducy and his group (60). A *bglap*-deficient mouse was generated to inspect its effect on bone formation. Surprisingly, the mice developed a phenotype marked by higher bone mass and bone of developed functional quality. Furthermore, histomorphometric studies have shown that lack of *bglap* leads to an increase in bone formation without impairing bone resorption (60).

1.16. Tartrate-resistant acid phosphatase

TRAP is an acid phosphatase metalloenzyme synthesised as a monomeric proenzyme (TRAP 5a, 35 kDa). TRAP is encoded by *ACP5* (61). There are two types

(isoforms) of TRAP, namely TRAP5a (found chiefly in immune cells) and TRAP5b (identified primarily on osteoclasts).

TRAP is predominantly responsible for regulating OPN activity, a protein formed by activated osteoclasts and macrophages (62), promoting osteoclast-genesis and osteoclast activity (63). Studies have shown that TRAP is associated with excessive bone resorption rates and fractures.

TRAP is released into the resorption lacuna of active osteoclasts throughout the process of bone resorption. It dephosphorylates OPN, which facilitates the detachment and migration of the osteoclasts (64).

Osteoclasts can bind to bones when OPN is activated throughout the bone remodelling process. Subsequent to the complete breakdown of bone, the TRAP5b deactivates the OPN, which results in osteoclasts discharge from the bone (65). Studies also identified skeletal abnormalities in homozygous *ACP5* knockout mice, which indicated that TRAP is also required for the ossification process. Progressive contracting and deformity were evident in these mice's long bones and axial skeleton. The epiphyseal growth plates also widen, whilst the cartilage mineralisation is delayed (66).

1.17. Matrix metalloproteinases

MMPs are family of zinc-dependent proteolytic enzymes that play a critical role in cleaving different ECM degrading proteins (67). For the most part, they can be categorised into 1) collagenases (MMP-1, -8, -13, and -18), 2) gelatinases (MMP-2 and -9), 3) membrane-type MMPs (MMP-14, -15, -16, -17, -24, and -25) and 4) others (MMP-7, -12, -19, -20, -23, -26, and -28). Common functional areas and activation systems exist between these enzymes, and they can be synthesised to create secreted transmembrane proenzymes (68). Moreover, amino-terminal pro-peptides

can be removed to convert the enzymes into active forms. MMP endopeptidases regulate osteoblasts and osteoclasts during cell growth, migration, and extracellular matrix re-modelling (69). MMP-13 plays a significant role in the extracellular matrix breakdown. MMP-13 effectively breaks down collagen type II and collagen types I, III, and X, which are crucial parts of bone and cartilage. It has been shown that mice lacking MMP-13 appear to have a striking defect in endochondral ossification (70, 71).

1.18. Osteomyelitis

OM is an inflammation of the bone and bone marrow cavity that results in local bone destruction and osteonecrosis (72). The term osteomyelitis includes bone or joint infections (73). Various pathogenic organisms such as fungi, parasites, mycobacteria, and Gram-positive and Gram-negative bacteria have been identified as causative agents of osteomyelitis (73). Most commonly, approximately 80-90% of pyogenic infection osteomyelitis cases are induced by *S. aureus,* while *Staphylococcal epidermis* is predominantly responsible for prosthetic osteomyelitis (introduced by joints/bone medical devices) (73). OM is classified by a broad spectrum based on duration, clinical presentation, and anatomy (74, 75).

According to Wald Vogel's classification, osteomyelitis can be acute or chronic. The term acute osteomyelitis is recognised recently as bone infection clinically manifested by extreme tenderness (74, 75). Usually, this type of infection is common in children under 17 years old, and it is not treatable since it is not responsive to any antimicrobial therapy. Conversely, chronic osteomyelitis is an infection relapse where clinical symptoms persist for over ten days. This type is expected in the elderly population and is associated with clinical conditions such as diabetes, neuropathy, and peripheral vascular diseases. Additionally, chronic osteomyelitis is characterised by the persistence of low-virulence microorganisms, which facilitate the development of

necrotic bone and the formation of pus and sequestrum (a compromised soft tissue envelope) (76) (Table 1-2). Moreover, osteomyelitis can be classified according to the mechanism of bone infection. OM due to contiguous infection accounts for the most prevalent type of OM and is associated with haematogenous infection or with direct inoculation of bone following an open fracture/ trauma or after joint replacement surgery such as post-traumatic OM, and infections related to prosthetic devices. It is common in patients with implanted surgical devices such as catheters and prostheses (76). Haematogenous osteomyelitis is the most common form in children and is characterised by blood-borne infection. It is initiated when blood is contaminated with a pathogenic agent that spreads through the bloodstream remotely, such as in impetigo or tonsillitis (74). This type is mainly caused by *S. aureus* and originates in the metaphyseal region of the long bone (the tibia and femur), where there are large numbers of blood vessels which facilitate the transfer of bacteria from the blood to the bone marrow (75). In the elderly, osteomyelitis, associated with vascular insufficiency, generally affects the lower extremities, such as the feet (74) and is characterised by an infection triggered by inadequate blood supply, diabetic wounds, neuropathy impaired immune systems (e.g. rheumatoid arthritis).

Table 1-1 Wald Vogel's classification of osteomyelitis according to the mechanism of bone infection. Adapted from (77).

Mechanism of bone infection	Characteristics
Hematogenous	Secondary to bacterial transport through the blood. Majority of infections in children
Contiguous	Bacterial inoculation from an adjacent focus. E.g., Post-traumatic Osteomyelitis, and infections related to prosthetic devices.
Associated with vascular insufficiency	Infections affecting the feet in patients with diabetes or peripheral vascular insufficiency

Table 1-2 Wald Vogel's classification of osteomyelitis according to the duration of infection

Duration of infection	Characteristics
Acute	Initial episodes of osteomyelitis. Oedema, formation of pus, vascular congestion, thrombosis of the small vessels
Chronic	Recurrence of acute cases. Large areas of ischemia, necrosis and bone sequestrate

Antibiotic administration and surgical debridement are the only therapeutic strategies offered to patients diagnosed with osteomyelitis, and both therapeutic options have disadvantages (78). Antibiotic therapy is challenged by the progress of antibiotic resistance of bacteria and the difficulty in delivering antibiotics to the site of infection (79). However, the removal of damaged tissues by surgery is associated with complications and disability, which may result in amputation of the affected limb in chronic, resistant cases (79).

1.19. Pathogenesis of osteomyelitis

Several studies were conducted in animal models (i.e., guinea pigs or rabbits) to identify the pathogenicity of OM. These studies showed that normal bone is highly tolerant to an infection, and an induction of infection requires inoculation of a high microorganism load at the site of infection, which may be originated by trauma or presence of implanted foreign bodies.

The pathogenesis of OM is a four-step process: (i) bacterial attachment to bone surface, (ii) recruitment of acute inflammation, (iii) abscess formation and (iv) destruction of bone integrity (75).

S. aureus is one of the major causes of bone infection, as they can adhere to bone through adhesion molecules expressed on their cell surface. These molecules, called adhesins, can bind to bone components such as fibronectin, laminin, collagen, and bone sialoglycoprotein (80). In addition, it has been reported that collagen-binding

adhesin enables *S. aureus* to attach to cartilage (81). *S. aureus* has the potential not only to adhere to bone and cartilage but also to attach to implanted devices in the bone. Moreover, *S. aureus* can survive intracellularly, which may contribute to the persistence of bone infection (81).

Once the pathogenic microorganism adheres to bone, the host immune system is activated by stimulating an acute inflammatory purulent reaction. In this phase, bacteria resist antimicrobial activity and avoid the phagocytic mechanisms of the host immune system (82). After microbial adherence, bone destruction mediated by osteoclast resorption takes place. In this stage, inflammatory cells release several cytokines such as interleukins (IL-1, IL-6 and IL-11) (83) and tumour necrosis factor (TNF), which in combination can activate osteoclast-driven bone resorption (84). Moreover, phagocytic cells produce oxygen radicals and release enzymes that lyse adjacent tissues, eventually leading to pathologic bone fracture (85). Furthermore, cell surface antigens of infectious pathogens promptly trigger the complement cascade, resulting in tissue oedema, local vasodilatation, and migration of polymorphonuclear cells to the site of injury (86). Subsequently, pus exudate increases in the intramedullary canal and exerts an intraosseous pressure that spreads towards endosteal vascular channels, causing impaired blood flow. This abscess will eventually lead to periosteal rupture and disruption of the blood flow in the periosteum. The ischemic necrosis of bone (demonstrated by the absence of living osteocytes) results in the separation of segmental cortical fragments known as a sequestrum (sequestra) (73) (73, 85).

1.20. *S. aureus* structure and morphology

Staphylococcus genus is a group of bacteria belonging to Gram-positive bacteria that are spherical and arranged in grape-like structures (87). *S. aureus* and *S. epidermis*

are two species known to be human commensals, as *S. aureus* normally colonizes nasal passage and axillae, whereas *S. epidermidis* commonly inhabits human skin (82, 87). *S. aureus* is one of the most pathogenic species that contribute to a wide range of diseases such as superficial skin lesions and localized abscesses in other sites and has potential to cause deep infections such as OM. *S. aureus* is also considered a major source of nosocomial and community-acquired infection (82). Figure 1-5 illustrates steps of bone infections.

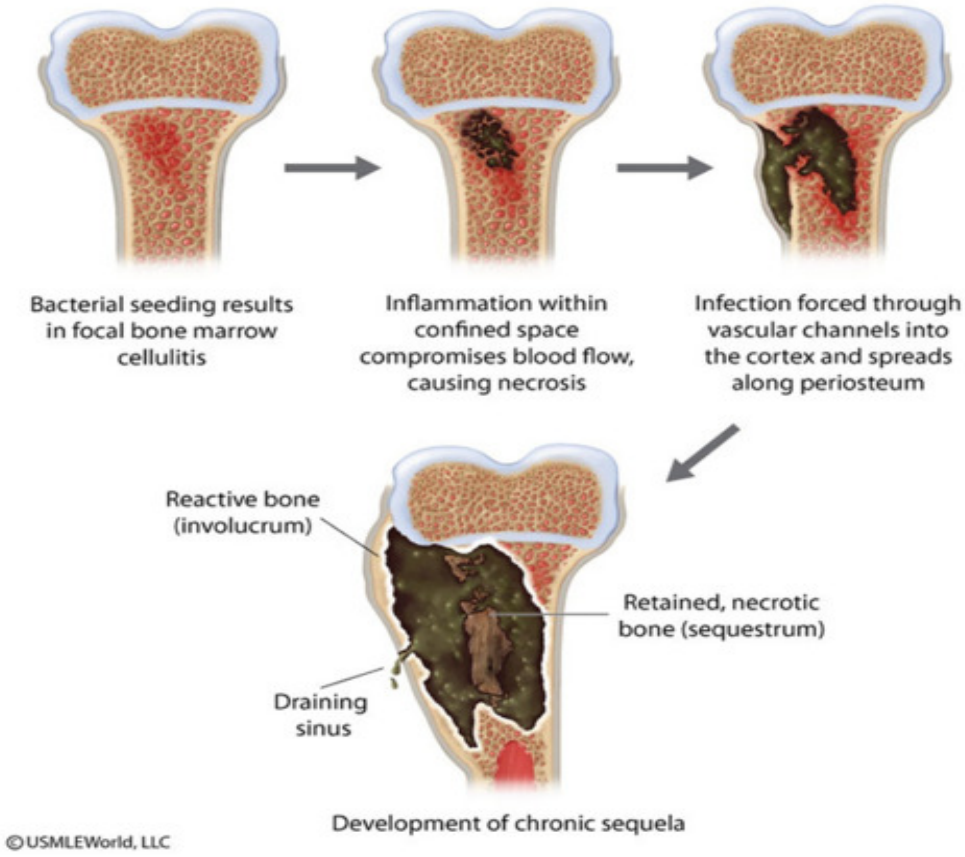

Figure 1-5 Osteomyelitis pathogenesis The original image was taken from (1) [Accessed 15 January 2023].

1.21. Virulence factors of *S. aureus*

S. aureus expresses a variety of virulence factors such as cell surface proteins which contribute to mammalian infection (82). These virulence factors are encoded by and are grouped according to the mechanism of infection; (i) surface proteins that promote adherence to host tissues, (ii) protein factors that inhibit phagocytosis and (iii) toxins (87, 88). Biofilm production is an additional virulence factor used by *S. aureus* which facilitates the bacteria to persist on plastic surfaces and resist host defenses or antibiotics (88). Additionally, small colony variants (SCVs) of *S. aureus* help the pathogen to survive in a metabolically inactive state under harsh conditions (88, 89). The small colony variants (SCVs) are slow-growing sub group of bacteria which exhibit uncommon colony morphology on agar plates and unusual biochemical traits (90, 91). Moreover, SCVs show a higher capacity to persist intracellularly within host cells and they are less susceptible to antibiotics than their original wild-type phenotype (92). Moreover, SCVs were noted to their virulent wild-type form when changing their intracellular location and reinfecting new cells (93). It was revealed that SCVs of *S. aureus* are associated with persistent, repeated, and antibiotic-resistant infections, and this investigation has impacted our understanding of the persistence of chronic infections of *S. aureus,* such as chronic OM (88).

S. aureus secrete an extracellular polymeric substance (EPS), a key component in biofilm formation, which helps microbes to resist and minimise the diffusion of antimicrobial drugs. Functionally, the biofilm protects cells against aggressive conditions, i.e., changes in temperature, dehydration, or nutrients deprivation and protects cells against antibacterial drugs. The biofilm formation of *S. aureus* is supported by a number of gene products, such as fibronectin-binding proteins (FnbA and FnbB), intercellular adhesion (IcaA, B, C and D), fibrinogen-binding

proteins (F*ib*) and collagen binding protein (CNA) (94). Due to the presence of biofilms surrounding bacterial cells, antimicrobial antibiotics drugs are increasingly becoming partially or fully inactive against *S. aureus* as they are either less penetrable or totally impenetrable (87). Bacterial cells covered in a biofilm have been reported to resist antibiotics 10–1000 times more compared to their corresponding planktonic forms (95).

Moreover, fibronectin (Fn) is one of ECM component acts as a linking bridge between *S. aureus* and osteoblasts. *S. aureus* binds to Fn receptors of host cells by their Fn binding proteins (fibronectin protein A) and the latter mediates *S. aureus* internalization into the cells through the mechanism of an α5ß1 integrin (96). The α5ß1 integrin is a cellular element (the most common virulence marker) promotes subsequent internalisation of *S. aureus* into osteoblasts. It was proven that *S. aureus* capability to infect cells reduced when this integrin gene was deleted (96, 97).

S. aureus may be internalized by osteoblasts. The uptake of *S. aureus* by osteoblasts is mediated by the major adhesins fibronectin protein B (FnBPs). FnBPs on the surface of *S. aureus* enable *S. aureus* to internalize into osteoblasts via the Fn junction with Fn receptors such as α5β1 integrins. Fn is a “bridge” between *S. aureus* and osteoblasts. This “Fn bridge” enables *S. aureus* to enter osteoblasts via internalization.

1.22. Interaction of *S. aureus* with bone cells

The balance between bone formation by osteoblasts and osteoclast resorption is necessary to maintain the integrity and strength of the bone. However, in pathological conditions such as infections, this homeostasis is impaired and results in bone loss and destruction. The process of bone infection undergoes 3 stages: (i) *S. aureus* attachment to bone extracellular matrix (ECM), (ii) the internalization of *S. aureus* into

osteoblasts (mediate by fibronectin receptors) and (iii) impaired osteoblast functions resulting in bone destruction (97).

S. aureus adherence to the ECM is the initial step in establishing bone infection. This allows bacteria to attack and invade the host cells (98) . *S. aureus* expresses several cell wall proteins (adhesins) capable of binding glycan and proteins of ECM such as type I collagen, sialoprotein, OPN and fibronectin (99). These microbial adhesins are alternatively named microbial surface components recognising adhesive matrix molecules (MSCRAMMs) (Figure 1-6). Studies have shown a link between microbial adhesin molecules and OM pathogenicity. For example, collagen adhesin and sialoprotein binding protein on the microbial surface of *S. aureus* are considered major markers of virulence that are associated with OM (98, 99).

The next stage of bone infection is the internalization of *S. aureus* into the osteoblasts which is the key element in spreading *S. aureus* in these cells. Internalisation allows *S. aureus* to live inside the osteoblasts where it is protected from the immune-system mediated phagocytosis, providing *S. aureus* with an opportunity to sustain infection (99, 100). This might explain the progress of the acute phase into the chronic stage of OM.

Subsequent to *S. aureus* internalisation into osteoblasts, *S. aureus* survives inside vesicles (99, 100). The absence of an efficient intracellular bacterial elimination program in osteoblasts may permit *S. aureus* to escape from the intracellular vesicles and released into cell cytoplasm to evade proteolytic activity of the lysosome (101). Other *S. aureus* virulence factors including membrane-damaging factors (e.g., haemolysins and phenol soluble modulins (PSM)) are involved in *S. aureus* escaping from intracellular vesicles (102). After the infection is established, osteoblast activity becomes less active and eventually become necrotic. Moreover, *S. aureus* produce

inflammatory mediators from osteoblasts (103). *S. aureus*-osteoblast interaction has been investigated. The infection led to a decrease in osteoblast proliferation, a decline in ALP activity, and a lower expression of ECM components such as type I collagen, and bglap (98). Moreover, it has been revealed that *S. aureus* counteract the mineralization process in infected osteoblast, as indicated by a reduction in calcium deposition in the infected osteoblasts (98).

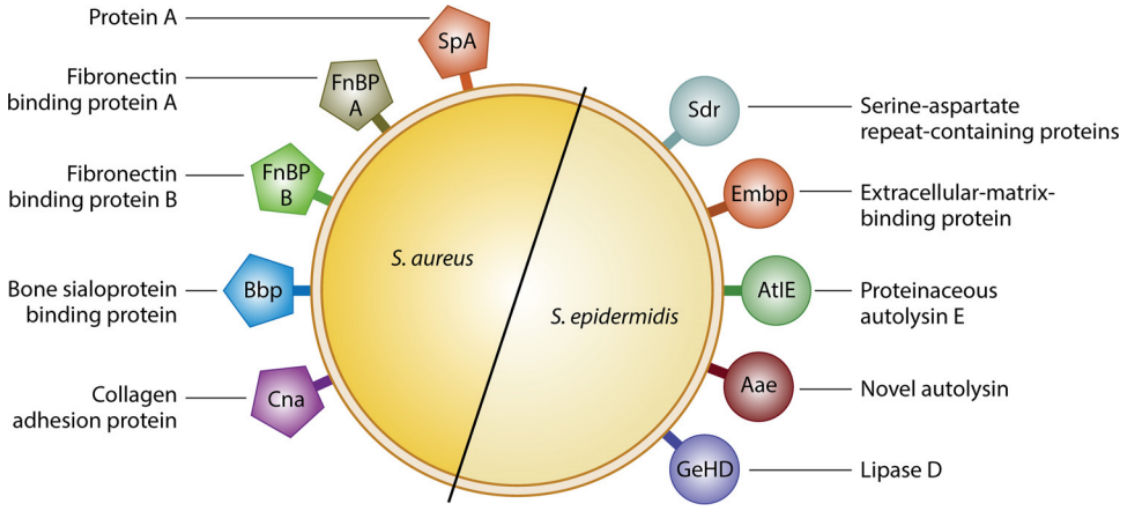

Figure 1-6 *S. aureus and S. epidermidis* cell surface proteins. Virulence factors known as MSCRAMMs are *S. aureus* surface proteins participating in interacting with bone cells and ECM. Cited from (73).

1.23. Mesenchymal stem cells

Mesenchymal stem cells (MSCs) are a population of self-renewing, multipotent, heterogeneous cells that originate mainly from bone marrow and other connective tissues of the body such as adipose tissue, chorionic villi of the placenta, umbilical cord blood, lung, amniotic fluid, foetal liver, and peripheral blood (104). They are undifferentiated and can potentially differentiate into functionally specialised types of cells, namely osteoblasts, chondrocytes and adipocytes, which form bone, cartilage and fat cells, respectively (105). This commitment of MSCs to differentiate into

specialised cell types requires the recruitment of different factors, such as growth factors. This specialised differentiation feature provides useful tools in regenerative medicine as MSCs can be developed to replace damaged tissues (104, 105). The population of MSCs, isolated from bone marrow possess several identifying surface antigen markers at variable levels. This variability in the expression of markers occurs as a consequence of many factors such as species, tissue source, culture conditions and the duration before individual passages. These markers include CD44, CD105 (SH2; endoglin), CD106 (vascular cell adhesion molecule; VCAM-1), CD166, CD29, CD73, CD90, CD117, STRO-1 and Sca-1 (106). Correspondingly, MSCs lack the expression of haematopoietic and endothelial cell lineage markers, i.e. CD11b, CD14, CD31, CD33, CD34, CD133, HLA-DR II and CD45 (107). These differences provide an advantage in distinguishing MSCs from the hematopoietic precursors. In vitro, MSCs are characterised by their ability to adhere to plastic culture surfaces (108). MSCs can be obtained by following various laboratory protocols. MSCs isolated from bone marrow aspirates can be obtained using the widely used density gradient centrifugation method which enriches the mononuclear cell fraction. Common media for this purpose include Ficoll, Percoll or dextran (109). On other hand, some studies performing clinical-grade isolation and expansion of MSCs follow the direct plating strategy to separate plastic adherent MSCs from the nonadherent hematopoietic cells (109, 110). MSCs can be grown and expanded when incubated with appropriate growth media. After several days (5-7 days) in culture, MSCs develop a fibroblastic-like morphology (111).

1.24. Antimicrobial peptides

AMPs are short, positively charged peptides found in a wide variety of multicellular organisms (112, 113). Numerous AMP molecules demonstrate a broad-spectrum

antimicrobial activity against both Gram-negative and Gram-positive bacteria as well as other infectious pathogens such as viruses, fungi and protozoa (113). The production of these antimicrobial peptides is either constitutive or inducible in response to inflammatory stimuli or infection (112). There are different mechanisms of action (MoA) of AMPs leading to the eradication of pathogens (114).

The majority of AMPs are cationic peptides that electrostatically interact with anionic membrane of bacteria, while hydrophobic part of AMPs (more strongly) interacts with hydrophobic bacterial membrane. This results in penetration of phospholipid bilayer (114). The bacterial cell death mediated by AMPs occurs by disturbing the membrane integrity and inhibiting, RNA, DNA or protein synthesis (115). AMPs firstly penetrate the polysaccharide surface of the bacterial membrane and then attaches to lipopolysaccharide or teichoic acid in Gram-negative or in Gram-positive bacteria respectively. This attachment results in creating pores in bacterial membrane and disturbing their integrity with subsequent bacterial killing (115, 116).

Moreover, AMP activity has been shown to depend on target cell membrane structure. Bacterial and eukaryotic cell membranes express different cell membrane components. Eukaryotic cells express a large amount of cholesterol whereas bacteria lack cholesterol in their cell membranes. The bacterial selectivity of most antimicrobial peptides has been attributed to the presence of abundant acidic phospholipids and the absence of cholesterol in bacterial membranes. For example, cholesterol has been shown to protect human erythrocytes from attack by magainin 2. Similar studies on model membranes have demonstrated that the presence of cholesterol reduces AMP binding and suppresses the disruption of lipid bilayer structure (117, 118).

1.25. Cathelicidin LL-37

Cathelicidin is a group of α-helical mammalian AMPs composed of about 20 members, but only one is present in humans, called LL-37 (41). Inactive 18 kDa protein precursor (hCAP180) of LL-37 is produced and on further processing by proteolysis of C-terminal, the small 37 amino acid functional peptide is formed. The C-terminal leucine-leucine residues of LL-37 are the active site against bacteria (119). Both Gram-positive and Gram-negative bacteria are susceptible to the actions of LL-37. Further, LL-37 contributes to many cellular activities, including apoptosis, phagocytosis, and effector immune cell chemotaxis (120, 121). Several studies also demonstrated a reduction in bacterial growth in response to LL-37 (120, 121). In a mouse model of sepsis, *in vivo* treatment by human MSCs produced significant improvements in survival and an overall decrease in bacterial growth (122). LL-37 was better than conventional antibiotics against *S. aureus*-infected osteoblasts, exhibiting improved bacterial killing, particularly against clinically relevant strains (120). LL-37 association with Toll-like receptor (TLR) modulation can be exploited to induce expression via TLR-2, TLR-4, and TLR-9 (123, 124). LL-37 expression is linked to several stimuli, including inflammatory mediators such as TNF alpha and interferon, and TLR receptors and microbial structures (125).

1.26. Defensin

Defensins are 2-5 kDa cationic peptides of AMP family. Based on cell origin, gene structure and sequence cysteine-residue (126), defensins are categorised into three sub-families; α-defensins, β-defensins, or θ-defensins. Defensins contribute to wound repair, expression of cytokines and chemokines, histamine production and improved antibody response (127). In humans, the primary functional β-Defensins are hBD-1,

hBD-2, and hBD-3 (37), and these are expressed by a variety of cells, including MSCs, epithelial cells and granulocytes (128). hBD-1 is expressed continuously, while other β-defensins are induced by either pro-inflammatory stimuli or microorganisms (129-131).

Studies have shown that mouse keratinocytes stimulated with PGN-SA can induce expression of mBD-3 (a homologue of hBD-2), and its lack of expression in a TLR-2-deficient mice (132). hBD-1 does not show an antimicrobial activity against *S. aureus*, while other experiments have shown that both hBD-2 and hBD-4 show weak bacteriostatic activity against *S. aureus* (133, 134). In contrast, hBD-3 has been shown to have potent bactericidal activity against some strains of *S. aureus* (129, 130) as there are antibiotic-resistant clinical strains of *S. aureus* to hBD-3 (135). Some studies have shown that some *S. aureus* strains (predominantly MRSA strains) tested for susceptibility survived in the presence of hBD3 (136). Moreover, other studies revealed that absence of wall teichoic acids (the major polyanionic polymers in the envelope of *S. aureus*) causes a selective increase in bacterial resistance to hBD-3 (137).

1.27. Indoleamine 2, 3-dioxygenase

Indoleamine 2, 3-dioxygenase (IDO) is a rate-limiting catabolic enzyme that plays a critical role in degrading the essential amino acid, tryptophan. IDO cleaves tryptophan's aromatic indole ring to create several tryptophan degradation products (kynurenines) which have vital immuno-regulatory functions such as preventing T cell replication, inducing T cell apoptosis, and facilitating regulatory T cell differentiation/suppressor function activation (138). They also help keep out invading microbes by generating hostile environments such as tryptophan depletion (139).

IDO is expressed predominantly in dendritic cells (DCs). In inflammatory tissues, Interferon - γ (INF-γ) can produce elevated levels of IDO. This, in turn, results in tryptophan reduction and release of its metabolites which can resolve inflammation and return tissue homeostasis. The antimicrobial effect of IDO against *S. aureus* has been investigated in different studies. It was found that tryptophan depletion, induced by IDO, resulted in considerable reduction in *S. aureus* growth (140). Moreover, IFN-γ stimulation of human cells promotes IDO activity, and as a result, this can cause inhibition in *S. aureus* multiplication in bacterial-endothelial cell co-culture (141). IFN-γ leads to L-tryptophan depletion and subsequently inhibits bacterial growth (142).

1.28. Antimicrobial peptides of MSCs

To date, MSCs have been shown to express four antimicrobial peptides, specifically, LL-37, defensin, hepcidin, and lipocalin-2 (Lcn2). Their secretion may be altered in response to different stimuli such as infection or inflammation (119). It has been demonstrated that bacterial preconditioning of MSCs provokes an increase in LL-37, beta defensin-2, and hepcidin, while pre-exposure of MSCs to inflammatory stimuli evokes increasing levels of LL-37 and Lcn2 (reviewed by (119)). It has also been shown that down-regulation of these AMPs can lead to greater susceptibility to bacterial infections (143). AMPs derived from MSCs have been shown to participate in bacterial clearance, and may be considered as “natural antibiotics” (119) with potential to be an alternative to antibiotics (144). This indicates that MSCs directly increase the innate immune system in response to bacterial infection.

1.29. The immunomodulatory features of MSCs

Beside their effective antimicrobial action through secretion of AMPs, MSCs play a major role in supporting the immune defence system with immunomodulatory

properties including stimulation of TLR and production of proinflammatory cytokines. These factors help in preventing harmful pro-inflammatory responses and contribute to bacterial clearance from the host. MSCs possess immunosuppressive properties mediated by interferon-γ, linked to pro-inflammatory cytokines such as IL-1α, IL-1β or TNF-α (145). Furthermore, MSCs can facilitate paracrine activity and mediate cell-to-cell interaction. These effects are influenced by the secretome components manufactured by MSCs including cytokines, chemokines, enzymes, and growth factors (60). However, MSCs do not exhibit immunogenic properties, as they lack the expression of major histocompatibility complex class II (146).

1.30. Microbe-associated molecular patterns

Microbe-associated molecular patterns **(**MAMPs) are structural secretory and conserved components in most microorganisms (147). The ability to identify MAMPs is based on the presence of pattern recognition receptors (PRRs) which play a critical role in inducing host immune responses. Several different host PRRs (including TLRs and nucleotide-binding oligomerisation domain (NOD)-like receptors (NLRs), or G-protein coupled receptors (GPCRs) can recognise conserved structures of pathogens called pathogen-associated molecular patterns (PAMPs). Many host PRRs are categorised based on their function, location, and ligand specificity. The prominent PRRs in identifying bacterial MAMPs are TLRs localised in the plasma membrane or endosomes and NLRs located in the cytoplasm (148). Each receptor responds to its unique bacterial MAMPs to recruit the host immune response and fight off invading microbes (149).

1.31. Toll-like receptors (TLRs)

TLRs are membrane-bound or intracellular cell-specific receptors that are the first line of recognition for microorganisms. They have alternatively PRP which discriminate between stimulants from a wide-range of microbial pathogen-associated molecular patterns (PAMPs) or self-derived damage-associated molecular patterns (DAMPs). TLRs can be further categorised into two subfamilies according to their location (150). There are cell surface TLRs that include TLR-1, TLR-2, TLR-4, TLR-5, TLR-6, and TLR-10 and intracellular TLRs, found in the endosome, that include TLR-3, TLR-7, TLR-8, TLR-9, TLR-11, TLR-12, and TLR-13 (151) (see figure 1-7).

Typically, cell-surface TLRs identify the lipids, lipoproteins, and proteins that make up microbial membranes. TLR-3 can identify viral double-stranded RNA (dsRNA), small interfering RNAs, and self-RNAs produced by damaged cells. TLR-4 can detect lipopolysaccharide from bacteria (LPS). Additionally, TLR-5 can detect bacterial flagellin (152). PAMPs such as lipoproteins, peptidoglycans, and lipoteichoic acids are all recognised by TLR-2, as well as TLR-1 or TLR-6 (151).

TLR-10 is a pseudogene in mice due to an insertion of a stop codon, but human TLR-10 collaborates with TLR-2 to recognise ligands which are recognized by TLR2/TLR1 heterodimer. By contrast, intracellular TLRs recognise nucleic acids produced by bacteria and viruses while identifying self-nucleic acids in many autoimmune diseases. Most importantly, TLR-7 is expressed plasmacytoid DCs and can differentiate single-stranded (ss) RNA from viruses. In humans, TLR-8 responds to bacterial and viral RNA. TLR9 is an example of intracellular receptor for the unmethylated DNA derivatives from the viruses and bacteria (152).

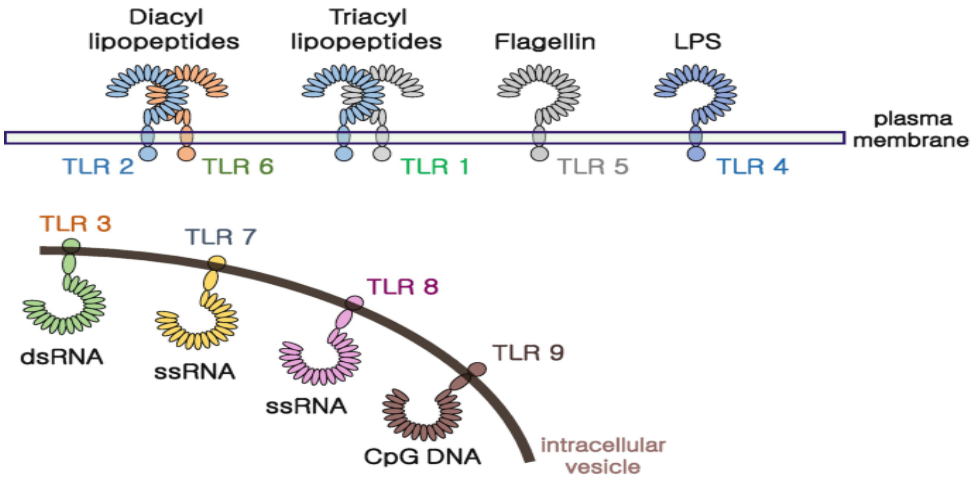

Figure 1-7 TLR subtypes and localisation. Taken from (153). [Accessed 07 January 2023].

1.32. The structures of TLRs

Every TLR is comprised of an ectodomain with leucine-rich repeats (LRRs), a transmembrane domain and a cytoplasmic Toll/IL-1 receptor (TIR) domain, and these components play individual roles in mediating PAMP identification which initiates downstream signalling (154). The ectodomain's structure displays a horseshoe-like structure. Internally, the cytoplasmic area of TLRs resembles the IL-1R family, called the TIR domain (Figure 1-8). TLRs interact with their corresponding PAMPs or DAMPs in the form of homo- or hetero-dimers. In some circumstances, TLR's function necessitates co-receptors or accessory molecules.

Some innate immune cells, dendritic cells, macrophages, and non-immune cells, including epithelial cells, fibroblast cells and MSCs express TLRs (155, 156). It is believed that TLRs have evolved primarily as sensors of exogenous stimuli. However, it is now widely accepted that their ability to detect and identify endogenous ligands plays a critical role in controlling inflammation. As TLRs can detect their specific ligands in the presence of a non-infectious threat, they are known as "danger signals" (156). TLRs play a critical functional role in establishing innate immunity. TLRs signal, by recruiting distinct adaptor molecules that activate transcription factors NF-kB and

IRFs (157). These factors initiate signal transduction pathways to control innate immune responses (158). It is interesting to note that TLR activation is involved in the pathology of many inflammatory diseases (i.e., rheumatoid arthritis or inflammatory bowel disease (IBD)) as constant exposure to TLR ligands either initiate or perpetuates chronic inflammation.

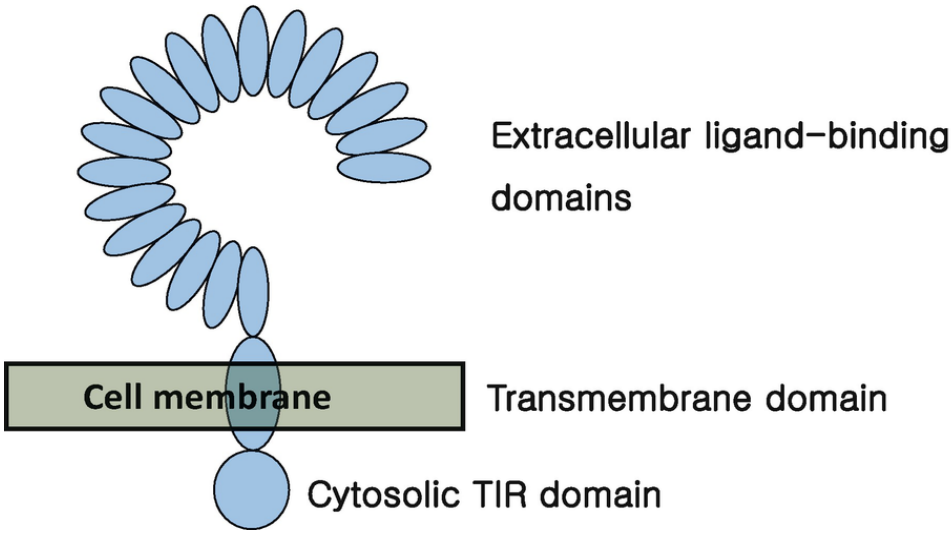

Figure 1-8 The TLR molecular structure. TLRs have ligand-binding domains in the extracellular region (horse-like structure), a transmembrane domain, and a TIR domain in the cytoplasmic area (cytosolic TIR domain). The original image was taken from (153). [Accessed 07 January 2023].

1.33. TLR signalling

Several different adaptor molecules recruited when TLR is activated, such as Toll-interleukin 1 receptor domain-containing adaptor protein (TIRAP), TIR-domain-containing adaptor-inducing interferon-β (TRIF), myeloid differentiation primary response gene 88 (MyD88) and Toll-like receptor four adaptor protein (TRAM) (159). In turn, these adaptor elements trigger other downstream transcriptional gene regulators, including protein-1, NF-κB, IRFs, or MAP kinases or interferon that regulate the expression of cytokines, chemokines, type I IFNs and antimicrobial agents (160). These regulators then protect host cells from infecting microbes and drive expression of chemokines, proinflammatory cytokines [tumour necrosis factor-alpha (TNF-α), IL-

6, IL-1β and IL-12] and/or costimulatory molecules. Costimulatory molecules must be upregulated to initiate a pathogen-specific adaptive immune response (161). These responses play a crucial role in eliminating infecting microbes and the resultant instruction of antigen-specific adaptive immune responses.

1.34. TLR-2 and *staphylococcal* infections

TLR-2 is a receptor that recognises Gram-positive bacterial components. TLR-2 can recognise ligands, including lipoarabinomannan, lipoproteins/lipopeptides, peptidoglycan (PGN), glycopolymers lipoteichoic acid (LTA) and zymosan.

Staphylococcal cell membrane components are involved in TLR-2 recognition. Bacterial lipoproteins were first found to trigger TLR-2 in 1999 (162), and lipoproteins are the most potent TLR-2 ligands in *S. aureus,* among other *staphylococcal* components known to activate TLR-2 (163). For example, TLR-2-deficient mice demonstrated impaired production of cytokine in response to *S. aureus* PGN and mycoplasma lipopeptide (164). Moreover, *in vivo* studies of TLR-2- and MyD88-deficient mice have shown higher susceptibility to *S. aureus* infection. This finding was the first to indicate that *S. aureus* is recognised by TLR-2 (165).

Functionally, TLR-2, in association with TLR-1, senses triacyl lipopeptides/proteins (represented by the synthetic tri-acylated lipopeptide, Pam3-Cys- Ser-Lys4, Pam3 CSK4), whereas an association with TLR-6 is necessary for TLR-2 to recognise diacyl lipoproteins (Pam2CSK4 or MALP2) (166, 167). Recent studies have shown that, after internalisation, peptidoglycan co-localizes with both TLR-2 and NOD2 receptors (168). The weak peptidoglycan may help host immune responses by promoting inflammation brought on by other more potent *staphylococcal* ligands (such as lipoproteins). The TLR-1 and TLR-2 ectodomains undergo conformational changes in response to the binding of Pam3CSK4, which leads to the production of a heterodimer; however,

Pam2CSK4 does not support this conformation, and thus TLR-2-TLR-1 could not be activated (169). Additionally, other accessory non-TLR molecules may take on the role of TLR-2 co-receptors (TLR-1 and TLR-6) (170).

1.35. Mesenchymal stem cells and toll-like receptors

According to published studies, isolated MSCs from bone marrow, adipose tissue, or umbilical cord blood exhibit different TLRs expression patterns (171). Depending on their tissue origin, all human MSCs exhibit inconsistencies in their functional properties. Previous studies have examined the difference in TLR function in human MSC from different sources at RNA and protein levels (171, 172).

To date, research findings in both humans and mice have consistently shown that TLR-1, TLR-2, TLR-3, TLR-4, TLR-5, and TLR-6 have high levels of mRNA expression in adipose derived MSCs (AD-MSCs) and bone marrow (bmMSCs). By contrast, TLR-7 to TLR-10 have variable levels of mRNA expression (173).

Previous findings have shown that TLR modulation impacts MSCs immunomodulatory functions, differentiation, migration, and survivability (174). It has been shown that the immunogenic properties of MSCs may be impacted by high levels of specific TLR ligands. For example, TLR-3 and TLR-4 stimulations might provoke pro-inflammatory phenotype in bmMSCs and AD-MSCs; however, Wharton's Jelly mesenchymal stromal cells (WJ-MSCs) are unresponsive to the stimulation of these TLRs (175).

Other studies have shown that TLRs play a vital role in the differentiation capacity of MSCs. TLR activation has inconsistency impacted MSC ability to differentiate into the three mesodermal lineages. For example, both chondrogenesis and osteogenesis of cord blood MSCs (CB-MSCs) could be promoted by TLR-2 activation with Pam3CSK4 and TLR-4 activation with LPS, albeit to a varying degree of differentiation (176). Similarly, it was reported that different types of TLRs have different impact on the level

of osteogenic differentiation of MSCs (176). The activation of LPS and peptidoglycan (PGN) was found to enhance osteogenic differentiation of human AD- MSC, and decreasing it in the presence of CpG oligodeoxynucleotides (CpG-ODN) (177). A different study has shown that stimulation of human amnion-derived mesenchymal stem cells (hAD-MSCs) with TLR-2 and TLR-4 agonists (PGN and LPS, respectively) led to increased expression of ALP, OPN, and BMP-2 in osteogenic differentiation medium (178). However, another group has shown that CpG-ODN stimulated MSCs abolish *OPN* and *RUNX2* expressions substantially. This indicated that osteogenic differentiation is impaired by TLR-9 ligation (179). In addition, TLRs were found to influence MSC survival and apoptosis. Studies involving humans have shown that activation of TLR-2, TLR-3, TLR-4, and TLR-9 in hAD- MSCs induce the downstream TLR signalling pathway molecules such as IL-6 and IL-8 (178). In inflammatory or injured tissues, the expression of these molecules promotes more effective engraftment and increases the chance of AD-MSC survival. On the whole, these discrepancies may be caused by the use of different TLR agonists, incubation times and different MSC sources (180).

Administration of antibiotics and surgical debridement are the only therapeutic options currently available to OM patients, with both strategies having significant shortcomings (181, 182). On the other hand, MSCs recently have shown immunomodulatory response to *S. aureus* infection by releasing anti-inflammatory and antimicrobial peptides which have an additive bacterial killing effect against *S. aureus* suggesting that MSCs can be used as an alternative therapeutic agent in infectious diseases (183). Therefore, better understanding of MSCs role in bone infection is an important factor for development of better remedial strategies for this disease.

1.36. Aims of PhD study

This PhD project will

1. Investigate the role of TLRs in MSCs during infection. Infected MSCs primed with TLR-2 agonist will be infected and monitored for cytokine and anti-bacterial peptide expression.
2. Compare the changes to infected bmMSC-derived osteoblasts osteogenic capacity before and after exposure to MSC-CM, S
3. Develop an *in vitro* explant culture system for bone infection in the presence or absence of exogenous MSCs and evaluate the therapeutic potential of injected MSCs in a model of osteomyelitis. Plugs of human cancellous bone obtained from surgery will be infected and incubated with MSCs.

2. Materials and Methodology

2.1. Materials

2.1.1. Reagents used for MSCs culture and passaging.

Low glucose Dulbecco's Modified Eagle's Medium (DMEM, Merck, D5546), 10% (v/v) foetal bovine serum (FBS, Merck, F7524), 1% penicillin/streptomycin (10,000 units penicillin and 10 mg streptomycin per mL, Merck, Germany, P0781), 1% (v/v) Glutamax (Life Technologies, 35050038), and 10 ng/ml of fibroblast growth factor-2 (FGF-2, PeproTech, London, UK), 1% (v/v) Insulin Transferrin Selenium (ITS, GIBCO, 41400045) were used for MSC culture.

Trypsin-Ethylene Diamine Tetra-Acetic acid (EDTA) solution (Sigma, Dorset, UK) and phosphate-buffered saline with no calcium/no magnesium (PBS, GIBCO, Paisley, Scotland) were used for MSC passaging.

2.1.2. Reagents used for bacterial maintenance.

Mueller Hinton agar (MHA) was used for bacterial streaking for maintaining *S. aureus* growth. The infection medium for MSC was prepared as the MSC culture medium but without adding penicillin/streptomycin.

2.1.3. Reagents used for TLR-2 activation of MSCs.

The following chemicals were used for TLR-2 stimulation of bmMSCs: Pam3CSK4 (10 µg/ml working concentration,1 mg/ml, TOCRIS, UK) and PGN-SA (10 µg/ml working concentration, 5 mg/ml, InvivoGen, UK).

2.1.4. Reagents used for molecular assays.

The following kits were used for the gene expression assay: PureLink® RNA Mini Kit (ThermoFisher Scientific, UK), High-Capacity cDNA Reverse Transcription Kit (ThermoFisher Scientific, UK), and TaqMan® Universal Mix II protocol for the StepOnePlus™ System (ThermoFisher Scientific, UK).

2.1.5. Reagents used for biochemical and protein assays.

Human CTX-I (cross-linked C- telopeptide of type I collagen; ELISA Kit was purchased from NOVUS Biologicals (NBP2-69073, USA).

The following chemicals were used for protein extraction and western blot assay; Radioimmunoprecipitation assay buffer (RIPA Buffer, SIGMA, R0278-50ml), PageRuler™ Plus Pre-stained Protein Ladder, 10 to 250kDa Thermo Scientific™, Catalogue number11832124), Ammonium persulfate (Sigma-Aldrich, Catalogue number A3678) and UltraPure™ TEMED (N, N, N´, N´-tetramethyl ethylenediamine) (ThermoFisher Scientific, Catalogue number 15524010).

2.1.6. Reagents used in western blot.

Gel preparation buffers were obtained from National Diagnostics company (Hessle, UK); ProtoGel 30% (w/v) acrylamide/methylene bis-acrylamide solution (Catalogue number EC-890), ProtoGel Resolving Buffer (4X) (Catalogue number EC-892, 1.5 M Tris-HCl and 0.1% SDS, pH 8.8), ProtoGel Stacking Buffer (Catalogue number EC-893, 0.5 M Tris-HCl and 0.1% SDS, pH 6.8).

Protein detection kit used was LumiGLO® Peroxidase Chemiluminescent Substrate kit (SERAcare KPL, Catalogue number 5430-0040) and CL-XPosure™ Film, 5 x 7 inches (ThermoFisher Scientific, Catalogue number 34090). Transfer Membrane PVDF/Filter Paper Sandwiches, 0.45 µm, 8.5 x 13.5 cm Immobilon®-P PVDF Membrane (Merk, Catalogue number IPVH00010).

The following antibodies were used; mouse anti- metalloproteinase-1 (MMP-1) antibody (abcam, catalogue number ab134184, 1:500), mouse anti- Indoleamine 2, 3-dioxygenase (IDO) antibody (abcam, catalogue number ab55305,1:500), mouse anti-alpha tubulin antibody (Sigma, Gillingham, UK, catalogue number T9026), mouse anti-RUNX2 antibody (abcam, catalogue number ab76956, 1:800), mouse anti-osteocalcin antibody (OC4-30, Insight Biotechnology, catalogue number GTX13418. 1:400),

secondary anti-mouse antibody (catalogue number ab97023 abcam, USA), rabbit anti-*S. aureus* antibody (4 µg/ml working concentration, ab20920, abcam) and Alexa fluor 594 anti-rabbit IgG secondary antibody (Invitrogen, UK)

2.2. Methodology

2.2.1. Human mesenchymal stem cell isolation

MSCs were isolated from samples of human bone marrow surgically extracted from patients undergoing knee replacement surgery and obtained under NHS ethics approval. MSCs were prepared following a protocol developed at the University of Bristol regenerative medicine laboratory and stored in liquid nitrogen. To avoid sample clotting, bone marrow samples were collected in sterile tubes containing heparin. One ml of bone marrow aspirate was dispensed in T175 flasks containing 25 ml of low-glucose DMEM supplemented with 10% (v/v) FBS, 1% penicillin/streptomycin, 1% (v/v) Glutamax and 10 ng/ml FGF-2 and incubated in 5% CO_2 and 95% humidity at 37°C for 4 days or until reaching confluency.

2.2.2. Human mesenchymal stem cell preparation

The protocol followed to prepare bmMSCs is based on regular medium change and trypsinisation for cell (sub-)culturing after they reach confluency. First, MSCs samples were brought from the liquid nitrogen supply and thawed in a 37°C water bath. Immediately after thawing, cells were transferred to 50 ml falcon tubes containing 10 ml of prewarmed DMEM media to reduce the shock to the cells. Then, the mixture was centrifuged at 1500 *g* for five minutes and the supernatant was discarded to remove any remaining freezing mix (10% DMSO: 90% FBS).

2.2.3. Human mesenchymal stem cell primary culture

MSCs were cultured in growth DMEM supplemented with 10% (v/v) FBS, 1% (v/v) Glutamax and 1 % penicillin/streptomycin. During culturing, FGF-2 (10 ng/ml) was added to enhance MSC growth. MSCs were cultured in T175 flasks and incubated with 5% CO_2 and 95% humidity at 37°C. The cells were checked frequently under an

inverted light microscope to check for their viability and morphology, and the medium was replenished every 2-3 days.

2.2.4. Human mesenchymal stem cell passaging

Once MSCs reached 70-80% confluency, they were harvested for further passaging/subculture by trypsinisation. During passaging, media were discarded, and the cells were washed using PBS, then approximately 7 ml of EDTA solution was added and the T175 flasks were incubated for 3-5 minutes at 37°C. After the flasks were removed from the incubator, their sides were tapped rapidly to ensure that the cells detach from the flask surface. Twenty-one ml of DMEM were added to the T175 flasks as FBS in the media would inhibit further action of trypsin. Next, the cell mixture was aspirated from the T175 flask, transferred into a conical 50 ml tube, and centrifuged at 1500 *g* for five minutes. The supernatant was discarded, and the pellet resuspended in fresh medium. 10 µl of suspension was transferred to a haemocytometer and cells were counted using a light microscope.

2.2.5. Bacteria preparation and culturing

This study used a wildtype *S. aureus* 8325.4 strain, this strain was kindly gifted by Dr Andrew Edwards, Imperial College London (184). *S. aureus* strains were stored as glycerol stocks and streaked at a Mueller Hinton agar (MHA) plate before being cultured at 37°C and 5% CO_2 incubator overnight. One day after inoculation, a 10-ml disposable loop was used to collect colonies of *S. aureus* from the MHA plate; these were transferred into 2 ml of PBS and gently suspended. To measure the optical density of the diluted bacterial suspension, 0.1 ml of the bacterial suspension was diluted in 0.9 ml of PBS and then transferred into a spectrophotometer cuvette. The absorbance was read by a light spectrophotometer at 600 nm. The following formula was used to calculate the CFU/ml: OD (reading from the spectrophotometer) x 10

(dilution factor) x $2x10^9$ (optical density of 1 at 600 nm is equal to 2x109 CFU for *S. aureus*) (185).

2.2.6. Multiplicity of infection

The multiplicity of infection (MOI) is the ratio of the number of infectious bacteria divided by the number of cells present in that well. The volume and number of bacteria per ml was derived according to the desired MOI (e.g., 10,100); the number of cells at confluency; the type of vessels to be infected; the volume of infection media required for infection. To calculate *S. aureus* suspension of MOI10, the number of cells in the well/flasks was estimated and then multiplied by 10 to get the required MOI10. The calculation for the number of *S. aureus* in CFU/ml detailed in the previous section (2.2.5) and then divided by the required number of bacteria.

2.2.7. RNA extraction

RNA was extracted from cells as described in the protocol of the PureLink® RNA Mini Kit. Briefly, cells were washed with PBS, and a volume of 1:100 lysis solution (containing β-mercaptoethanol and washing buffer) was added to the wells. The cells were lysed by gently patting the plate and continuously scraping the cells with yellow tips (200 µl) for five minutes. The cell lysate was transferred to RNase-free Eppendorf tubes and stored at -80°C or subjected to needle homogenisation 8-10 times by passing the cell lysate through a 19-gauge needle. An equal volume of 70% (v/v) ethanol was added to each homogenised cell lysate and mixed through a vortex. A 700 µl amount of the mixture was transferred into a spin cartridge and centrifuged for 15 seconds at 12,000 *g* at room temperature. The flow through was discarded; this step was repeated until all the remaining samples were processed. The spin cartridge was then washed with Buffer I and Buffer II consecutively before being transferred into a clean collection tub. A 50µl of elution RNase-free water was added to the centre of the spin cartridge and incubated for one minute. This was followed by 2 minutes

centrifugation (at 12000 *g*) to elute the RNA from the membrane to the recovery tube. The extracted RNA was measured for concentration and purification, and this was either used for cDNA synthesis or stored at -80°C. RNA concentration was measured using a Nanophotometer® (Implen, Germany) and RNA purification was assessed by calculating the A280/260 ratio. A ratio of ≥1.8 indicates good RNA purity to proceed to cDNA synthesis step.

2.2.8. cDNA synthesis

cDNA was prepared using the High-Capacity cDNA Reverse Transcription Kit (ThermoFisher Scientific, UK) protocol. For each RT-PCR reaction, RNA samples were normalised to 20 ng/µl in RNase-free water up to 20 µl. This was followed by the addition of reaction cDNA master mix (20 µl), giving a total volume of 40 µl/reaction. RT-PCR Master mix was prepared by adding 4 µl of RT buffer, 1.6 µl of 25 dNTP, 4 µl 10x RT random primers, 8.4 µl RNase-free water and 2 µl MultiScribe Reverse Transcriptase. The reaction was mixed gently using a vortex to ensure uniform distribution of the contents before being transferred into a thermocycling machine (Bio-Rad, UK). The RT-PCR thermocycler was adjusted to the following parameters: 25°C for 10 minutes, 37°C for 120 minutes and then 85°C for five minutes. The last step was to cool down the samples by decreasing the temperature to 4°C to conserve the cDNA integrity.

2.2.9. qPCR assay

To determine the gene expression level, a real-time qPCR assay was performed using the TaqMan® Universal Mix II protocol for the StepOnePlus™ System. Each qPCR reaction (1X) consisted of a mixture of TaqMan® Universal Mix II, TaqMan primers, cDNA template and RNase-free water. The cDNA mixture (2 µl of cDNA and 2.5 µl of RNase-free water) and gene master mix (5 µl of master mix and 0.5 µl of gene assay) were prepared in two separate tubes according to the protocol followed.

A volume of 10 µl of PCR reaction mixture containing 5.5 µl gene master mix and 4.5 µl cDNA mixture was transferred into corresponding wells of a 96-well qPCR plate. During the qPCR run, amplification was performed during thermocycling with an initial denaturation step at 95°C for 30 seconds, followed by 40 cycles of denaturation at 95°C for 3-5 seconds, then an annealing/extension step at 60°C for 60 seconds. The ΔΔCT method was used to determine the relative gene expression compared to the control group and expressed as a fold change.

The relative expression of the genes of interest (GOI) compared to the CT mean of their corresponding housekeeping genes (*ACTNB* and *B2M*) was calculated by using (ΔΔCt) method: ΔΔCt = (Ct gene of interest − Ct housekeeping genes). Finally, the experiment calculated the fold change by using comparative Ct method ($2^{-\Delta\Delta Ct}$). Fold change was compared between different conditions employing the One-Way ANOVA test.

2.2.10. Western blotting

2.2.11. Protein lysate preparation

Protein lysis buffer was prepared by adding 700 µl of proteinase solutions (inhibitors phosphatase inhibitor (1/100) and protease inhibitor cocktail (1/100) into radioimmunoprecipitation assay (RIPA) buffer.

The media were removed to prepare protein lysates from cells in the 12-well plate, and the cells were washed 1X with ice-cold PBS. 70 µl of freshly prepared lysis buffer were added to the well and mixed up and down thoroughly. The cell lysate was then transferred into Eppendorf tubes, and the plates were checked under the microscope to ensure the complete removal of cell lysate. Then, the tubes were incubated for 30 minutes with constant agitation in the rotator in the cold room followed by centrifugation at 12000 *g* for 5 minutes at 4°C. The supernatant was transferred to

labelled tubes and stored at –20°C, and the pellet was discarded. All protein lysis steps were conducted on ice.

2.2.12. Gel electrophoresis and protein transfer

Mini-Protean 3 Electrophoresis Cells (Bio-Rad, Hemel Hempstead, UK) were used to cast 7.5–15% acrylamide resolving gels and 4.5% stacking gels, using 1.5mm spacers. According to the size of the proteins, different percentages of acrylamide were formulated to achieve good resolution for different molecular weight ranges of protein bands. Table 2-1 shows the proportion and volume of the acrylamide and buffers used to prepare the resolving and stacking buffers.

Table 2-1 Composition of SDS-PAGE gels

% Acrylamide gel	15%	12.5%	10%	7.5%	Stack (4.5%)
Approximate Protein Size	<30 kDa	30-50 kDa	50-100 kDa	>100 kDa	
30% Acrylamide/1% Bis	8.7 ml	7.3 ml	5.8 ml	4.4 ml	1.2 ml
Resolving Buffer (8.8)	4.4 ml	4.4 ml	4.4 ml	4.4 ml	
Stack Buffer pH (6.8)					2.0 ml
Distilled Water	4.4 ml	5.8 ml	7.3 ml	8.7 ml	4.4 ml
Ammonium Persulphate (1 g in 1 ml DW)	110 µl	110 µl	110 µl	110 µl	58 µl
TEMED	3.6 µl	3.6 µl	3.6 µl	3.6 µl	1.8 µl

At the electrophoresis step, the gel was constructed with resolving gels beneath the stacking gels. Once the gels solidified, the boiled protein samples mixed with 5X Laemmli Buffer (Table 2.2) loaded into the wells of the gel alongside a Protein ladder. To denature the sample, samples in a loading buffer were heated at 95 –100°C for 5 min. The prepared hand-cast gel was placed in the inner tank and immersed in running

buffer (Table 2-2) and the inner tank was placed within an outer running tank and connected to the power.

Protein electrophoresis was primarily run at 80 V for approximately 15 minutes allowing the samples to move through the stack and reach the resolving gel. The voltage was raised to 180V for an hour. The electrophoresis process was terminated prior to the dye front leaving the gel. The segregated proteins were transferred from the gel onto polyvinylidene difluoride (PVDF, Invitrolon™). The blotting sandwich was assembled by placing one piece of foam sponge on the black side of the cassette holder followed by adding 3-4 sheets of filter paper (dipped into the transfer buffer), followed by placing the gel with resolved proteins over it (the stacking part was removed). A PVDF membrane sheet was placed over the gel covered using another pre-soaked sheet of filter paper and foam pad.

The blotting apparatus was positioned inside the tank filled with transfer buffer with an ice block placed beside the cassette. The transfer system was subjected to 350 mA for 1 hour and 15 minutes. Following the transfer step, the PVDF membrane was soaked int blocking solution (see table 2-2) for a minimum of 60 minutes at room temperature with gentle rocking to reduce background noise. The proteins in the membrane were probed by incubating the membrane with primary antibody diluted at a specific concentration in 0.5% (w/v) milk dilution buffer overnight on a rotator in the cold room. Subsequently, the membrane was washed and incubated with matching secondary antibody for 1 hour at room temperature with gentle rocking.

2.2.13. Protein detection

Protein bands were detected using the LumiGLO Peroxidase Chemiluminescence Substrate kit. LumiGLO is a luminol-based chemiluminescent substrate constructed for detection of HRP-labelled antibodies. After washing, the membrane was coated

with an equal amount of solution A and solution B for approximately 3 minutes. The light emission from LumiGLO reaches maximum intensity within five minutes and lasts for 1-2 hours. The membrane was placed in transparent plastic and exposed to three of X-ray films inside a lightproof cassette. A Compact X4 Film Processor (XOgraph Imaging Systems Ltd., Stonehouse, UK) was used to develop the light-sensitive films, which were exposed according to the signal strength.

Table 2-2 Buffers and solutions for western blot

Buffer	Components
5X Laemmli Buffer	10% w/v SDS, 5% v/v 2-mercapto-ethanol, 50% v/v glycerol, 0.1% w/v bromophenol blue, 312.5 mM Tris HCl, pH 6.8
Running Buffer	192mM glycine, 25mM Tris, 0.1% (w/v) SDS
Transfer Buffer	192mM glycine, 25mM Tris, 20% (v/v) methanol
Tris-Buffered Saline -Tween 20 (TBS-T)	50 mM Tris.HCl, pH 7.4, 150 mM sodium chloride, 0.1% Tween 20
0.5% Milk Blocking Buffer	0.5% (w/v) non-fat milk powder in TBS-T

3. Chapter Three

Impact of TLR-2 stimulation on human mesenchymal stem cells antimicrobial capacity.

3.1. An overview

OM is bone tissue inflammation that typically arises due to bacterial infection, and it is highly detrimental to bone structure (97). It has a high chronicity and recurrence rate, even when treated appropriately (186). Current strategies for addressing orthopaedic infections such as surgical removal of necrotic tissues and antibiotic administration to eradicate bacteria to facilitate healing and thereby decrease the pain of inflammation, re-establish function in infected joints, and consolidate fractures, whilst restricting OM insofar as possible (85, 97). However, antibiotics that are typically utilised in the clinical management of bone-associated infections are generally ineffective in driving bone regeneration or differentiation (187). An unsuccessful response to current treatment can also due to changing bacterial isolation patterns and susceptibilities as time passes, with a growing rate of multidrug resistance (187). Hence, it is essential to develop innovative strategies and effective antibacterial medications to address infections.

On the other hand, MSCs are crucial contributors in normal tissue regeneration. These potential cells promote healing via angiogenesis, epithelialization, build-up of collagen, development of granulation tissue, and discharge of inflammatory mediators (188). There is increasing evidence to indicates that besides their regenerative characteristics, MSCs and their paracrine secretome also have antimicrobial and anti-inflammatory traits in response to infectious conditions such as OM. The antimicrobial peptides released by MSCs result in bacterial cell membranes depolarisation and bacterial growth inhibition. These effects provide further benefits over conventional antibiotic therapy by reducing inflammation combined with infection, accelerating the health improvement time, relieving pain, and reducing sequelae linked with infection

(174, 189, 190). Therefore, MSCs appear to be advantageous as alternative therapies to antibiotics because antimicrobial resistance does not develop (191, 192).

One mechanism by which MSCs play a role in the inflammatory response to infection is through the expression of TLRs and antimicrobial potential activity (174, 190). Recent studies demonstrated that cellular properties of MSCs, including stimulation of TLRs and inducing anti-microbial peptides (AMPs), have transformed the explorations of the innate immune system (193). The expression of TLRs on MSCs can be an alternative and more effective approach MSCs contribute to addressing the inflammatory response to infection (194). However, there is still much to elucidate about the mechanism of TLRs activation and AMPs secretion.

Recent studies have discovered that activation of MSCs using TLRs ligands can amplify their anti-bacterial properties. Johnson *et al.* demonstrated that activated MSCs with TLR-3 ligand polyinosinic: polycytidylic acid (pIC) were more effective in decreasing bacterial load than antibiotics alone or MSCs alone in a mouse model with chronic implant infection and a canine model with wound infections (195, 196). Moreover, some studies have shown that AMP gene expression can be induced in various cells following TLR-2 stimulation both *in vitro* and *in vivo* models. Kumar A *et al.* have reported that intravitreal injections of Pam3Cys (a synthetic ligand of TLR-2) in a mouse model of *S. aureus*-induced endophthalmitis has induced *CRAMP* gene expression (LL-37 mouse version antimicrobial gene) which led to the greater bacterial killing and lower *S. aureus* pathogenesis (197).

These early findings support a more comprehensive examination of human MSCs immune/antibacterial properties upon activation of these receptors. This understanding could aid with enhancing the immune properties of MSCs towards the treatment of OM.

In this chapter, it hypothesised herein that activation of MSCs would increase the secretion of cytokines and antimicrobial elements associated with recruiting natural immune effector cells, improve bacterial extermination, and upregulate the expression of the antimicrobial peptides, ultimately increasing the overall bactericidal impact.

3.2. Aim

The work covered in this chapter aimed investigate the molecular mechanism of TLR-2 receptor-stimulated bmMSCs in initiating antibacterial activity against *S. aureus* infection *in vitro*. It hypothesised that stimulating TLR-2 receptors using synthetic agonists (Pam3CSK4 or PGN-SA) might modulate bmMSCs and enhance their secretion of anti-inflammatory cytokines and antimicrobial peptides, which may eventually improve clearance of *S. aureus*.

3.3. Objectives of the study

1. Stimulate bmMSCs using synthetic TLR-2 agonists at various concentrations and different incubation times and measure the viability of bmMSCs via an Alamar Blue assay.
2. Infect bmMSCs following TLR-2 stimulation with TLR-2 agonists and measure the impact of the stimulation on the bacterial number using CFU count assay.
3. Stimulate bmMSCs with TLR-2 agonists and collect the conditioned media (TLR-2-CM) and subsequently measure the impact of TLR-2-CM on bacterial viability using Alamar Blue and CFU count assays.
4. Investigate bmMSCs gene expression in response to TLR-2 stimulation and during infection by measuring gene expression of antimicrobial peptides, IDO, and anti-inflammatory cytokines.

3.4. Methods

3.4.1. Cytotoxic effect of TLR-2 agonists on bacterial viability using an Alamar Blue assay.

S. aureus bacterial suspension was prepared as MOI10 in DMEM (assuming that human bmMSCs were seeded in 96 well plates at a density of 5000 cells/cm2 and reached confluency). Different concentrations of Pam3CSK4 (0.1, 1 and 10 µg/ml) and PGN-SA (0.1, 1, 10 and 20 µg/ml) were prepared in DMEM.

A volume of 10 µl of bacterial suspension was mixed with 190 µl of different concentrations of TLR-2 agonists Pam3CSK4 or PGN-SA using 96-wells flat-bottom plates. The plate was incubated at 37°C for 1, 4, and 24 hours. At the end of each incubation time, an Alamar Blue assay was performed using Resazurin salt.

Resazurin solution was prepared by dissolving 337.5 mg of resazurin powder in distilled water in 50 ml falcon tube. The tube was given a proper vortex mixer to ensure homogeneity. The mixture is sterilised using 0.2 um syringe filter (Sartorius 16532-K). The working solution for Resazurin dye was prepared by 1:100 dilution of the prepared stock solution using DMEM. The plate then was incubated in in dark for 2 hours. Then, the plate was read using a plate reader. The change in fluorescence intensity was measured using a BIOTEK plate reader with fluorescence monitored at a 530–560 nm excitation wavelength and 590 nm emission wavelength. The percentage difference between the treated and control cells was calculated according to the manufacturer's instructions. The formula is as follows:

$$\text{Percentage difference between treated and control cells (\%)} = \frac{\text{FI 590 of treated agent}}{\text{FI 590 of untreated (control)}} \times 100$$

Where: FI 590 is the fluoresce intensity at 590 nm emission (560 nm excitation).

3.4.2. Viability of bmMSCs following TLR-2 stimulation Alamar Blue using an Alamar Blue assay.

bmMSCs were cultured in 96-well plates at a density of 5000 cells/cm^2 until confluency was reached (approximately 72 hours) using 96-wells flat-bottom plates. Different concentrations of Pam3CSK4 (0.1, 1 and 10 µg/ml) and PGN-SA (0.1, 1, 10 and 20 µg/ml) were prepared in DMEM. The media was aspirated from cells and replaced with 200 µl of different concentrations of TLR-2 agonists Pam3CSK4 or PGN-SA. The bmMSCs were incubated at 37°C with TLR-2 agonists for 1, 4, and 24 hours. At the end of the incubation, the media was removed, and 150 µl of a Resazurin dye was added to each well and incubated at 37°C for 1 h in the dark. The change in fluorescence intensity was measured using a BIOTEK plate reader Alamar Blue viability assay of bmMSCs following TLR-2 stimulation at a 530–560 nm excitation wavelength and 590 nm emission wavelength. The percentage difference between the treated and control cells was calculated according to the manufacturer's instructions. The formula is as follows:

$$\text{Percentage difference between treated and control cells (\%)} = \frac{\text{FI 590 of treated agent}}{\text{FI 590 of untreated (control)}} \times 100$$

Where: FI 590 is the fluorescent intensity at 590 nm emission (560 nm excitation).

3.4.3. The impact of TLR-2 stimulated and infected bmMSCs on bacterial viability by CFU assay.

bmMSCs were seeded in 24-well plate at a density of 5,000 cells/cm^2. After confluency (usually within 3 days), the media was replaced with 500 µl of antibiotic-free media supplemented with 10 µg/ml of TLR-2 agonists to the corresponding wells, then the plate was incubated at 37°C for a period of 24 hours. Cells were washed and a volume of 500 µl of *S. aureus* suspension at MOI10 was inoculated into the corresponding

wells. The plate was incubated at 37°C and 5% CO_2 for 60 minutes. Control wells include normal bmMSCs or infected bmMSCs without TLR-2 stimulation. At the end of the infection period, cells were washed three times to remove unbound bacteria; then, the cells were incubated in serum-free media for 24 hours.

The same experiment was conducted omitting the pre-infection washing step (the media containing TLR-2 agonists) and the infection step was carried out with *S. aureus* without washing step between stimulation and infection.

After 24 hours of incubation with serum-free media, the media was discarded, and 60 µl of 1% saponin was added to each well and incubated for 10 minutes at 37°C. The wells were scraped using yellow tips, and 20 µl of cell suspension was transferred into a 96-well round-bottomed plates for serial dilution (1 in 10 dilution factor) across 5 wells. Subsequently, 10 µl of the final three wells was inoculated onto an MHA plate and incubated for 24 hours at 37°C. Finally, the number of bacterial colonies were counted using a colony counter and the results were plotted on an Excel sheet.

3.4.4. The impact of TLR-2-CM on bacterial viability by Alamar Blue assay.

bmMSCs were seeded in 24-well plate at a density of 5,000 cells/cm^2 until achieving confluency (usually within 72 hours). Subsequently, the media was removed and replaced with 500 µl of antibiotic-free media supplemented with 10 µg/ml of TLR-2 agonists (Pam3CSK4 or PGN-SA) or antibiotic-free DMEM (control wells). The plate was incubated for 24 hours at 37°C. The supernatant was collected in a sterile tube. This supernatant is referred to as TLR-2 conditioned media (TLR-2-CM) or MSCs conditioned media (MSC-CM).

The next step was carried out by adding 190 µl of the prepared conditioned media and incubated with 10 µl of *S. aureus* suspension (prepared as MOI10, see 3.4.1) in the 96-wells plate. Control included wells containing bacteria with normal DMEM. The

plate was incubated for 1 hour or 24 hours at 37°C. At the end of incubation time, an Alamar Blue assay was carried out, as described in section 3.4.1.

3.4.5. The impact of TLR-2-CM on bacterial viability by CFU assay

A volume of 190 µl of either TLR-2-CM or MSC-CM (as detailed in section 3.4.4) was incubated with 10 µl of bacterial suspension of *S. aureus* in a 96-wells plate. Control wells included wells containing bacteria with only normal DMEM. The plate was incubated for 1 hour or 24 hours at 37°C. At the end of the infection time, 20 µl of each condition was mixed with 180 µl of PBS in a 96-wells round-bottom plate for serial dilution (1 in 10 dilution factor) across 5 wells. Subsequently, 10 µl of each well (typically the final three wells) was inoculated to an MHA plate and incubated overnight at 37°C. CFU counting of viable *S. aureus* colonies using a plate counter was carried out and the results were plotted on an Excel sheet.

3.4.6. Gene expression of cytokine, *IDO* and antimicrobial peptide in infection of bmMSCs following TLR-2 stimulation

bmMSCs were seeded in 24-wells plate at a density of 5,000 cells/cm^2 at 37°C in 5% CO_2 until the cells reached confluency. Cells were then stimulated with the TLR-2 agonists Pam3CSK4 or PGN-SA at 10 µg/ml for 24 hours. An infection assay was carried out at MOI10 for 1 hour. Cells were washed three times with DMEM media and incubated in a serum-free medium for 24 hours. At the end of infection, bmMSCs were washed once with PBS, and 100 µl of RNA lysis solution was added to the wells. The cells were lysed by gently tapping the plate and swirling the lysis buffer around the plate surface for 5 minutes. The cell lysate was transferred to Eppendorf tubes, and stored at -80°C. Subsequently, *LL-37, hBD-2, IDO, CCL2, IL-6, and IL-8* gene expression analysis was performed following the qPCR protocol.

3.5. Results

3.5.1. The effect of TLR-2 agonists on the viability of bmMSCs.

This experiment aimed to analyse the cytotoxic effect of applying synthetic TLR-2 agonists on human bmMSCs. This was accomplished by employing Alamar Blue assay, which is used to measure metabolic activity of live cells. A higher rate of absorbance corresponds to greater metabolic activity. Thus, bmMSCs were incubated with the TLR-2 agonist Pam3CSK4 or PGN-SA for 1, 4, and 24 hours, then Alamar Blue assay was performed.

Our results demonstrated that TLR-2 agonists Pam3CSK4 (at the designated concentrations) did not exhibit cytotoxic effect against bmMSCs viability when cells were incubated with Pam3CSK4 at 1 and 24 hours. However, there was a significant reduction in the viability of bmMSCs when cells were incubated with Pam3CSK4 for 4 hours. When bmMSCs were incubated with Pam3CSK4 at the higher concentration of 10 µg/ml, the viability of cells was decreased by approximately 10% at 4 hours ($p=0.0087$ (*)), (Figure 3-1-A).

The relative viability of bmMSCs was not affected when cells were treated with PGN-SA at lower concentration (0.1, 1 and 10 µg/ml) for 1, 4 or 24 hours, compared to untreated cells. When the concentration of PGN-SA was increased to 20 µg/ml, the viability of cells significantly reduced by approximately 10% at 1 ($p=0.279$ (*)), 4 ($p=0.0279$ (*)) and 24 ($p=0.0351$(*)) hours compared to untreated control groups, indicating a cytotoxic effect of PGN-SA at higher concentrations (Figure 3-1-B).

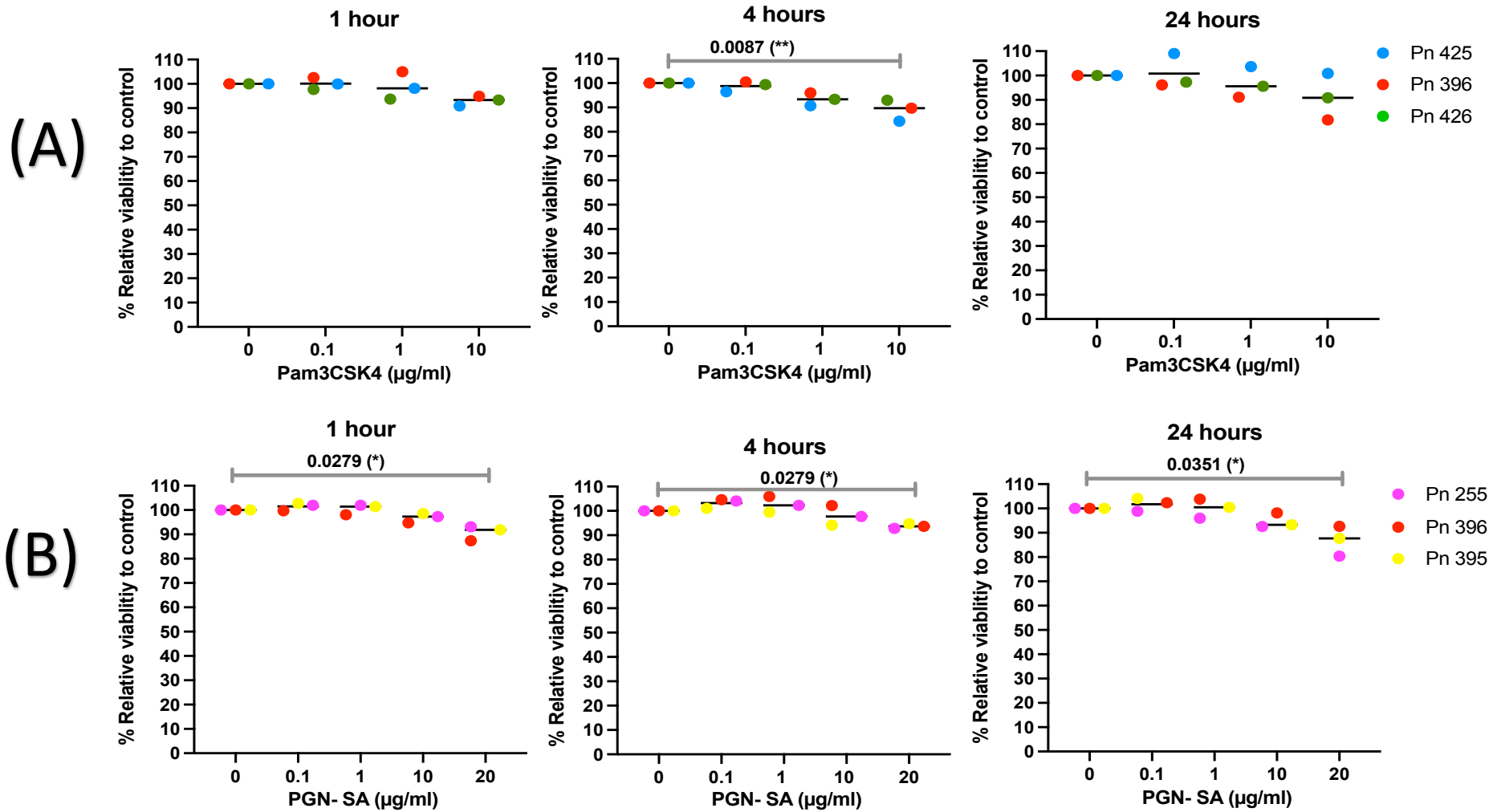

Figure 3-1: Cytotoxic effect of TLR-2 agonists (Pam3CSK4 or PGN-SA) on bmMSCs. Confluent bmMSCs in a 96 wells flat bottom plate were incubated with different concentrations of Pam3CSK4 (A) or PGN-SA (B) for 1,4, and 24 hours. At the end of incubation, cells were mixed with Alamar Blue dye (Resazurin). The fluorescence change was measured via a plate reader at excitation 545 nm and emission 590nm. The percent relative viability of treated to control wells (untreated cells) was calculated. The coloured symbols represent three individual patient samples (n=3). Bars indicates the mean. *** = $p \leq 0.001$, ** = $p \leq 0.01$, * = $p \leq 0.05$.

1.1.1. The effect of TLR-2 agonists on bacterial viability with Alamar Blue assay

This experiment aimed to examine the cytotoxic effects of the TLR-2 agonists on bacterial viability. The goal was to ascertain whether these synthetic chemicals could kill bacteria directly. To accomplish this, different concentrations of TLR-2 agonists were incubated with *S. aureus* for 1 and 24 hours.

The results showed that there was no cytotoxic effect of incubation of TLR-2 agonists on *S. aureus* viability at 1-hour incubation (Figure 3-2). The percentage of relative viability of bacteria (compared to normal) was close to that of 100% of the background level as the normal cells.

On the other hand, there was a fluctuating change in the percentage difference at 24 hours post-TLR-2 stimulation. At low concentrations of Pam3CSK4 and PGN-SA (0.1 and 10 µg/ml), there was an induced bacterial cell death as there was a reduction in fluoresce intensity of bacterial cells reduced by approximately 10% to 20%. An exception was the group incubated at 10 µg/ml for 24 hours where metabolic activity of *S. aureus* increased to 120% (Figure 3-2).

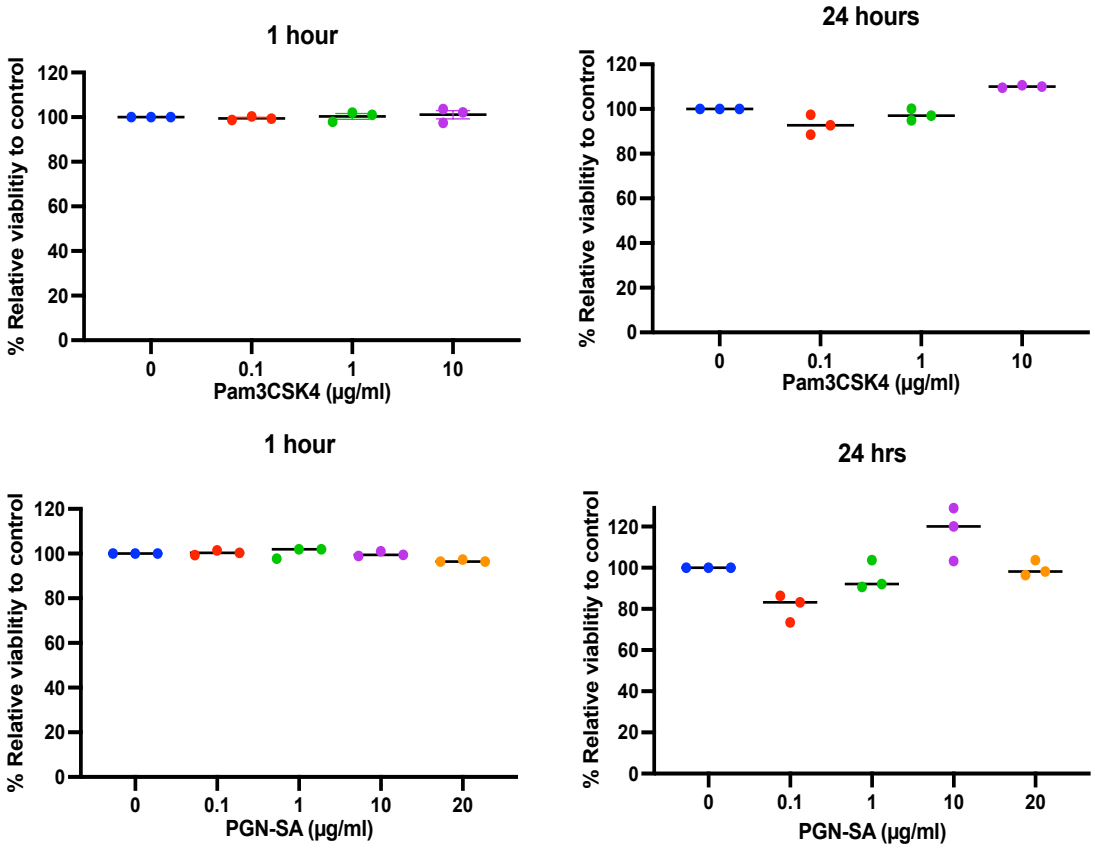

Figure 3-2 Cytotoxic effect of TLR-2 agonists (Pam3CSK4 or PGN-SA) on *S. aureus* viability. Different concentrations of Pam3CSK4 or PGN-SA were incubated for 1 and 24 hours with *S. aureus*. At the end of the incubation, cells were mixed with an Alamar Blue dye (Resazurin salt). The fluorescence change was measured via a plate reader at an excitation of 545 nm and an emission of 590 nm. The percent relative viability of treated to control wells (untreated cells) was calculated. The coloured dots represent three technical repeats. Bars indicate the mean, n=1.

3.5.2. The impact of TLR-2-stimulated bmMSCs conditioned media on bacterial viability

This experiment aimed to investigate the effect of TLR-2-stimulated bmMSCs on bacterial count of *S. aureus.* Thus, normal bmMSCs were preincubated with the TLR-2 agonists Pam3CSK4 or PGN-SA at 10 µg/ml for 24 hours. Cells were washed and infected with *S. aureus* at MOI 10, and the number of bacterial colonies were counted.

The result showed that bmMSCs had less *S. aureus* colonies recovered than from TLR-2 stimulated bmMSCs than unstimulated infected bmMSCs.

There was $5x10^8$ CFU/ml of *S. aureus* recovered from unstimulated infected bmMSCs compared to $4x10^8$ and $2.5x10^8$ CFU/ml at stimulated bmMSCs with Pam3CSK4 or PGN-SA, respectively (Figure 3-3). Although there was a reduction in bacterial count in infected bmMSCs stimulated with Pam3CSK4, that reduction was not statistically significant. On the other hand, there was a statically significant reduction of *S. aureus* colonies when infected bmMSCs cells were pre-treated with PGN-SA, with a p-value of 0.0327(*). These results suggested that there was a stimulated cellular response that enhanced the antibacterial activity of human MSCs by PGN-SA agonists leading to greater bacterial clearance.

In another experiment setting, bmMSCs were pre-treated with TLR-2 agonists for 24 hours and then infected without a prior washing step. For this experiment, the numbers of viable bacteria significantly decreased when the MSCs were treated with Pam3CSK4 or PGN-SA, with a p-value of 0.0003 (***) and 0.0001 (***) respectively. The viable bacteria recovered from the unstimulated infected MSCs was approximately $2x10^8$ CFU/ml. There was a noticeable reduction of *S. aureus* colonies counted ($1x10^8$ CFU/ml and $8.7\ x10^7$ CFU/ml) after bmMSCs were stimulated with Pam3CSK4 or PGN-SA, respectively.

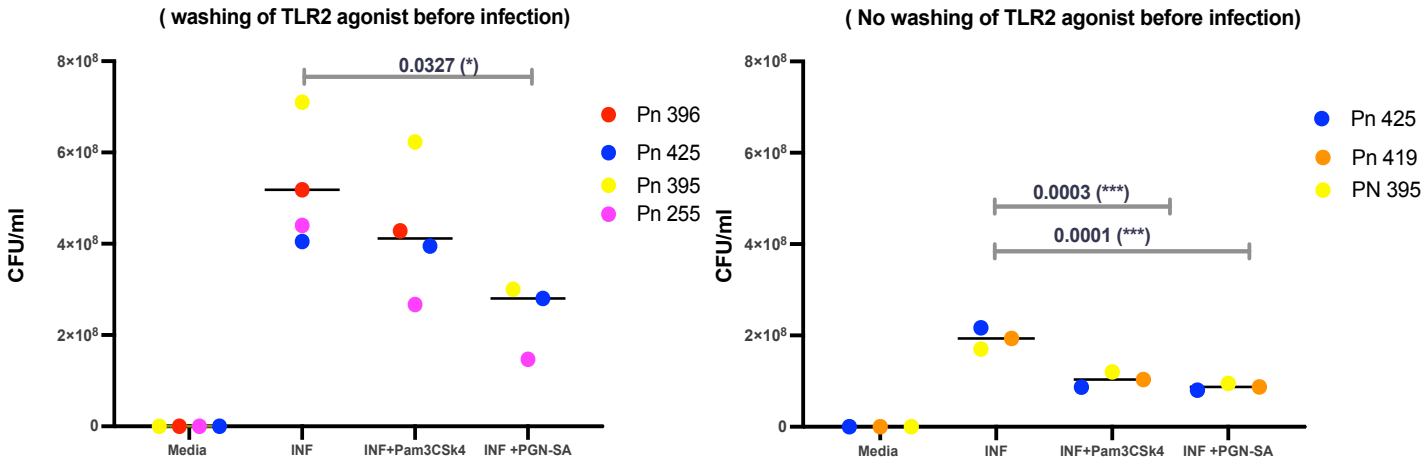

Figure 3-3: Total bacterial count (CFU/ml) of *S. aureus* recovered from infected bmMSCs after TLR-2 stimulation. Confluent bmMSCs in 24-well plates were stimulated with 10 µg/ml of TLR-2 agonists (Pam3CSK4 or PGN-SA) for 24 hours. The cells were then either washed and subsequently infected with *S. aureus* or directly infected with *S. aureus* (no washing prior to infection). The infection time was 1 hour. Cells were washed followed by bmMSCs incubation for 24 hours in serum-free media. Serial dilution was carried out and inculcated at MHA plates overnight. CFU count was then performed. INF= infected cells. The coloured dots represent biological repeats. Bars indicate the mean. (n = 3 or 4). *** = $p \leq 0.001$, ** = $p \leq 0.01$, * = $p \leq 0.05$.

3.5.3. The impact of TLR-2-CM on bacterial viability

This experiment aimed to determine whether TLR-2 stimulated bmMSCs secreted factors impact the bacterial viability. Thus, *S. aureus* was cultured in TLR-2-CM or MSC-CM for 1 or 24 hours before measuring the effect on bacterial viability using Alamar blue. The bacterial viability of *S. aureus* after 24 hours of incubation with different conditioned media showed significant inhibition when the bacteria were exposed to MSC-CM and TLR-2-CM. These findings suggest that the reduction of *S. aureus* growth was due to factors released from MSCs alone (unstimulated) (Figure 3-4).

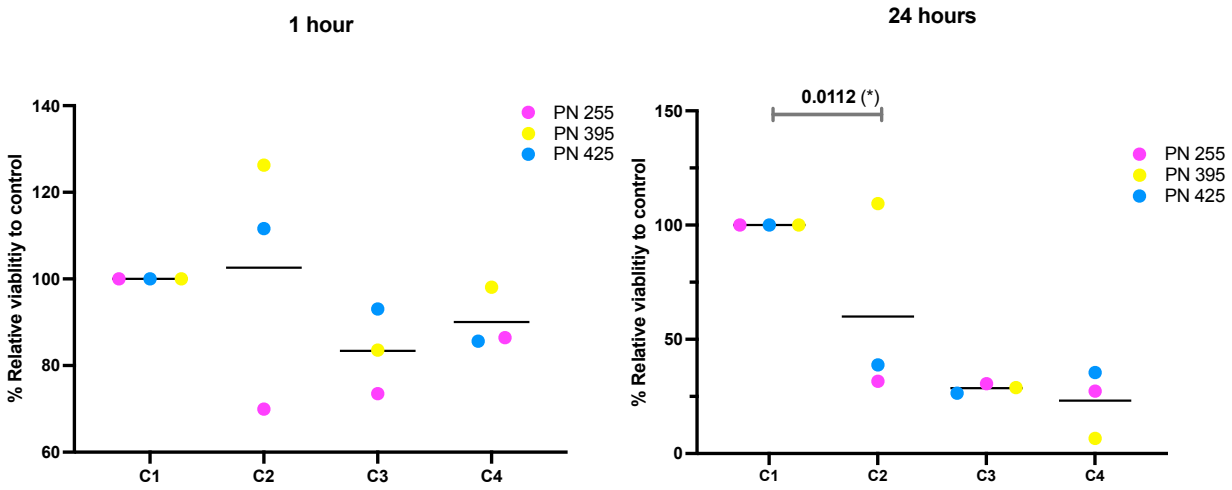

Figure 3-4: The impact of TLR-2-CM on bacterial viability by Alamar blue. *S. aureus* suspension was incubated with TLR-2-CM or MSC-CM in 96 wells plate for 1 or 24 hours. Then, bacteria were mixed with Alamar Blue dye (Resazurin) and incubated for 1 hour in the dark. The fluorescence change was measured by plate reader at excitation of 545nm and emission of 590nm. The percentage difference in the reduction of Alamar Blue between treated and control wells (untreated cells) was calculated. C1= only *S. aureus*, C2= conditioned media of MSCs, C3= conditioned media of MSCs stimulated with Pam3Ck4, C4= conditioned media of MSCs stimulated with PGN-SA. The coloured dots represent three biological repeats. Bars indicate the mean, n=3. *** = $p \leq 0.001$, ** = $p \leq 0.01$, * = $p \leq 0.05$.

3.5.4. The impact of TLR-2-CM on bacterial viability using CFU Assay

We investigated the impact of TLR-2-CM on viable bacteria counts by CFU count assay. We found there is no effect on the relative bacterial count during early incubation (1 hour). However, after 24 hours post-infection, we found that the relative bacterial growth was significantly inhibited in the presence of MSC-CM, and TLR-2-CM when compared to conditioned media of unstimulated MSCs (Figure 3-5).

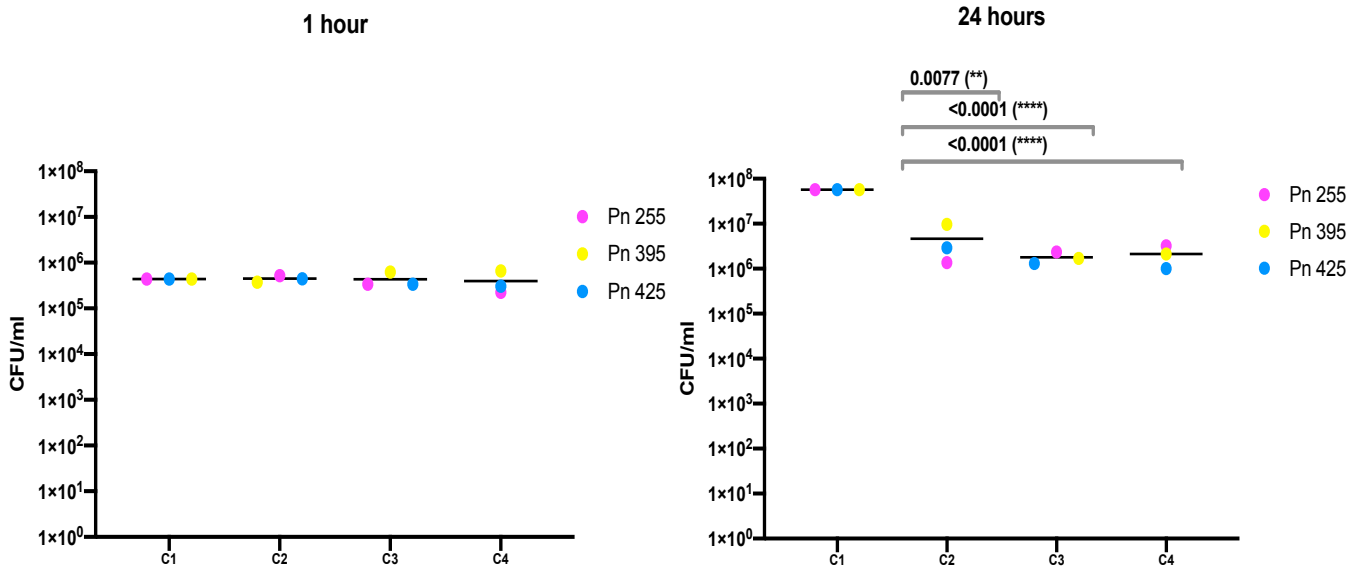

Figure 3-5: The impact of TLR-2-CM on bacterial viability by CFU assay. *S. aureus* suspension was incubated with TLR-2-CM or MSC-CM in 96 wells plate and incubated for 1 or 24 hours. At the end of incubation times, serial dilution was performed, and bacterial colonies were counted. C1= only *S. aureus*, C2= conditioned media of MSCs, C3= conditioned media of MSCs stimulated with Pam3Ck4, C4= conditioned media of MSCs stimulated with PGN-SA. The coloured dots represent three biological repeats, n=3. Bars indicate the mean. *** = $p \leq 0.001$, ** = $p \leq 0.01$, * = $p \leq 0.05$.

3.5.5. Gene expression of anti-microbial genes and *IDO* in infected MSCs following TLR-2 stimulation.

In the previous experiments, a significant reduction was found in bacterial count when bmMSCs were stimulated with PGN-SA. It was hypothesised that this reduction could be due to the stimulation of antimicrobial peptides or inflammatory cytokines. Gene expression analysis was performed to measure changes in mRNA of antibacterial peptide genes to investigate whether there is significant antimicrobial activity (either via AMPs or IDO) triggered when bmMSCs were stimulated with TLR-2 agonists during infection. Our result showed that there was a small increase in *IDO* expression by bmMSCs infected with *S. aureus*. reaching 70-fold compared to uninfected

bmMSCs (Figure 3-6), however this *IDO* overexpression was not statistically significant. *IDO* expression was also evaluated in *S. aureus* infected bmMSCs pre-treated with TLR-2 agonist, Pam3CSK4. As shown in figure 3-6, *IDO* was upregulated when infected bmMSCs were pre-treated with Pam3CSK4 agonist. The expression increased significantly, reaching 300-fold over normal bmMSCs (Figure 3-6). In separate experiments, *IDO* expression was evaluated in *S. aureus* infected bmMSCs pre-treated with PGN-SA. There was minor increase in *IDO* expression by 4-fold change when bmMSCs were infected by *S. aureus*. This change was no statistical difference between this group and the group of infected bmMSCs pre-stimulated with PGN-SA (Figure 3-6).

LL-37 and *hBD-2* gene expression was examined; there was undetermined CT values, indicating no expression of these genes (data is not shown).

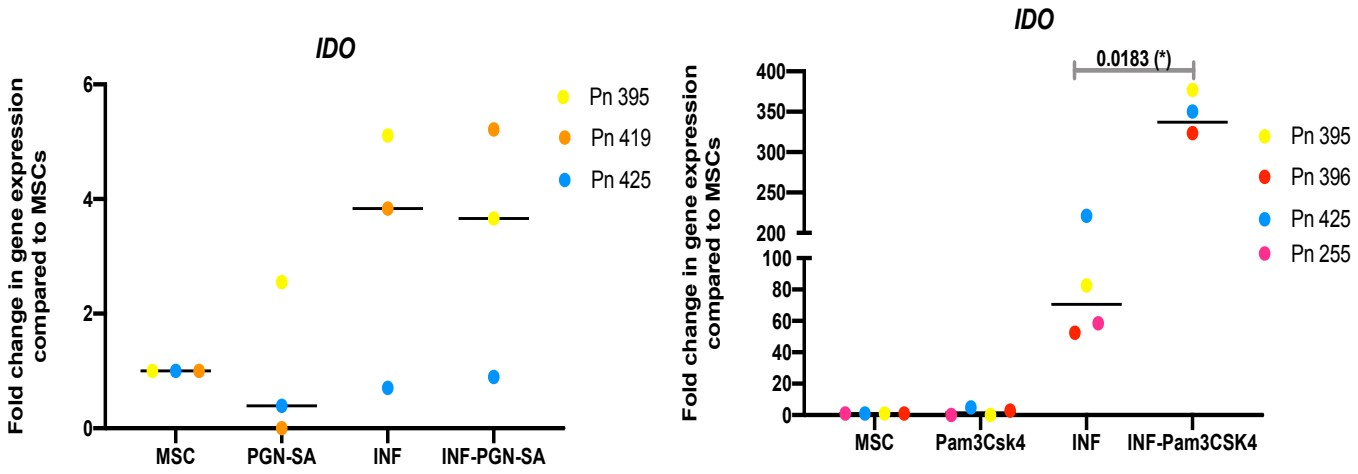

Figure 3-6: qPCR analysis of *IDO* expression in infected bmMSCs TLR-2 pre stimulated bmMSCs followed by infection with *S. aureus*. Confluent MSCs in a 12-well plate were stimulated with TLR-2 agonists and incubated for 24 hours. Cells were then infected with *S. aureus* at MOI 10 for 60 minutes, followed by washing, and the cells were subsequently immersed in serum-free medium for 24 hours. Cell lysis was performed, and samples were analysed using qPCR for the *IDO* gene expression. *IDO* = Indoleamine 2, 3-dioxygenase. All values are normalised to BACTN and B2m (housekeeping genes) CT values. n = 3 or 4. *** = $p \leq 0.001$, ** = $p \leq 0.01$, * = $p \leq 0.05$.

3.5.6. Gene expression of cytokine genes in infected bmMSCs following TLR-2 stimulation.

The mRNA changes of three cytokines (i.e., *IL-6, IL-8,* and *CCL2)* were measured. The results showed that there was a post-infection increase in *IL-6* and *CCL2* in bmMSCs when stimulated with *S. aureus*, however, this increase was not statistically significant (Figure 3-7). It was observed that there was a 10- fold change and 60- fold increase of *IL-6* in infected bmMSCs after Pam3CSK4 and PGN-SA, respectively, compared to untreated bmMSCs control. Similarly, Pam3CSK4 and PGN-SA have induced *CCL2* overexpression to approximately 15-fold in infected bmMSCs. This overexpression of *IL-6* and *CCL2* in infected bmMSCs stimulated with TLR-2 agonists was statistically significant (*IL-6*; p=0.0267 and *CCL2*; p=0.0357).

IL-8 gene expression in *S. aureus* infected bmMSCs was between 10 to 1333-fold higher compared to uninfected cells at 1-hour post-infection. Due to the large variance among samples the changes were not statistically significant (Figure 3-7). When infected bmMSCs were pre stimulated with TLR-2 Pam3CSK4, the relative expression of *IL-8* by infected bmMSCs shows an upregulation reaching a 21-fold without statistical significance. Similarly, when infected bmMSCs were pre stimulated with PGN-SA, there was an increase in *IL-8* expression in infected bmMSCs close to 800-fold higher than uninfected PGN-SA stimulated bmMSCs without statistical significance.

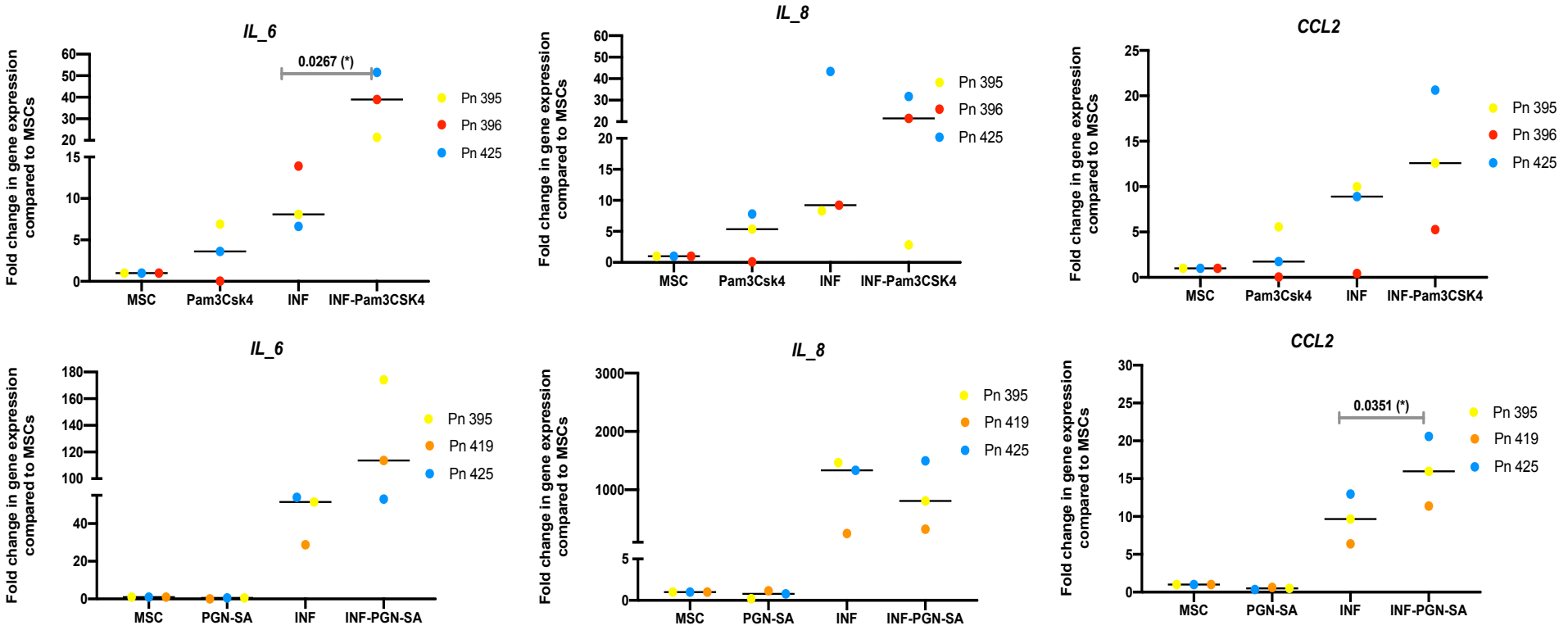

Figure 3-7: qPCR analysis of cytokine genes in infected bmMSCs pre stimulated with TLR-2. Confluent bmMSCs in a 12 wells plate were stimulated with TLR-2 agonists Pam3CSK4 and PGN-SA at 10 µg/ml for 24 hours. After stimulation, cells were infected with *S. aureus* at MOI 10 for 60 minutes, subsequently cells were incubated in a serum-free medium for 24 hours. Samples were analysed using qPCR *for IL-6, IL-8* and *CCL2*. All values were normalised to BACTN and B2m CT values. n = 3 or 4. *** = $p \leq 0.001$, ** = $p \leq 0.01$, * = $p \leq 0.05$.

3.6. Discussion

Our study has been built upon the previous knowledge that MSCs exhibit direct antibacterial properties and when stimulated, they can induce an activated immune response to battle infection through their paracrine mechanism (198-201). A strong correlation has been identified between the activation of TLRs and the expression of antimicrobial peptides during infections (202). Several studies demonstrated the significance of TLR function in the presence of infections and investigated how TLR expression on MSCs can help in promoting their antimicrobial activity (203). A previous report had shown that grafted skin of TLR-2 knockout mice resulted in impetigo following the inoculation with *S. aureus*. This is a powerful indication that TLR-2 expression is essential for the anti-microbial protection (204). The key goals of the study described in this chapter were to investigate the interaction of TLR-2 stimulated bmMSCs and *S. aureus*, to explore the impact of stimulated bmMSCs on the bacterial growth, and to examine the mechanism behind the antimicrobial activity of stimulated MSCs in the bacterial clearance. This is the first study to demonstrate that the activated TLR-2 receptors of human bmMSCs may support possess antibacterial properties by inhibiting the growth of *S. aureus.*

In our study, TLR-2 receptors on human bmMSCs were stimulated using two different TLR-2 agonists, *staphylococcal* peptidoglycan (PGN-SA) and lipoproteins (such as Pam3CSK4), to determine which cell wall elements of *S. aureus* involved in triggering the TLR-2 signalling pathway. Although both agonists are recognised mainly by the

TLR-2 receptors, they can have diverse cellular responses based on the specific pathway triggered by either TLR-2/TLR-1 or TLR-2/TLR-6 6 heterodimers (205). Therefore, we have considered these two agonists for TLR-2 activation in our study.

The most significant test cytotoxic impact on bmMSCs was observed only following bmMSCs incubation with 20 µg/ml of PGN-SA for 24 hours; however, there was an approximately 10% decrease in MSC viability. Nevertheless, we employed 10 µg/ml of PGN-SA for TLR-2 activation in our further studies; this concentration of PGN-SA did not generate any cytotoxic effects on the bmMSCs. This preliminary experiment is critical to ensure if there was an observed reduction in *S. aureus* viability when incubated with activated MSCs was not due to the presence of these chemical agonists but is solely due to the activity of stimulated MSCs by TLR-2 ligands. However, none of other research groups utilising TLR-2 agonists (as a stimulator of their cell models) have investigated the cytotoxic effects of TLR-2 agonists on the cells (206, 207).

In this chapter, we hypothesised that stimulation of bmMSCs with our TLR-2 agonists, Pam3CSK4 or PGNS-SA, may improve secretion of antimicrobial substances from bmMSCs into the supernatant, thereby reducing bacterial growth. Our results revealed that the stimulation of bmMSCs with PGN-SA and Pam3CSK4 caused a decline in *S. aureus* growth, and it was found to be more significant with PGN-SA stimulation.

Through a deep literature search, there was no exact comparable research to our study. We could not find studies that tested the impact of TLR-2 activated human

bmMSCs on *S. aureus* growth. However, Hertz *et al.* discovered a minor reduction in *P. aeruginosa* recovered from infected epithelial cell cultures pre-stimulated with lipopeptide (TLR-2 agonists) (208). Another published research investigated the TLR-2 activation of microglial cells in mice to test their antimicrobial effect on *S. aureus* growth. Nevertheless, both studies utilised different experimental settings, i.e., MOI, TLR-2 agonists, and different infection period.

Furthermore, we examined the effect of conditioned media derived from unstimulated bmMSCs (MSC-CM) and TLR-2 stimulated bmMSCs (TLR-2-CM) on bacterial growth using Alamar Blue and CFU count assays. We aimed to find if TLR-2-stimulated bmMSCs can exhibit powerful antimicrobial activity by secreting more substances into the conditioned media. Using Alamar Blue and CFU count assays, we observed no noticeable changes in bacterial cells viability (Alamar Blue assay) or bacterial count (CFU count assay) when *S. aureus* was challenged with conditioned media groups for 1 hour. This might propose that the mode of action of AMPs secretion in the conditioned medium requires a longer time to trigger their effects on bacterial growth. When *S. aureus* was challenged for 24 hours with MSC-CM and TLR-2-CM, a decline in *S. aureus* growth was observed in both the TLR-2-stimulated and unstimulated bmMSCs conditioned media. We found that conditioned media following TLR-2 agonist stimulation had the same impact on bacterial viability as MSC conditioned media alone, implying that TLR-2 stimulation was not affecting secreted components. In this study, we could not determine that this bacterial reduction was due to secreted AMPs in the conditioned media. Further protein-based analysis of other factors

released by MSCs into the supernatant is suggested but not conducted in this study. to explain the sharp decline in *S. aureus* growth.

The antimicrobial effects of MSC-CM (unstimulated) on bacterial load have been examined in several previous studies. It has been revealed that the growth of *S. aureus* was significantly decreased when exposed to bovine-conditioned media generated from bmMSCs and adipose tissue-derived MSCs (AT-MSCs) *in vitro* (209). Correspondingly, another study has demonstrated that MSC-CM from equine MSCs could inhibit the bacterial growth of *E. coli* and *aureus* (210). All these studies focused on the antimicrobial effects of unstimulated MSCs. On the other hand, there is no other study in the existing literature investigated anti-bacterial activity of TLR-2 MSC-CM on bacterial viability. However, Pezzanite and his group did report that MSC-CM stimulated with TLR-3 agonists (polyinosinic-polycytidylic acid-PIC) lead to decreased planktonic bacterial colonies and inhibited biofilm formation (203).

Evaluation of changes in the mRNA expression of AMPs in TLR-2 activated MSCs might provide valuable information about the key mechanism behind the antimicrobial activity of these TLR2 activated MSCs. Therefore, we hypothesised that the TLR-2 activation plays a role in mediating the overexpression of genes such as *LL-37*, *hBD-2* or *IDO* (encodes for IDO enzymes involved in antibacterial activity) in bmMSCs that could have led to bacterial clearance. Our results revealed significant *IDO* and *IL-6* mRNA overexpression when bmMSCs were stimulated with Pam3CSK4 and a

significant increase of *CCL2* when bmMSCs were stimulated with PGN-SA during *S. aureus* infection.

Regarding IDO*,* MSCs can act against *S. aureus* attack by releasing IDO protein (211). Various cell types exhibited superior production of IDO protein or amplified IDO activity when stimulated with TLRs agonists. For example, it was shown that stimulation with TLR-3 Poly(I: C) and TLR-9 CpG results in the upregulation of IDO expression from different types of cells, such as monocyte-derived dendritic cells or umbilical cord MSCs (UC-MSCs) (212-214). On the other hand, IDO activity was shown to be TLR-2 dependent and was mediated by the TLR-2 signalling pathway in murine dendritic cells during *Mycobacterium leprae* infection (215). This is indicative that TLRs stimulation plays a role in IDO induction.

In this study, observed *IDO* overexpression was found to reach up to 350-fold in infected bmMSCs when pre-stimulated with Pam3CSK4 but not PGN-SA. To date, no study has attempted to demonstrate TLR-2 agonist-Pam3CSK4 stimulation of *IDO* expression in human bmMSCs during bacterial infection using *S. aureus.* It was not possible to prove that *IDO* overexpression in our experiment was the reason behind bacterial growth inhibition because our data revealed no difference in viability between TLR-2-CM and MSC-CM against *S. aureus*. Moreover, the studies were based on mRNA analysis which could be transient, Further investigation as to whether there are other proteins produced by the bmMSCs that could be involved in this inhibition is warranted.

We investigated gene expressions *LL-37* and *hBD-2,* antimicrobial peptides. MSCs produce both cathelicidin *LL-37* and *hBD-2* which exhibit potent activities capable of killing *S. aureus* (216). In our study, the expression level of *LL-37* and *hBD-2* mRNA was undetermined (data not shown) either during the bacterial challenge, stimulation of TLR-2, or in both treatments. Through a deep literature search, several studies have found strong association between TLR-2 stimulations and AMPs expression (mainly *LL-37* and *hBD-2*) in different cells at either gene or protein level (217). However, those studies were not equivalent to our study design and experimental settings. For example, in one study different TLR ligands (natural and artificial) and different stimulation length were used (218). Another study used different TLRs concentration and cell phenotyping assays (219). In a third study, a different infectious agent and hence infection environment was used (220). Taken together, these indicate that antimicrobial production is influenced by many factors which can explain the reported inconsistencies in AMPs expression.

Additionally, we sought to identify other factors that may contribute to anti-bacterial effects of TLR-2-stimulated bmMSCs by examining chemokines and cytokines expression involved in the inflammatory response. A slight increase was found in the expression of pro-inflammatory cytokines *IL-8* or *CCL2* and IL-6 in *S. aureus*-infected bmMSCs compared to uninfected bmMSCs, but that was not significant. However,

TLR-2 stimulation of MSCs with Pam3CSK4 or PGN-SA exhibited significant increase in the expression levels of IL-6 and *CCL2*, respectively.

MSCs can release IL-6, a multifunctional cytokine that can act as both a pro-inflammatory and anti-inflammatory cytokine. IL-6 plays a crucial role in host defence mechanisms by regulating the immune response. We have found an upregulation of IL-6 in *S. aureus*-infected MSCs with or without TLR-2 stimulation. It is well established that activation of TLRs in adipose-derived stromal cells (ASCs) can result in the production of pro-inflammatory cytokines such as IL-6 (221, 222). In another study, it has been demonstrated that the secretion levels of IL-6 increased when the MSCs were incubated with PGN (a TLR-2 agonist), LPS (a TLR-4 agonist) and poly (I: C) (TLR-3 agonist) and this IL-6 overexpression was abolished when neutralised TLR-2 antibodies were used, indicating that the expression of IL-6 is TLR-2 mediated (223).

We observed that TLR-2 stimulated MSCs cells and MSC-CM showed antimicrobial activity against *S. aureus*. However, we did not evaluate protein constituents released from the stimulated bmMSCs. It would be useful in the future to measure the secreted proteins via multiplex analysis or a similar proteomics approach, as this might enable a broad screen of the protein profiles, which could facilitate the identification of appropriate protein targets for amelioration.

In conclusion, we found in our study that TLR-2 stimulated bmMSCs showed an enhanced antibacterial activity against *S. aureus.* Pam3CSK4 treatment of bmMSCs

results in significant upregulation of expression; however, this overexpression was not guaranteed to be the reason behind the observed bacterial growth inhibition. Further investigations might be suggested to measure protein level in the conditioned media and examine other intracellular pathways to elucidate the molecular mechanisms which cause the bacterial reduction. Overall, this *in vitro* study supports further studies of TLR-2 stimulated human bmMSCs enhanced antibacterial activity towards finding be a therapeutic agent for the control of *S. aureus* infection.

4. Chapter Four

Changes occurring in infected osteoblasts before and after exposure to conditioned media of MSCs.

4.1. Overview

4.1.1. Bone and mesenchymal stem cell therapy

The bone regeneration process coordinates the formation of new bone cells and the surrounding extracellular matrix, thus maintaining bone structure and function (224). Under physiological conditions, osteoblasts are responsible for new bone formation by synthesising mineralised bone matrix (225). The osteoblastic activity can be malformed in some pathological conditions, such as bacterial infections, which can impair bone homeostasis. In this context, *S. aureus* represents the most common pathogen responsible for increased risk of OM. This invading pathogen is capable of bone colonisation, resulting in bone destruction. On the other hand, during infection, the immune response of the host may dysregulate the mineralisation of bone matrix by osteoblasts and/or disrupt the bone resorption process by osteoclasts, leading to bone loss. This invited exploring new alternative therapies, with regenerative medicines aiming to displace or replenish tissues or organs to revive and maintain their normal function (226, 227).

Cellular therapy, represented by MSCs, has become an alternative and promising candidate in regenerative medicine (228). MSC therapy is considered a risk-free and effective technique for treating diseases and pathological conditions due to their potential for proliferation and multilineage differentiation into the cells of interest and their competency to replenish damaged tissue. Additionally, the therapeutic effect of MSCs can be accredited to the potent factors and substances secreted in MSC-CM. These substances are called secretomes and include growth factors, cytokines,

chemokines, and extracellular vesicles which, stimulate cell differentiation of the recipient stem cells, thus promoting the formation of new tissues. Various studies have illustrated the beneficial therapeutic outcomes of MSCs and MSC-CM in disease conditions such as Alzheimer's, diabetes, rheumatoid arthritis, focal cerebral ischemia, and acute renal failure (229).

4.1.2. Differences between MSCs and MSC-CM

Applying MSCs or MSC-CM for cellular remedies has been the subject of various comparative studies. These studies compared the biological impacts of secretome in the MSC-CM with the administration of MSCs cells (230, 231). Porzionato and his collaborators (232) achieved good results and displayed enhanced pulmonary and vascularity performances when employing MSC-CM secretome in a bronchopulmonary dysplasia model. On the other hand, a different research group observed no significant difference in morphological, radiological or histological features between the administration of MSCs (as a cell-based therapy approach) and the application of MSC-CM in a rabbit mandibular bone defect model (233).

Despite the safe application of MSCs therapy, using substances they secrete rather than using the cells proved to have more advantages. The application of MSC-CM avoids the risk of some complications associated with MSC based therapy, like inadequate cellular survival after transplantation, depriving the ability of the differentiation of transplanted cells and the failure of cells to graft (226).

4.1.3. Effects of MSC-CM on bone regeneration

Improving bone regeneration by using MSC-CM is possible because MSC-CM contains numerous growth factors that boost bone formation without triggering severe inflammatory response in the host (234).

In bone fracture models, MSC-CM improves osteogenesis, angiogenesis and fracture integration (235). Studies of animal models evaluated the application of MSC-CM to bone regeneration during bone defect conditions. The results suggested that secretome of MSCs enhances the development of new bone cells and bone formation, leading to fewer treatment periods required (233, 236). A study by Nakamura demonstrated that MSCs secretome accelerated skeletal muscle regeneration (237), whilst Zheng and others displayed encouraging results and efficaciousness of MSC-CM in repairing cartilage (235, 238).

In some histological examinations, it was noted that in bone defects aided with MSC-CM, there was more significant development of new, primarily mineralised regenerated bone with barely any inflammatory cell infiltration. In contrast, control groups demonstrated diminished osteogenesis with less mineralisation, more significant amount of regenerative material and enhanced infiltration of inflammatory cells (233, 234). Most experimental investigations noted that MSC-CM containing cytokines and growth factors are able to stimulate the migration and proliferation of osteoprogenitor cells, support osteogenesis and bone regeneration and enhance early vascularisation (239). In this chapter the therapeutic potential of MSC-CM in a 2D model of infected human bone as a basic model of OM was investigated. We

hypothesised that loading MSC-CM on infected osteoblasts could provoke antibacterial activity and consequently influence osteogenic differentiation, thereby supporting a role for the secretome in this process.

4.2. Aims

The chapter investigated the antimicrobial and cytoprotective effects of MSC-CM on infected bmMSCs differentiated into osteoblasts. In addition, we attempted to determine the changes in gene expression behind the bmMSCs therapeutic effect on infected osteoblasts exposed to MSC-CM. To this end, bmMSCs were differentiated into osteoblasts and infected with *S. aureus*, followed by culturing cells in MSC-CM. The effects of MSC-CM on infected osteoblasts were assessed by bacterial count assay (CFU assay), RUNX2 gene expression and other markers of osteogenesis at mRNA and protein levels.

4.3. Objectives of the study

1. Characterise the efficiency of bmMSCs differentiated osteoblasts by Alizarin red staining.
2. Establish a cellular model of osteomyelitis using cultured osteoblasts (differentiated from bmMSCs) infected with *S. aureus* and utilise this model to examine the infection by Immunofluorescent assay.
3. Examine possible antimicrobial effect of bmMSCs on *S. aureus*-infected osteoblasts by CFU count assay.
4. Use qPCR analysis to determine changes in gene expression of osteogenic markers and matrix metalloprotease enzymes.
5. Examine protein expression of osteogenic factors and IDO using western blotting.

4.4. Methods

4.4.1. Osteogenic induction

For induction of osteogenic differentiation, bmMSCs were seeded at a density of 4.2×10^3 cells/cm^2 in an osteogenic medium. Osteogenic differentiation was induced with osteogenic differentiation medium based on standard cultivation medium (α minimum essential medium supplemented with 10% FBS, 1% penicillin/streptomycin, 1% (v/v) Glutamax) and osteogenic supplements containing 50 µM α-ascorbate-2-phosphate, 10 mM β-glycerophosphate, and 0.1 µM dexamethasone. The medium was changed every 3-4 days for three weeks.

4.4.2. Alizarin red S staining

At day 21 of osteogenic induction, osteoblasts phenotype was verified by histological stain using Alizarin red. The osteogenic differentiation media was discarded. The cells were washed once with PBS and fixed by adding 1 ml of methanol, and the plate was incubated for 1 hour at room temperature. Following fixation, the methanol was removed, and the cells were washed with distilled water twice. 1 ml of freshly prepared 2% (w/v) Alizarine red dye was added to each well and incubated for 45 minutes. At the end of incubation, cells were washed thoroughly with PBS carefully until the supernatant became clear. The cells were then examined under a microscope at 20x and 40x magnification.

4.4.3. Osteoblast infection

At the end of osteogenic induction, differentiated osteoblasts were washed four times with PBS to remove any residue of antibiotics used in the osteogenic differentiation media. On the day of infection, *S. aureus* of 10 MOI was calculated according to the number of osteoblasts in the wells. The MOI10 bacterial suspension media was

prepared as in sections 2.8 and 2.10. A volume of 1 ml of *S. aureus* MOI10 was added to corresponding wells, and the plate was incubated at 37°C and 5% CO_2 for 1 hour.

1.1.2. Immunofluorescence staining of infected osteoblasts.

After the infection, osteoblast cells were washed three times with infection media. An amount of 200 µl of 4% paraformaldehyde (PFA) was added to each well, and the plate was placed at room temperature for 30 minutes; then, the PFA was discarded and replaced with PBS and kept in the fridge overnight. The following day, a blocking solution of 500 µl of 3% bovine serum albumin (BSA) was added with 0.1% (v/v) Triton™ X-100 (Sigma-Aldrich Catalogue No.9036-19-5) and incubated for an hour at room temperature. Primary, secondary, and control working antibody solutions were prepared with a specific concentration of 1% BSA. An amount of 500 µl of prepared primary antibody (1° antibody rabbit anti-*S. aureus* and 1° antibody mouse anti-osteocalcin) and control antibody (control antibody rabbit IgG and control antibody mouse IgG) was added to the corresponding wells and incubated overnight at 4° C. On the next day, the wells were washed three times with washing buffer (PBS with 0.05% v/v Tween 20). Subsequently, the secondary antibody (2° antibody rabbit Alexa fluor 594 and 2° antibody mouse Alexa fluor 488 (Invitrogen, UK) was prepared in PBS with 0.05% v/v Tween 20, added to the corresponding wells, and incubated in the dark for an hour at room temperature. Wells were then washed three times with ELISA wash (prepared as tris buffered saline with Tween 20, pH 8.0). 100 µl of DAPI (4',6-diamidino-2-phenylindole was prepared in PBS (1/1000) and added to all wells, and the plate was incubated in the dark at room temperature for 30 minutes. This was followed by one ELISA wash and the addition of 300µl of PBS containing 0.05% sodium Azide to all wells. An inverted (model) fluorescence microscope was used to

acquire the images. This method was applied to three biological repeats to prove the adhesion of *S. aureus* to the osteoblasts, which ensures the infection step.

4.4.4. *S. aureus* CFU recovery from infected osteoblasts cultured with MSC-CM

Osteoblasts were infected, as stated in section 4.5.3. Then, cells were washed 3X with PBS. After that, cells were cultured with MSC-CM by adding 1 ml of different conditions of MSC-CM and subsequent incubation of the plate for 24 hours. MSC-CM was prepared by seeding human bmMSCs at different concentrations of cells into 24 wells plate. i.e., 37500 cells /well (CM1), 7500 cells / well (CM2), and 15000 cells/ well (CM3). The cells were incubated at 5% CO_2 and 37°C for 48 hours. The supernatant was then transferred into sterile 15 ml tubes and stored at -80°C until required. At the end of infection, infected osteoblasts were washed with PBS and 3 ml of different conditions of MSC-CM (harvested from different cell densities) was added to the corresponding wells and the cells were incubated for 24 hours. Then, the MSC-CM was discarded, and 100 µl of 1% saponin was added to each well and incubated for 10 minutes at 37°C. The culture plate wells were scraped using the yellow tips, and 20 µl of the suspension was added to the corresponding wells of 96 well rounded bottom plate for the serial dilution (1 in 10 dilution factor). A 10 µl volume of the diluted suspension (the last three dilution wells) was inoculated on MHA and incubated overnight at 37°C. Finally, *S. aureus* CFU was counted using a plate counter and the results were plotted on an Excel sheet.

4.4.5. qPCR of osteogenic genes of infected osteoblasts cultured with MSC-CM

Osteoblasts were infected, as stated in section 4.5.3, then cells were cultured in MSC-CM harvested from different cell densities prepared as indicated in section 4.5.5 and

the osteoblasts were incubated for 24 hours. At the end of incubation time, cells were washed 1X with PBS, and 300 µl of lysis buffer was added. RNA was extracted using the method described in section 2.2.9 then reverse transcribed to cDNA, and qPCR assay was performed as described in sections 2.2.7 to 2.2.9 *for RUNX2, ALP, bglap, MMP-1* and *MMP-13*.

4.4.6. Western blotting for matrix metalloproteinase enzyme and RUNX2 proteins.

Western-blotting assay was conducted to measure protein expression levels of RUNX2, IDO and MMP-1. Osteoblasts were infected, as stated in section 4.4.3. Then cells were cultured with three conditions of MSC-CM. At the end of incubation, cells were washed 1X with PBS, and 700 µl of lysis radioimmunoprecipitation assay buffer (RIPA buffer) was added. Cell lysates were separated using SDS-polyacrylamide gel electrophoresis and transferred onto PVDF membranes. The membrane was blocked in 5% non-fat milk (w/v) and probed with the appropriate primary antibody overnight at cold room with constant agitation. Unbound antibody was removed by rinsing the membrane with TBST buffer. The protein bands were detected using species-specific HRP-conjugated secondary antibody for 1 hour at room temperature. Bands were determined by chemiluminescence. The exact method was described in Section 2.2.11 to 2.2.13.

4.5. Results

4.5.1. Alizarin red S stain detection of osteogenic differentiation

We determined the osteo-differentiation of bmMSCs used in our experiments using Alizarin Red S staining. After 21 days in an osteogenic medium, osteoblasts showed positive Alizarin red staining, which labels the deposits of calcium phosphate deposits (hydroxyapatite $Ca_5(PO_4)3(OH)$) in differentiated bmMSCs as compared to control undifferentiated bmMSCs (Figure 4-1).

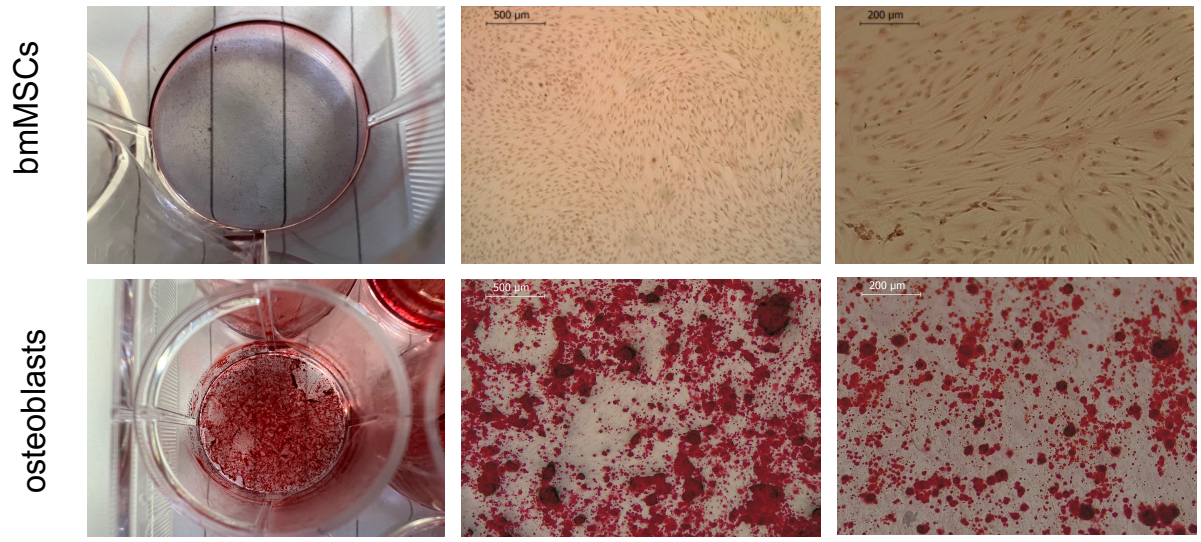

Figure 4-1 Alizarin red staining for osteoblasts (differentiated from bmMSCs). Osteogenesis was induced by using alpha MEM, supplemented with dexamethasone, ascorbic acid and β-glycerophosphate. On day 21, the medium was removed, and cells were fixed with methanol and stained with Alizarine red S for calcium deposits for 45 minutes. Undifferentiated bmMSCs cultured in basal bmMSCs medium were used as a control. Images were taken at magnifications x4 and x10. The images are representative of 3 independent experiments.

4.5.2. *S. aureus* infection of human osteoblasts

Osteoblasts were infected with *S. aureus* at MOI 10 for 1 hour. Infection media was aspirated, and cells were washed with PBS and fixed in 4% PFA. To validate the infection and osteogenic differentiation, infected osteoblasts were stained with an antibody specific to *S. aureus* and antibody for the osteogenic marker, osteocalcin, respectively (Figure 4-2).

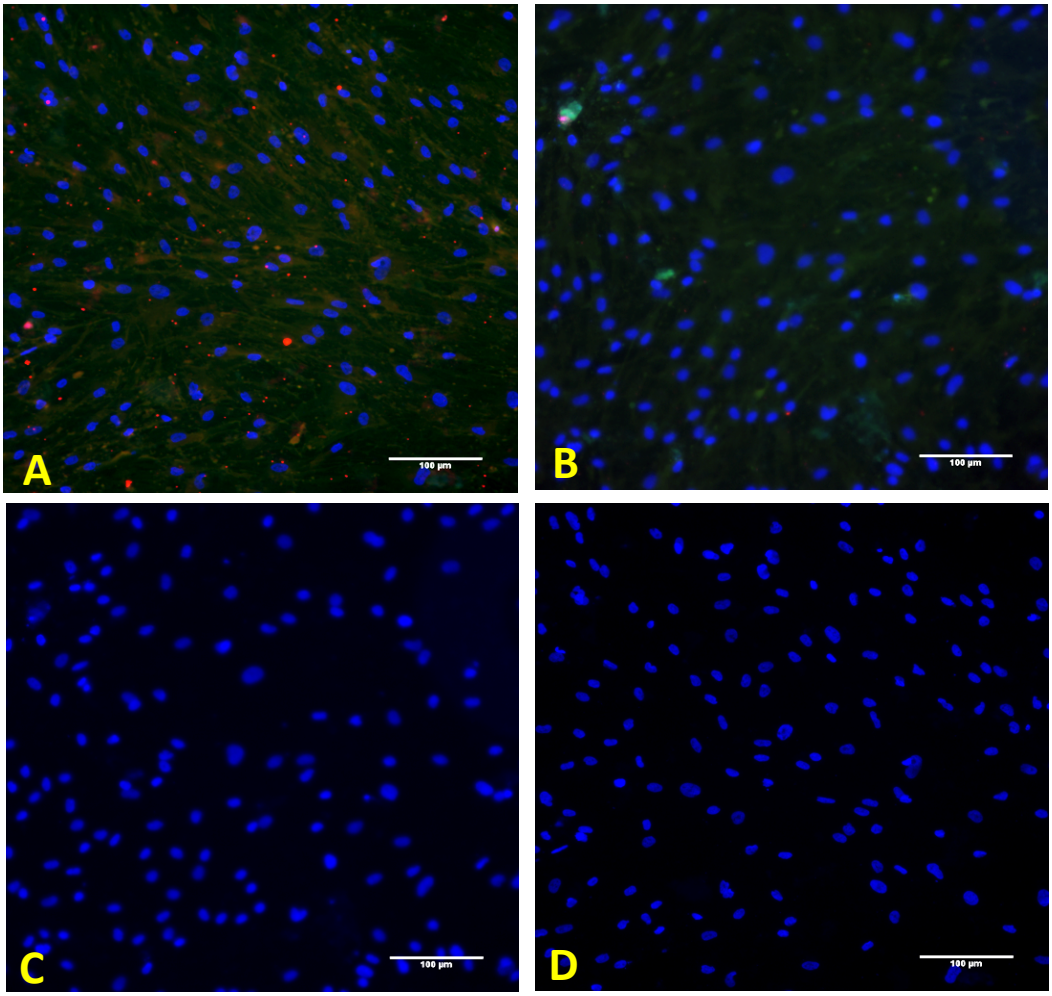

Figure 4-2 *S. aureus* infection of MSC-differentiated osteoblasts. bmMSCs were differentiated into osteoblasts and infected with *S. aureus* at 10 MOI. Cells were stained using an antibody for osteocalcin (green), nuclei were stained with DAPI (blue), and *S. aureus* with a specific antibody (red dots). The primary antibodies were detected using secondary antibodies conjugated to a fluorophore. (A) Osteoblasts stained with anti-osteocalcin and anti-*S. aureus* antibodies (B) Uninfected osteoblasts stained with anti-osteocalcin (C) osteoblasts stained with mouse isotype control IgG (D) osteoblasts stained with rabbit isotype control IgG. Magnification: x100, Scale bar 100µm, n=1.

4.5.3. MSC-CM induces inhibition of *S. aureus* growth.

To determine an appropriate capacity of MSC conditioning that can achieve an antimicrobial effect against *S. aureus* infected osteoblasts, we investigated the effect of three conditions of MSC-CM (i.e., MSC-CM harvested from different cell densities) on infected osteoblasts. MSC-CM were added onto infected osteoblasts and cells were incubated for 24 hours. We observed that infected osteoblasts treated with CM2 (MSC-CM harvested from seeding 7500 cells/well) and CM3 (MSC-CM harvested from seeding 15000 cells/well) had significantly lower *S. aureus* viable colonies than those infected osteoblasts alone. The number of bacteria recovered from infected osteoblasts was approximately $1.5x10^9$ CFU/ml. On the other hand, the number of *S. aureus* decreased to a level close to $3.2x10^8$ CFU/ml and $1.5x10^8$ CFU/ml when infected osteoblasts were supplemented with CM2 ($p=0.0374$ (*)) and CM3 ($p=0.0143$(*)), respectively. This demonstrated that bacterial growth could be attenuated after addition of MSC-CM on infected osteoblasts (Figures 4-3). These effects suggested antimicrobial agent(s) were secreted in the MSC-CM.

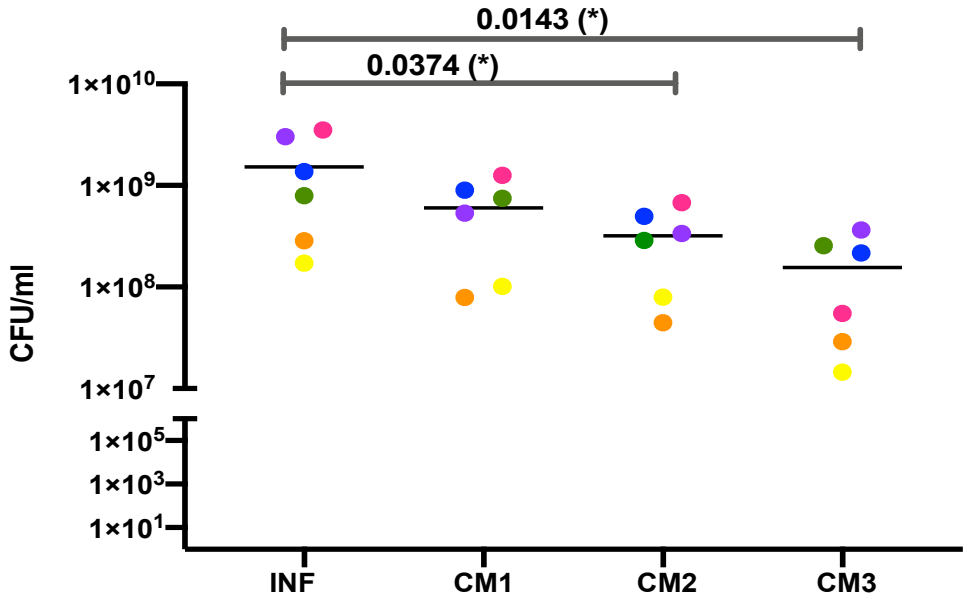

Figure 4-3 *S. aureus count* recovered from infected osteoblasts cultured with MSC-CM. Confluent osteoblasts in 24 well plates were infected with *S. aureus* at MOI 10 for 1 hour, followed by adding MSC-CM to cells and culturing for 24 hours. Media were collected and CFU count was performed. INF= infected osteoblasts, CM1 = conditioned media from seeding 3750 cells/well, CM2 = conditioned media from seeding 7500 cells/well and CM3 = conditioned media from seeding 15000 cells/well. The data samples 6 repeats, n=6. Bars indicate the mean. *** = $p \leq 0.001$, ** = $p \leq 0.01$, * = $p \leq 0.05$.

4.5.4. Gene expression of osteogenic markers and matrix degradation enzymes genes in infected osteoblasts cultured with MSC-CM

To investigate how MSC-CM could impact osteoblast differentiation, infected osteoblasts treated with MSC-CM were examined for the expression of osteoblastic markers, *RUNX2* and *bglap* and the matrix degradation enzymes, *MMP-1* and *MMP-13.*

The effect of MSC-CM on *bglap* expression in infected osteoblasts and after culture with MSC-CM were analysed. The level of *bglap* expression significantly decreased continuously when osteoblasts were cultured with increasing cell density MSC-CM compared to infected osteoblasts alone (Figure 4-4). To further confirm the impact of MSC-CM on osteogenic differentiation, the osteoblastic transcription factor, *RUNX2*

was analysed. Little change was observed in *RUNX2* expression in infected osteoblasts treated with various MSC-CM compared to control group.

We sought to investigate the impact of MSC-CM on two other essential genes that play critical roles in extracellular matrix degradation; *MMP-1* and *MMP-13*. *MMP-1* exhibited an increased expression with a 10-fold and 8-fold when infected osteoblasts cultured with CM2 and CM-3, respectively. However, these differences were not statistically significant (Figure 4-4). Very little change that was statistically not significant was observed in the expression of *MMP-13*.

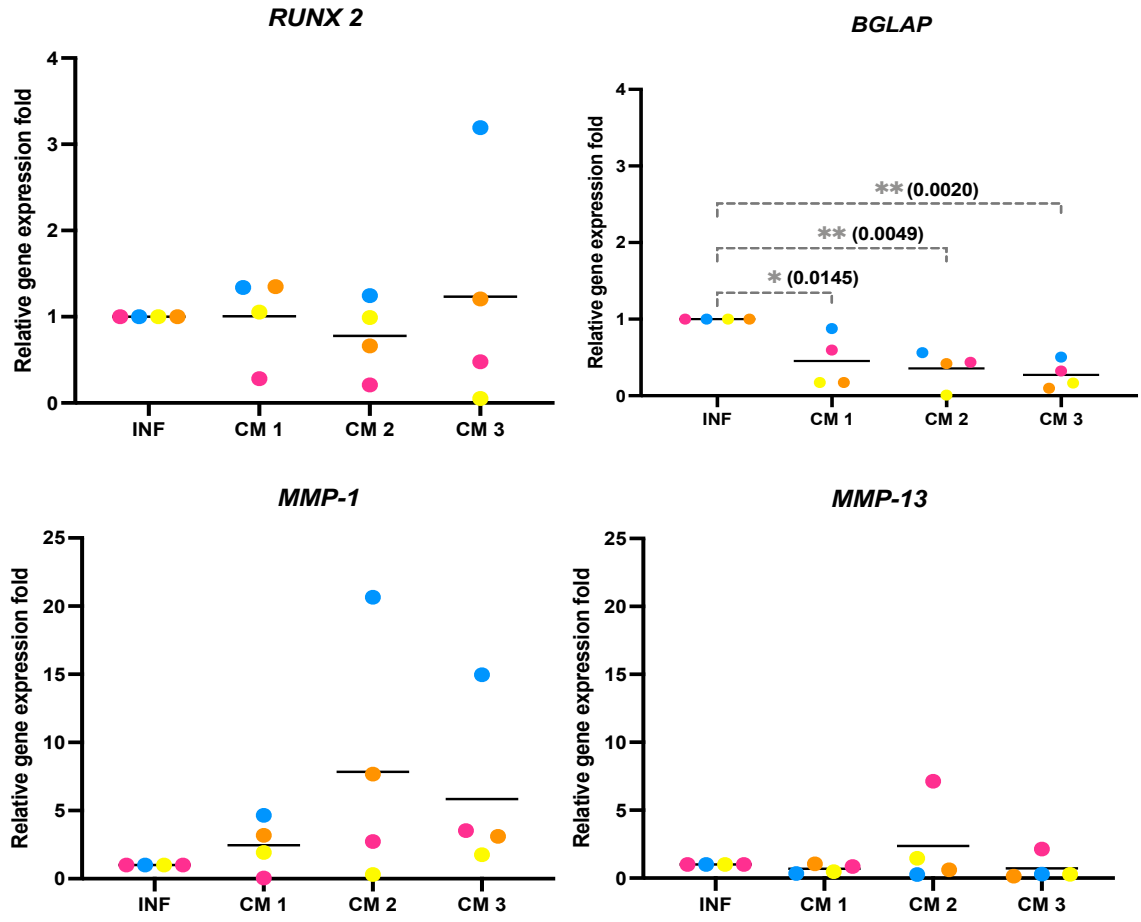

Figure 4-4 qPCR analysis of osteoblastic and ECM degradation genes of infected osteoblasts cultured with CM-MSC. Confluent osteoblasts in 24 wells plate were infected with *S. aureus* at MOI 10 for 1 hour, followed by adding MSC-CM for 24 hours. Cells were analysed using qPCR for *RUNX2, bglap, MMP-1* and *MMP-13*. INF= infected osteoblasts, CM1 = conditioned media from seeding 3750 cells/well, CM2 =conditioned media from seeding 7500 cells/well and CM3= conditioned media from seeding 15000 cells/well. n=4. Bars indicate the mean. *** = $p \leq 0.001$, ** = $p \leq 0.01$, * = $p \leq 0.05$.

4.5.5. Western blotting for IDO, RUNX2 and MMP-1

In order to validate mRNA analysis, western blotting analysis was conducted to detect protein expression of IDO, RUNX2 and MMP-1. The data has shown detectable overexpression of the MMP-1 and IDO compared to control uninfected osteoblasts (N). The expression in MSC-CM treatment groups was similar to infected control group without MSC-CM. This data was in agreement with mRNA analysis (Figure 4-4). RUNX2 expression was lower in infected cells compared to uninfected control group. The gradual increase in cell density of MSC-CM appears to correlate with decrease in RUNX2 expression where it becomes hardly detectable in MSC-CM3 treatment group Without semi-quantitative densitometric analysis, the appearance reflects little change among infected groups with or without MSC-CM treatment (Figure 4-5).

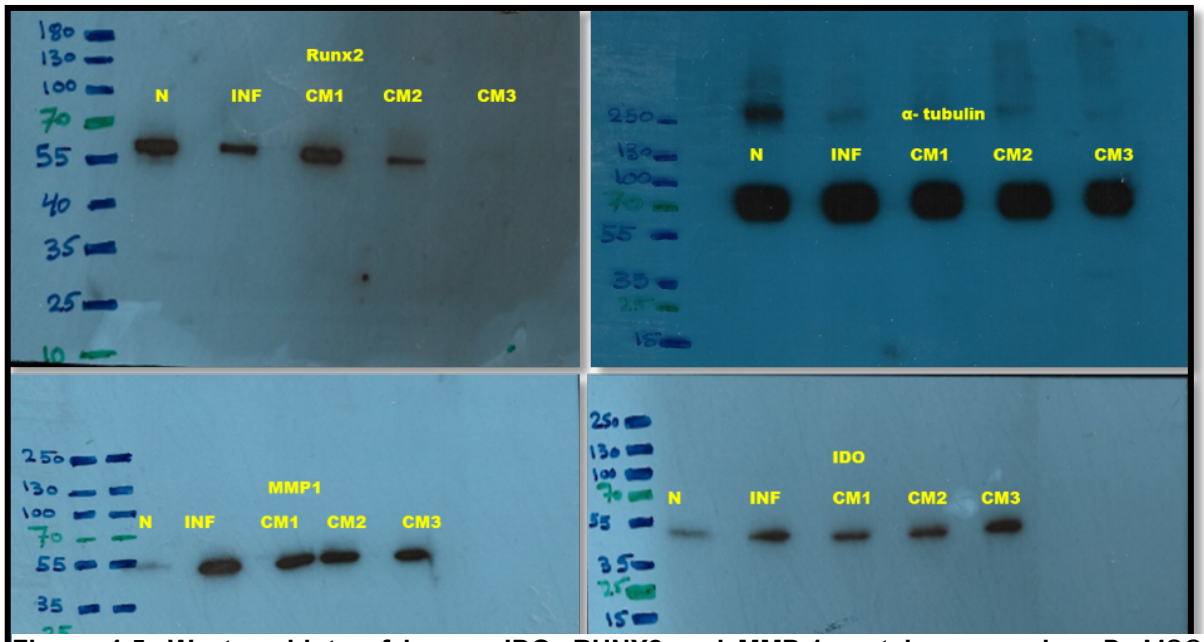

Figure 4-5: Western blots of human IDO, RUNX2 and MMP-1 protein expression. BmMSCs differentiated osteoblasts seeded in 12 wells were infected with *S. aureus* MOI10 for 1 hour. After washing, infected osteoblasts were exposed MSC-CM for 24 hours. Cell lysis was prepared, and protein levels was assayed using western blot, probed with monoclonal antibodies against IDO, MMP-1 and RUNX2. Protein bands were visualised with an anti-mouse secondary antibody conjugated with horseradish peroxidase and developed with a chemiluminescence reagent. INF= infected cells. CM1 = 3750 cells / well, CM2 = 7500 cells / well, CM3 = 15000 cells /well. Alpha-tubulin was used as the loading control. n=1

4.6. Discussion

Osteoblasts are the only fundamental cells for mineralising bone matrix and supplying new bone in addition to MSCs, which are crucial cells for bone regeneration due to their ability to differentiate into osteoblasts, making them potentially significant or essential in bone healing (240). The content of MSC-CM could support the therapeutic effects of MSCs to induce cell differentiation into osteoblasts, thus encouraging formation of new tissues and increasing bone repair (227, 241). The mechanism by which MSC-CM affects infected osteoblasts has been unknown in terms of osteogenic differentiation activity. Our study findings could contribute to developing therapeutic strategies for bone defects, bone tissue engineering and an alternative for treating OM through minimising antibiotic use, thereby limiting antibiotic resistance complications, and avoiding ineffective and complicated therapies.

In the present study, we hypothesised that the secretome generated by bmMSCs might improve antimicrobial functions and osteogenic activity of infected osteoblasts. In this study, an *in vitro* 2D model was established of the infected osteoblasts using *S. aureus* infected osteoblasts differentiated from MSCs. The model was used to investigate the antibacterial activity and regenerative potential of infected osteoblasts in response to exposure to MSC-CM.

MSC-CM was found to inhibit *S. aureus* growth using three different concentrations MSC-CM, produced by harvesting medium from increasing density of MSCs. The MSC-CM at any concentration was not found to influence osteoblast differentiation.

Initially, the lowest threshold of MSC-CM that triggered bactericidal effect in infected osteoblasts was investigated. This was evaluated by quantifying the number of viable

S. aureus recovered from infected osteoblasts (CFU assay). A key finding was the capacity of human MSC-CM to significantly inhibit growth of *S. aureus* at a dose of MSC-CM (CM2 - conditioned media from seeding 7500 cells/well of bmMSCs).

A number of studies have suggested an antimicrobial effect for MSC-CM on different cells. These studies investigated the impact of equine or mice MSC-CM in infected models, including models of rodent lung infection or mice with skin wounds. Their results have shown that MSC-CM could inhibit bacterial growth, such as *S. aureus* and *E. coli* (227). All of these studies have shown an evidence that MSC-CM has antimicrobial properties through the release of soluble factors, including the antimicrobial proteins cathelicidin LL-37, lipocalin-2, hBD-2, cystatin C and elafin, that enhance bacterial clearance (242-244) (210, 245, 246). However, to our knowledge, these studies have not explored the potential of human MSC-CM impacts on bone healing.

In this present study, bacterial reduction in infected osteoblasts post-culture with MSC-CM for 24 hours was found. This prompted exploring possible anti-bacterial mechanisms mediated by MSC-CM by investigating potential antibacterial factors in the supernatant. To this end, IDO protein level was assessed using western blot assay. Whilst a slight increase in IDO protein level was observed with increasing MSC-CM concentration, produced by increasing cell density, that might be associated with the reduction of *S. aureus*, no clear correlation between IDO levels and increased MSC-CM concentration was found. This suggested the contribution of other antimicrobial factors secreted in the MSC-CM which warranted further investigation.

Osteoblastic differentiation was examined by measuring gene expression of osteoblast-specific markers (*bglap* and *ALP*) and bone extracellular matrix degrading enzymes (*MMP-1* and *MMP-13*) in order to investigate the influence of MSC-CM on osteoblastic differentiation capacity during infection.

bglap is a crucial marker in osteoblastic differentiation. *bglap* gene encodes osteocalcin which is a non-collagenous protein produced abundantly by osteoblasts. This bone formation marker is expressed in the late stage of osteogenic differentiation. The results demonstrated that MSC-CM significantly inhibited *bglap* expression in infected osteoblasts, 24 hours post-exposure, when compared to infected osteoblasts control. Additionally, this reduction in *bglap* mRNA level was found to be MSC-CM concentration dependent.

Through a deep literature search, no other similar study was found investigating the role or effect of MSC-CM on the expression of osteoblast specific genes in infected osteoblasts. Previously Jing Sun *et al.* (247) studied the impact of different concentrations of MSC-CM on *bglap* expression during osteoblast differentiation. They found that *bglap* expression was significantly diminished by MSC-CM compared to control group on day 3 and returned to its normal level after 7 days (247).

In the current study, whilst MSC-CM downregulated *bglap* expression in infected osteoblasts, it was not possible to discern whether this downregulation was due to the presence of MSC-CM or *S. aureus* infection, since uninfected osteoblasts in standard medium were not included in the study as a control to allow comparing the expression of osteogenic markers among normal osteoblasts, infected osteoblasts and infected osteoblasts cultured with MSC-CM.

In order to understand the molecular mechanism(s) underlying the suppression of *bglap*, levels of the osteoblastic transcription factors *RUNX2* was investigated at both mRNA and protein levels. RUNX2 is a multifunctional transcription factor that regulates skeletal development by controlling the differentiation of chondrocytes and osteoblasts (48). Moreover, it has been found that *RUNX2* deficiency or mutation can cause severe abnormalities in the bone. Our study found that infected osteoblasts exposed to MSC-CM had no change in *RUNX2* gene expression. Taken together with bglap analysis, MSC-CM appears to arrest the osteoblast in an immature state, reducing their capacity to mature and express *bglap*.

The effect of MSC-CM on MMP expression at the mRNA and protein levels for MMP-1 and MMP-13 was investigated. MMPs are proteolytic enzymes expressed in both osteoblasts and osteoclasts and responsible for the degradation of the organic matrix in the bone during bone resorption. MMP-1 and MMP-13 are important osteoblastic differentiation markers. MMP-1 (known as interstitial collagenase) is one of the MMP members responsible for degrading collagen and enhancing bone calcification. *MMP-1* knockdown was found to inhibit alkaline phosphatase activity and mineralisation and decrease the expression of *RUNX2, OSX, OPN* and *bglap* in bmMSCs, which indicates that activating MMP-1 has a role in osteogenesis. In relation to infection, it was found that human monocytes upregulated *MMP-1* expression during tuberculosis (248).

MMP-13 (collagenase 3) is an essential enzyme that plays a crucial role in dissolving bone matrix and cartilage degradation (249). Studies have demonstrated that MMP-13 overexpression can be associated with pathological conditions such as malignant

tumours, breast tumours or infection *(*as *P. aeruginosa*) and develops a spontaneous osteoarthritis (OA)-like articular cartilage destruction phenotype (250). Genetic models of *MMP-13* and *MMP-9* deficiency exhibit skeletal defects resulting from impaired enzyme activity (251). Additionally, *MMP-1*3 overexpression is believed to lead to increased pre-osteoclast differentiation and subsequent activation. In the current study, culture of MSC-CM with infected osteoblasts had no impact on *MMP-1* and *MMP-1*3 expression.

Protein levels of RUNX2 and MMP-1 were investigated in order to affirm the mRNA results and discern an active presence of the proteins in MSC-CM. Whilst there was no marked change in *MMP-1* gene expression compared to control there was a slight decrease in the level of protein when infected osteoblasts were incubated with MSC-CM. Similarly, *RUNX2* gene expression was unchanged markedly in infected osteoblasts post culture with MSC-CM. At the protein level however, RUNX2 showed a slight decrease when osteoblasts were infected. RUNX2 levels increased when infected osteoblasts were cultured with CM1 followed by a gradual decrease with higher doses of CM2 and CM3.

The findings in this chapter include a critical limitation which impact outcome in different settings. In this study, we measured MSC-CM effect on gene expression after 24 hours of MSC-CM culture. Extended incubation time periods of MSC-CM culture with infected osteoblasts could enhance their osteogenic functions to different degrees. A long-term study with at least two more incubation time points might be

conducive to a conclusive understanding of the influence/effect of MSC-CM on the gene expression of infected osteoblast.

In conclusion, MSC-CM revealed a broadly positive and beneficial impact on an infected 2D model. This study showed that exposure to the MSC-CM inhibits bacterial growth, and (ii) does not prompt osteogenic differentiation whilst causing downregulation of osteocalcin. To confidently claim the effect of MSC-CM on osteoblastic differentiation, osteocalcin quantification from the media and ALP activity of treated osteoblasts would be needed. However, the exact mechanism by which human MSC-CM inhibits the bacterial growth in the infected osteoblasts remains to be investigated.

5. Chapter Five

The molecular and functional responses of bone cells to *S. aureus* infection and during the administration of MSCs.

5.1. Overview

Osteomyelitis (OM) is an infectious disease of the bone, primarily caused by the opportunistic pathogen, *S. aureus*. Once *S. aureus* colonises bone cells, a cascade of inflammatory events occurs that eventually results in dramatic modifications in bone tissue and a loss of diverse bone units such as cortical and trabecular bone, bone marrow, periosteum, and the surrounding soft tissue (252). The molecular mechanism of OM pathogenesis which involves the host-pathogen interface by osteoblasts, has yet to be fully understood. Therefore, OM has been modelled in different experimental approaches. Most studies aiming to understand the mechanism of OM have employed clinical patient-derived data and laboratory-based models. Developing models that partially or entirely replicate the infection process on bone cells and tissues will help us better understand multifaceted processes that cause bacterially induced bone destruction. Moreover, this will aid researchers to develop new methods for combatting such infections. However, the strengths and the limitations of existing models must be understood to create an effective new model.

5.1.1. In vivo models of bone

In vivo studies, which employing bone disease models, are used to investigate biochemical factors involved in metabolic bone diseases, examine bone development and growth, and test new bone substitutes. For decades, such *in vivo* models have been widely used to study the remedial of impaired bone resulting from clinical conditions, such as diabetes and metastatic tumours (253). Moreover, *in vivo* models have several benefits over *in vitro* models. For example, they can employ a large number of cells. They can also contain complicated but intact cell-to-cell or cell-ECM interactions that are vulnerable to the host system's influences. Additionally, different

types of animal species can be used to develop *in vivo* models. Several *in vivo* studies, focusing mainly on bone infections, have employed a range of mammals, from dogs to rodents and rabbits. Outcomes of these *in vivo* studies have improved scientific understanding of OM. For instance, *in vivo* studies clearly found that *S. aureus* are able to internalise osteoblasts and osteocytes (254) and utilises the canalicular network of the cortical bone (255). Nevertheless, it is essential to note that animal studies are sophisticated, time-consuming, and expensive. Moreover, to prove relevant effects in *in vivo* studies, a huge sample quantity is required. De Mesy and his group conducted *in vivo* study using 30 mice (i.e., 10 for each experiment) to develop an infected model of *S. aureus* in mouse long bone tissue (255). Additionally, Craig *et al.* (256) used 42 rabbits to develop a knee defect model to examine biomaterial infection effect and revealed a vast number of animals were required in such studies, which can have many ethical implications. Therefore, *in vitro* studies often precede *in vivo* testing to assess factors such as cytotoxicity, mechanism, and the proliferative impacts of new treatments on bone cells.

5.1.2. In vitro models of bone

In vitro studies use standard plastic culture vessels to grow 2D single- or dual-cell cultures. Thus, they are easy to perform and cost-effective. It is also possible to carry out reproducible and high throughput experiments due to the excellent control that such studies facilitate over culture conditions (i.e., cell number and differentiation) (257). Over years, the complexity and relevance of such studies have advanced significantly, with 3D cell cultures being used on cell spheroids or scaffolds (258). Nonetheless, no original extracellular matrix (ECM) or 3D arrangement exists under *in vitro* conditions. This can cause changes in cell morphology and protein expression

in 2D cultures. Thus, findings of *in vitro* studies are often non-representative of *in vivo* findings, making it challenging to translate these results into clinical practice. In vitro bone disease models tend to be simplistic in nature, as they are designed to represent the multicellular bone marrow complex by using one or multiple cells within a culture system (259). Regarding bone development, our understanding of osteoclast development, osteoblast mineral production, immune cell response to bacterial inducements, and different bone marrow cell responses to *S. aureus* have been greatly enhanced due to *in vitro* cultures that have used primary osseous cells and other cell lines. Nonetheless, these models fail to consider sophisticated cellular interactions or the 3D positioning of various cells in cell niches that are commonly observed in situ (253).

5.1.3. Ex vivo models of bone

Explant cultures (sometimes referred to as organ or *ex vivo* cultures) are used to grow and maintain explanted tissues *in vitro*. Therefore, these cultures are thought to be ideal for investigating cells in the native ECM whilst preserving cell-cell and cell-matrix interactions, mimicking the *in vivo* condition. Additionally, *ex vivo* models can uphold cellular diversity within the skeletal system of a natural ECM, as present in *in vivo* models.

Ex vivo cultures support to eliminate systemic variables caused by complexity of *in vivo* animal experiments (258). This complexity can be reduced by designing a controlled environment where biological and mechanical factors can be independently examined. Another advantage of *ex vivo* models is facilitating direct access to specific tissues, allowing cells to be controlled and manipulated during culture with other cells and reagents. This will enable researchers to examine important cellular, biological,

or mechanical factors that can be independently studied in a 3D space, ultimately enabling control and manipulation of these models (258, 260, 261). Therefore, *ex vivo* model combines the advantages of *in vitro* and *in vivo* models whilst also considering ethical considerations (262).

Ex vivo models are also used to analyse essential the mechanisms of skeletal development, matrix turnover, growth, endochondral ossification, and the impacts of mechanical loading (258). Experimental settings have mimicked the host-pathogens, including MgHA/Col scaffolds (system based on a magnesium-doped hydroxyapatite/collagen I), collagen glycosaminoglycan scaffolds, titanium substrates coated with MgHA, or mouse bone explants (253). Overall, *ex vivo* studies can generate meaningful insights which can resolve the gap between *in vitro* and *in vivo* studies. Additionally, *ex vivo* studies effectively address ethical issues of animal testing. In this respect, using an *ex vivo* human bone explant can produce a critical picture, a novel innovation of the bone matrix. In contrast to *in vivo* studies, which require large numbers of experimental animals, *ex vivo* models demand much fewer animals as multiple experiments can be carried out on various tissues taken from a single animal.

In past decades, several types of *ex vivo* bone models have been developed, including extended bone models, calvaria models, limb bone models, organic slice models, femoral head models, and bone core models (263). These *ex vivo* models were established to analyse events that may cause inflammatory bone destruction, osteoarthritis, and periodontitis.

5.2. Aim

This study aimed to establish an *ex vivo* model of bone infection and to test the efficacy of therapeutic approaches using MSCs in OM in order to investigate molecular and functional responses of bone cells to *S. aureus* infection and during the administration of MSCs. This work mainly focuses on creating a novel 3D model of bone infection using a human bone tissue explant, which better represents physiological bone microenvironment in which bone cells, specifically osteoblasts/osteocytes, are present.

5.3. Objectives

1. Culture bone plugs and evaluate cell viability using Alamar Blue Assay.
2. Harvest the plugs and conduct histological analysis to establish t=0 appearance.
3. Harvest the plugs and conduct a gene expression study of osteogenic genes, degradative enzymes and inflammatory cytokines using qPCR.
4. Infect bone plugs with bacteria and assess histology.
5. Analyse infected plugs as in (2) and (3) and assay supernatant for osteogenic/ osteoclastic proteins associated with osteogenesis by western blotting.
6. Load MSC-CM onto infected bone plugs and analyse their biology.

5.4. Methods

5.4.1. Preparation of human cancellous bone explant model

Human femoral head bones were obtained from patients undergoing hip replacement surgery at Southmead hospital in Bristol who had written informed consent. The femoral head samples were provided by Mr Niall Sullivan (A surgeon in Southmead hospital, Bristol, UK) and collected in sterile containers. The femoral head was washed several times to remove the contaminating blood and fat. By using biopsy punch tools (gifted from Ying Fei, a PhD student in Dr Mo Sharif group), cylindrical bone plugs were generated. Cartilage and debris were removed, and bone plugs were washed in PBS. The femoral head was made into small cylindrical-shaped, cancellous bone plugs with 3 mm thickness using an aseptic instrument with the help of cutting punch biopsy tools and transferred into a 12-wells plate containing 3 ml DMEM without antibiotics and the plate was placed in the incubator at 37°C.The human femurs size enabled many blocks to be cut from the cancellous region of an individual bone. These cancellous bone explant models were cultured with DMEM medium supplemented with 1% Glutamax and 1% ITS and incubated at 37˚C and 5%CO_2.

5.4.2. Bacterial strains and bone infection

On the day of infection, bacteria were adjusted to different concentrations of $3X10^6$, $1X10^7$ and $3x10^7$ CFU/ml in DMEM media (no antibiotics/ no FBS). Each bone plug was transferred into a 12-wells plate using sterile forceps. A 3 ml of each of *S. aureus* suspension was added into each well. Control bone plugs were incubated with DMEM as a negative control. The plate was incubated for 1, 4, and 24 hours at 37°C. At the end of each infection time, bone plugs were washed with infection media to remove unbound bacteria.

In some studies, *S. aureus* was fixed in 4% PFA. A 10-ml disposable loop was used to collect colonies of *S. aureus* from the MHA plate and transferred into bijoux tubes containing 2 ml of 4% PFA. The bacterial suspension was given constant agitation using vortex mixer and the tube was centrifuged at 4,000 *g* for 10 min. The supernatant was discarded, and bacterial pellet washed 3x times using PBS. After washing, 2 ml of PBS was added into the pellet and bacterial suspension was given proper homogenisation with gentle mixing. The absorbance was read by a light spectrophotometer adjusted at 600 nm. After bacterial concentration calculated, the bacteria were adjusted to $3x10^6$ or $1x\ 10^7$ and $3x10^7$ CFU/mL in DMEM media (no antibiotics/no FBS).

5.4.3. Determining bone cell viability in the presence of *S. aureus*

At the end of infection, Alamar Blue assay (resazurin salt) was used to measure the metabolic activity of bone cells. Alamar Blue was added to each well of bone plugs in the media to a final concentration of 10% (v/v). The plate was incubated for 2 hours at 37˚in CO_2 in the dark. After 2 hours of incubation, 200 µl of the mixture was transferred into 96 well plates, and fluorescence intensity was read at 560 nm for excitation and 590 nm for emission on a spectrophotometer. The percentage difference between treated and control cells was calculated according to manufacturer instructions, as described in section 3.4.1.

5.4.4. Recovery of viable *S. aureus* from infected bone plugs and CFU count assay.

At the end of the infection, each bone plug was removed from the well and washed with PBS to remove the unbound bacteria. Bone plugs were placed in folded foil and pulverised using mortar. Crushed bone plugs were transferred into a tube containing

3 ml sterile PBS. The bone fragments were vortexed for 1 minute and serially diluted in saline (1:10 dilution). The bacterial CFU of *S. aureus* was determined by plating each dilution on an MHA plate and incubating overnight at 37°C. The number of bacterial cells as CFU/mL was determined.

5.4.5. Fixation and decalcification of bone plugs for histological staining

At the end of the infection period, bone plugs were washed with infection media to remove unbound bacteria. The bone plugs were transferred into a bijoux tube containing 2 ml of 4% PFA for 24-48 hours for fixation. Then, bone plugs were rinsed with PBS and processed for decalcification. The decalcification solution is composed of hydrochloric acid (12%), EDTA (0.07%), sodium tartrate (0.014%), potassium tartrate (0.8%) and distilled water. The bone plugs were placed in 4 ml decalcifying solution under constant agitation for three weeks and with continuous change of solution every two days.

5.4.6. Haematoxylin and eosin staining

At the end of the decalcification step, bone plug samples were sent to the histology service facility at the University of Bristol for tissue processing, sectioning, and staining. Bone plugs were wax embedded and sectioned using a microtome. Afterwards, slides were processed for staining by haematoxylin and eosin stain. Briefly, decalcified paraffin-embedded sections were dewaxed by soaking the slides in histo-clear for 30 minutes. Afterwards, the slides were immersed in descending concentrations of alcohol (100%, 90% and 70%) for 5 minutes in each concentration. After a quick wash of slides with tap water, HE stains was performed to stain bone tissues.

For HE stains, slides were placed in Ehrlich haematoxylin dye for 7 minutes. The haematoxylin stains the cell nuclei as blue/ dark dots. Tissue slides were then placed under tap water, followed by quick dip into alcohol for seconds to remove haematoxylin (differentiation). Subsequently, tissue slides were transferred into Scott's tap water (NAHCO3MgSO4) for seconds, and the tissue was counterstained with eosin stain for 10 seconds. Eosin stain stains the extracellular matrix and cytoplasm pink. A subsequent quick wash with tap water, followed by transient dip the tissue slides in ascending concentrations of alcohol (70%, 90% and 100%) for 5 minutes.

Bone tissue slides were placed in xylene, mounted using mounting medium (DPX), and covered with coverslips on the top to protect the tissue samples. Slides were left to air-dry before examination. All the staining procedures were performed inside a fume hood and at room temperature. Sections were then examined under a light microscope.

5.4.7. RNA extraction from bone tissues

At the end of infection period, bone plugs were washed with PBS, wrapped in foil, placed into liquid nitrogen (snap freeze), and then pulverised in liquid nitrogen-cooled mortar. The TRIzol method was used for RNA isolation. Following pulverisation, the powdered bone sample was transferred into RNase-free tubes. A volume of TRIzol was added (according to weight of the bone sample), and the tubes were stored at -80˚C until further RNA extraction.

On the day of RNA extraction, samples were centrifuged for 10 minutes at 4^{o}C, 11,500 rpm to move solid tissue. The clean supernatant containing the DNA and RNA was transferred to sterile 15-ml tube. A phase separation step was carried out to obtain the pure RNA. A volume of chloroform was added to the sample (according to the volume

of TRIzol) and the tube was vortexed for 15 seconds. Samples were centrifuged for 15 minutes at 4°C and at 11,500 rpm to separate the nucleic acid phase, and the upper aqueous layer was transferred to an RNase-free tube. An equal volume of isopropyl alcohol (isopropanol) was added and incubated for 10 min. The samples were centrifuged for 10 min at 12,000 rpm at 4°C.

For RNA precipitation, the supernatant was removed, and the RNA pellet was washed with 1 ml of 75% ethanol and centrifuged for 5 min at 8,000 rpm at 4°C. The supernatant was discarded, and the RNA pellet was air-dried for 5 to 10 min before the RNA was re-suspended in RNase-free water. RNA was reverse transcribed to cDNA following the method described in section 2.2.9.

5.4.8. Enzyme-linked immunosorbent assay (ELISA)

To investigate the effect of *S. aureus* infection on bone resorption, the release of cross-linked C-terminal telopeptide of type I collagen (CTX) from the bone matrix into medium was quantified using ELISA. The CTX level released into the media was analysed according to the manufacturer's instructions using Human CTX-I (NBP2-69073) ELISA kit. A standard curve was established using a four-parameter logistic curve, with standard concentration on the x-axis and OD values on the y-axis.

5.4.9. Western blot of osteocalcin and MMP-1 in bone supernatant media

At the end of the infection of the bone plugs, the culture media from each well was transferred into clear tubes and stored at -20°C. The supernatant was concentrated using ultra-centrifugal filtration tubes. The concentrated medium was separated using SDS-polyacrylamide gel electrophoresis and transferred onto PVDF membranes. The membrane was blocked in 5% non-fat milk (w/v) and probed with the appropriate primary antibody overnight at 4°C with constant agitation. Unbound antibody was

removed by rinsing the membrane with TBST buffer. The protein bands were detected using species-specific horseradish HRP-conjugated secondary antibody for 1 hour at room temperature. Bands were determined by chemiluminescence. The detailed method is described in Section 2.3.

5.4.10. Gene expression in infected bone cultured with MSC-CM

To investigate potential therapeutic effect of MSCs on infected bone explants, bone plugs were infected and treated with MSC-CM. Bone plugs were cultured with 3 ml of culture medium (DMEM without antibiotics + ITS) in a 12-well plate. On the day of the infection, bone plugs were washed with PBS, then studied under different conditions: (1) bone plugs were incubated in 3 ml of DMEM media (control group, no bacteria added), (2) bone plugs were infected with *S. aureus* at a final concentration of $3x10^7$ CFU/ml in DMEM media and incubated for 24 hours, (3) bone plugs were cultured with *S. aureus* at a final concentration of 3x107 CFU/ml in MSC-CM and incubated for 24 hours and (4) bone infected with *S. aureus* for 24 hours and then MSC-CM was added and incubated for 24 hours.

In all conditions, bone culture was performed in a CO_2 incubator at 37°C. At the end of incubation, bone plugs were washed and processed for RNA extraction and qPCR assay as described in section 2.2.9.

5.5. Results

5.5.1. Macroscopic analysis of bone femur head model

The human femoral trabecular model was used in the study. Figure 5-1 shows a representative sample of the femoral head and extracted plugs used in the study.

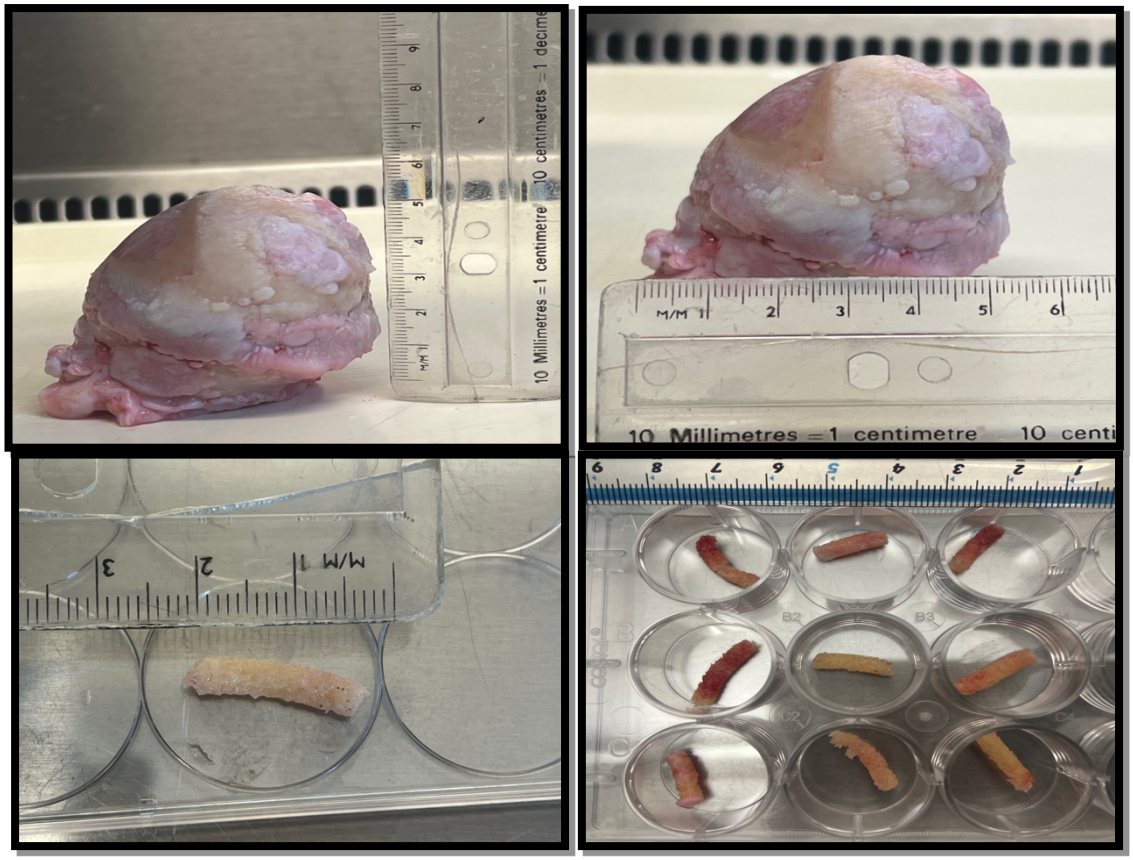

Figure 5-1 Macroscopic appearance of human bone sample. Femoral head was collected from patient following hip replacement surgery. Bone plugs were created using bone biopsy punch instrument. Top photos show a whole femoral head taken from an osteoarthritic joint. Bottom photos show extracted bone plugs used in the experiments.

5.5.2. The metabolic activity of bone cells during *S. aureus* infection of human bone explant

First, we investigated if bone cells viability was sensitive or altered following an infection with live *S. aureus* using increasing concentrations of the bacteria (Figure 5-

2). The metabolic activity of bone cells post infection was assessed using Alamar Blue assay (resazurin salt). We found that the presence of live *S. aureus* altered the mitochondrial activity of bone cells in the plugs (Figure 5-2A). The metabolic activity of infected bone cells increased reaching a maximum between 200 and 400% of uninfected control when cultured with all concentrations of live *S. aureus* for 4 hours. The metabolic activity at 4 h appears to correlate with the apparent increase in bacterial CFU seen at 4 h (Figures 5-3). The activity declined for all concentrations however, following infection for 24 hour, to approximately 20% of uninfected bone plugs. The Mean±SD values were for the 1-hour point, 132.4±130.26, for 4 hours point, 224.40 ± 262.90, and for 24 hours point, 47.55 ± 46.81).

To ascertain that this metabolic activity is dependent on the viability of *S. aureus*, we infected bone plugs with increasing concentration of dead *S. aureus* (fixed with 4% PFA). There was statistically not significant reduction in the metabolic activity of bone plugs infected with dead *S. aureus* at all concentrations used (Figure 5-2B). The lower metabolic activity seen with fixed cells likely indicates that there was a contribution made to the assay by viable bacteria. This indicated that *S. aureus* viability impacts the metabolism and fate of bone cells in the plugs independent of the bacterial concentration, with the caveat that the assay may also detect bacterial metabolic activity.

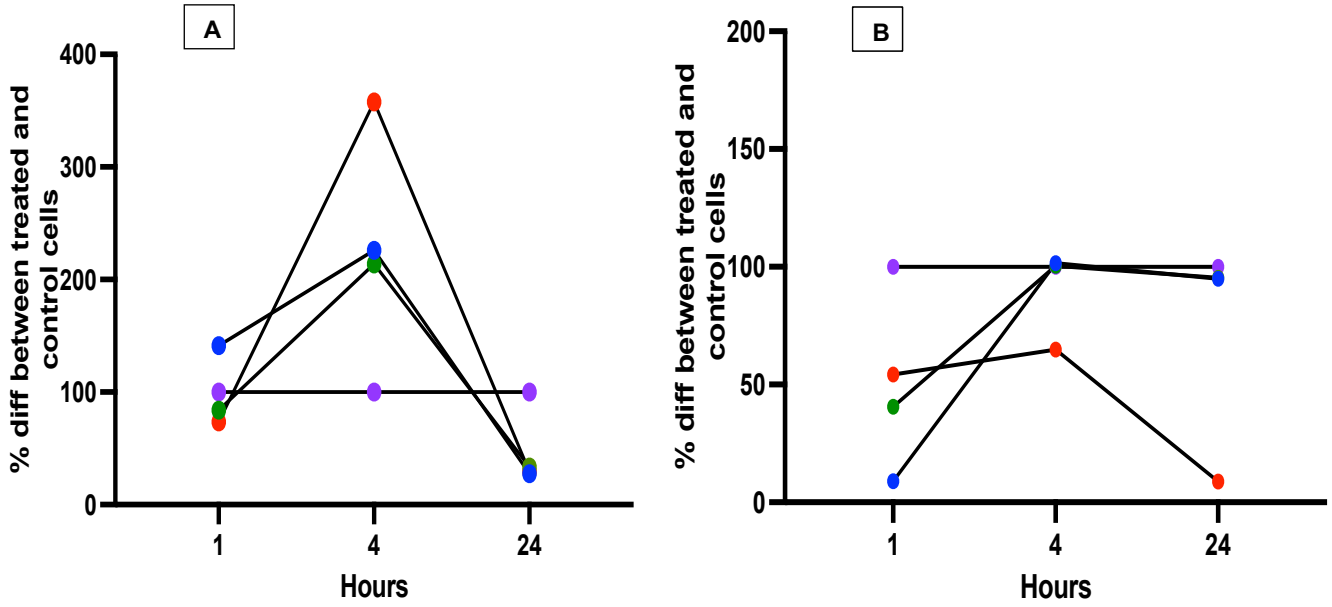

Figure 5-2 Assessment of bone cells metabolic activity in *S. aureus* infected bone explants. Bone plugs were infected with different concentrations of live *S. aureus* (A) or dead (PFA fixed) *S. aureus* (B) for 1, 4 and 24 hours. At end of incubation, Alamar Blue (resazurin salt) was added to the media for 2 hours, an aliquot of 200 µl was transferred into 96 wells flat bottom plate for fluorescence was measurement. The metabolic activity of viable cells was expressed as % difference between treated and control cells. A and B are performed in triplicate. Purple dots represent = 0 CFU/ml (control), red dots indicate= $3x10^6$ CFU/ml, green dots represent = $1x10^7$ CFU/ml, blue dots represent =$3x10^7$ CFU/ml. (n = 3)

5.5.3. Recovery of viable bacterial colonies from bone human bone plugs

Our experiment aimed to establish an infected 3D model bone. The development of bone infection was evaluated by quantifying the bacterial burden on and adhesion to bone cells during the early phase of infected. Three different concentrations of *S. aureus*, $3x10^6$, $1x10^7$ and $3x10^7$ CFU/ml were added to human bone plug cultures and incubated for 1, 4 and 24 hours. Bone plugs were washed to remove unbound bacteria then homogenised using a mortar and pestle. Little difference was found in the total *S. aureus* recovered across the three doses of bacteria in the experiment (Figure 5-3). The general trend was an initial increase in total *S. aureus* CFU/ml between 1 and

4 hours and a subsequent drop after 4 hours post-infection with approximate reading of $1x0^6$ CFU/ml at 1 hour, $1x10^{10}$ CFU/ml at 4 hours and $1x10^8$ CFU/ml at 24 hours post-infection (Figure 5-3). Remarkably, we noticed that the metabolic activity of bone cells was seemingly elevated at 4 hours (Figure 5-2), and this might correlate with the apparent increase in bacterial CFU seen at 4 hours (Figures 5-3), also indicative of a possible contribution to the assay by the bacteria.

To understand the bacterial load recovered from the bone plugs, we compared the number of bacteria in the supernatant (i.e., the culture media from bone plug wells) and *S. aureus* number alone (i.e., wells containing *S. aureus* only) (Figure 5-4). *S. aureus* count from the supernatant wells (alone in the wells) between 1 and 4 hours was quite steady and compared to that from bone plugs; however, between 4 hours and 24 hours, *S. aureus* CFU count increased dramatically for *S. aureus* only wells, reaching approximately $1x10^{14}$ CFU/ml. The bacterial count plug supernatant was far less, with an estimated $1x10^8$ CFU/ml. The number of *S. aureus* retrieved from crushed bone plugs was less than other groups except at 4 hours. The range of inoculation appears not to influence the observed outcome; the lowest concentration ($1x10^6$ CFU/ml) showed similar trend to higher concentrations, potentially indicating saturation of media at the lowest concentration.

Taken together the presence of bone appears to limit the growth of *S. aureus* in this system over time, possibly due to ECM hindrance or the release of antibacterial factors from bone plug cells.

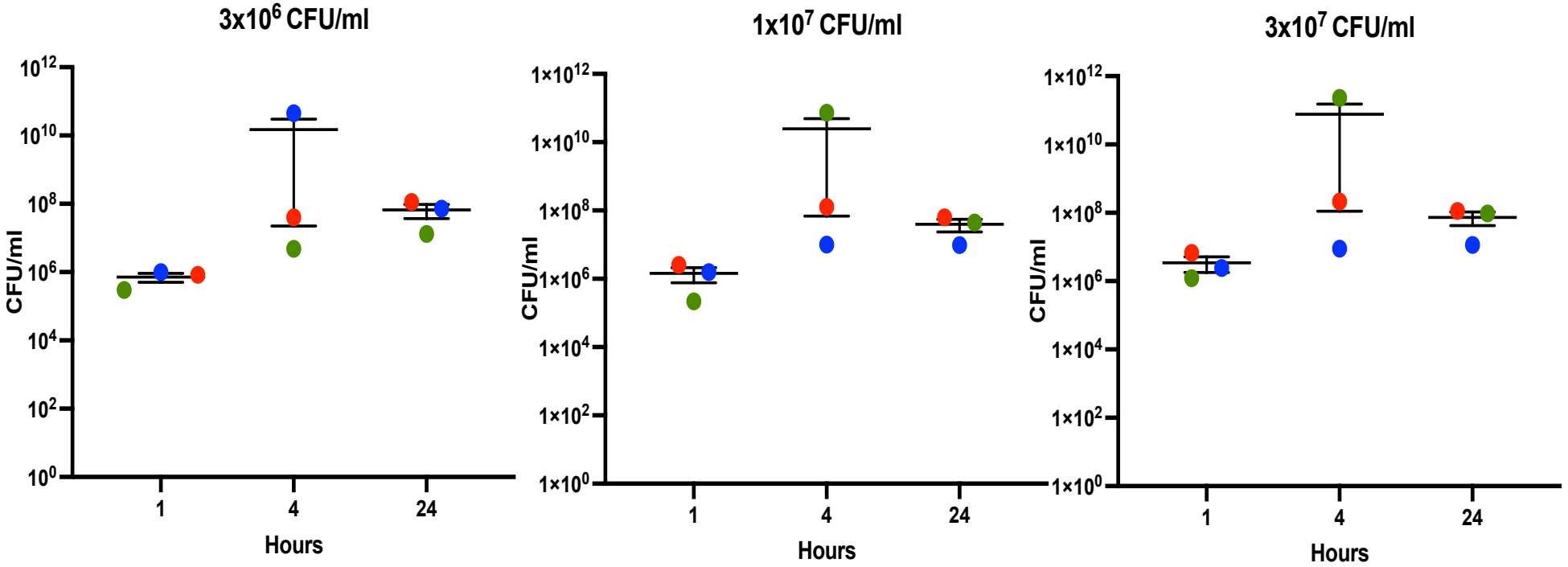

Figure 5-3 Quantification of viable *S. aureus* recovered from the infected bone explant: Human bone plugs were infected with *S. aureus* at $3x10^6$, $1x10^7$ and $3x10^7$ CFU/ml for 1,4 and 24 hours. The recovered bacteria from plug washing were plated on MHA plate. The number of viable bacteria was counted and calculated as CFU/ml. Results represents 3 independent experiments. Each dot represents the mean of 3 technical replicates and the coloured dots represent 3 biological samples (n=3).

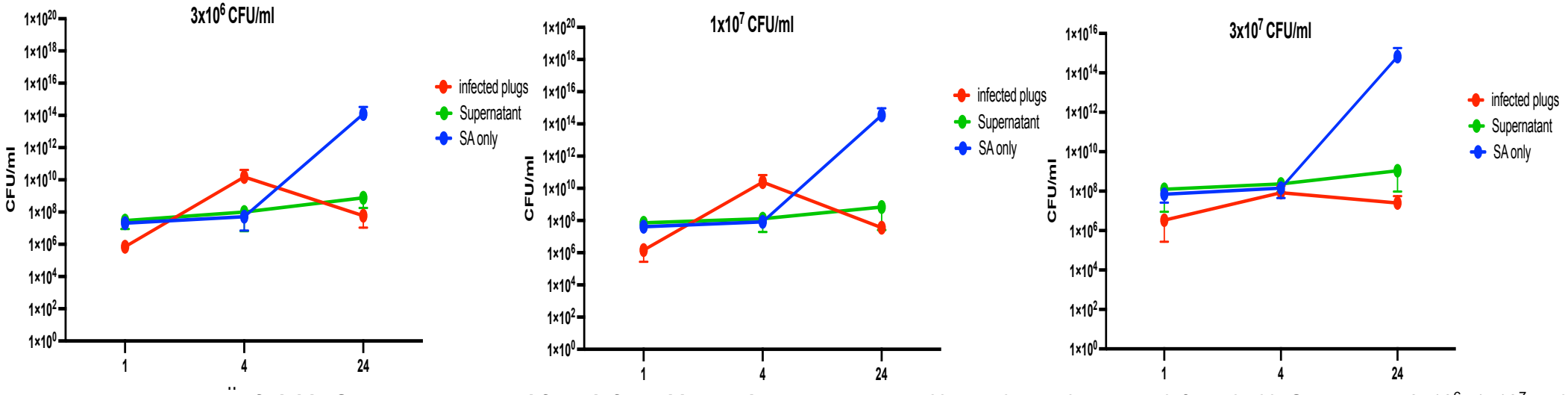

Figure 5-4 Quantification of viable *S. aureus* recovered from infected bone plugs supernatant. Human bone plugs were infected with *S. aureus* at $3x10^6$, $1x10^7$ and $3x10^7$ CFU/ml for 1, 4 and 24 hours. At the end of infection, the supernatant of infected bone was plated on MHA and the viable bacteria was counted (green line). Bacteria were counted from crushed, infected bone plugs (red line). Supernatant from wells containing *S. aureus* only (control) was plated onto MHA plate and the number of viable bacteria counted. Count was expressed as CFU/ml. Results represents 3 independent experiments. Each dot represents the mean of the 3 technical replicates and the three coloured dots represent 3 biological samples.

5.5.4. The stimulatory effect of *S. aureus* on CTX release from the infected bone explant

In this experiment, the matrix degradation fragment (CTX) released into the bone culture media from the infected bone plugs was analysed using ELISA. The serum level of CTX is used as a marker of osteoclastic activity; a high level of CTX indicates bone resorption (Figure 5-5). *S. aureus* did not stimulate CTX release from infected bone plugs at concentrations of $3x10^6$ and $1x10^7$ CFU/ml. The level of CTX was similar to the baseline seen in the control group (approximately 0.2 ng/µl). The observed trend was independent of the infection period. There was gradual increase in the release of CTX from bone plugs at the highest concentration ($3x10^7$ CFU/ml). The increase was statistically not significant among groups however (Figure 5-5).

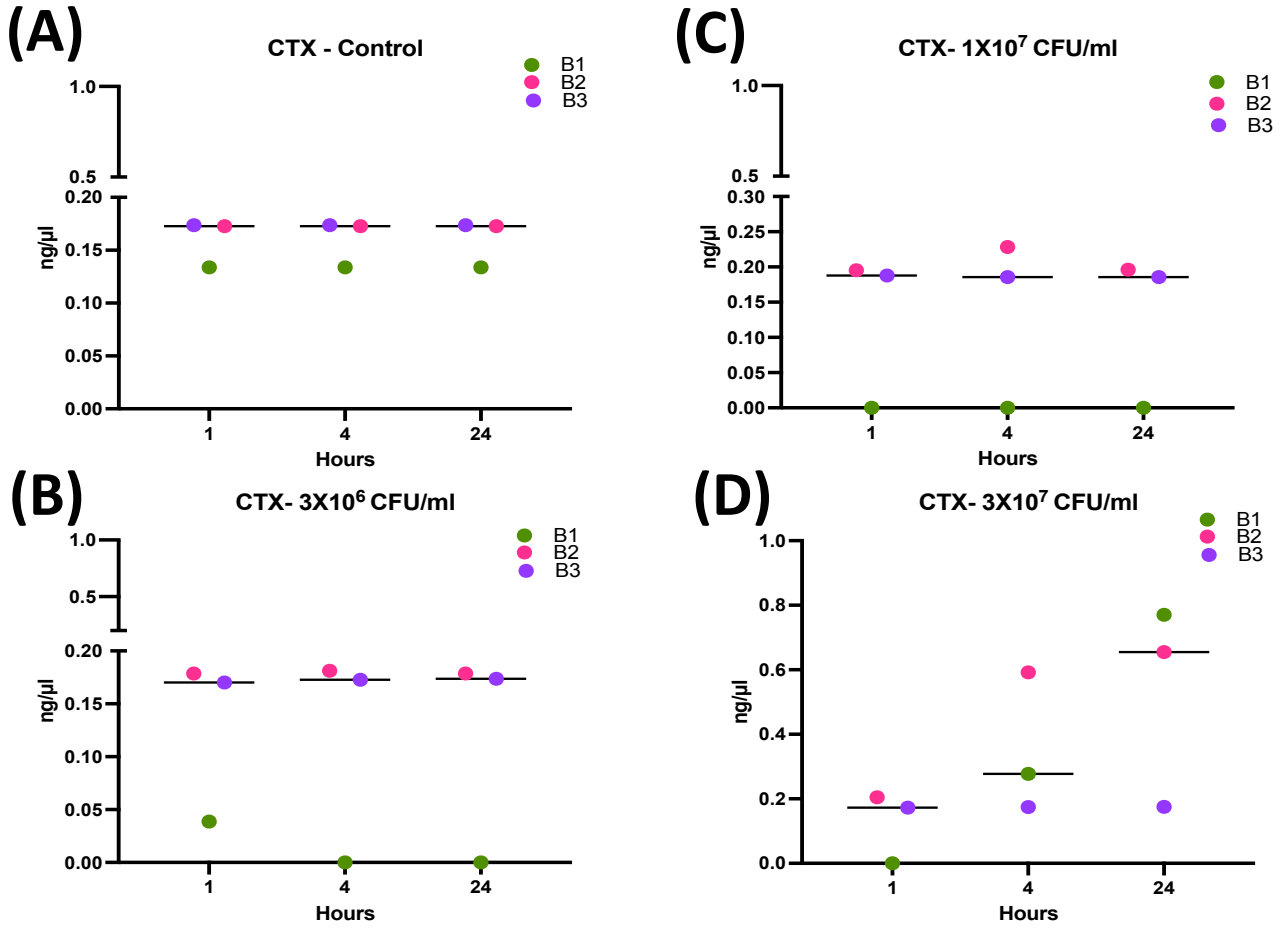

Figure 5-5 The stimulatory effect by *S. aureus* on CTX release. Human bone plugs were infected with *S. aureus* at $3x10^6$, $1x10^7$ and $3x10^7$ CFU/ml and incubated for 1, 4 and 24 hours. At the end of infection, the supernatant from each condition was collected in sterile tubes and the CTX level analysed by ELISA. (A) control (B) $3x10^6$ CFU/ml *S. aureus* (C) $1x10^7$ CFU/ml *S. aureus* (D) $3x10^7$ CFU/ml *S. aureus.* Bars indicate the mean. (n = 3)

5.5.5. qPCR analysis of osteogenic/osteoclastic markers, inflammatory cytokine and bone matrix degrading enzymes in infected bone explants

Real-time qPCR experiments were performed to investigate if *S. aureus* infection of human bone explants caused changes in the expression of osteogenic/osteoclastogenic activity genes, inflammatory cytokines, and matrix metalloproteinases enzymes in explant cells.

S. aureus impact on bone formation in the human bone explant was assessed by evaluating the osteogenic markers *ALP*, *bglap* and the osteogenic transcription factor RUNX2. *RUNX2 and ALP* in infected bone cells were differentially expressed compared to normal untreated bone. The expression varied with infection period and bacterial load; however, the detectable levels were similar to control with non-significant statistical difference. *bglap* expression was quite unchanged compared to control group at the two low bacterial concentrations used. On the other hand, significant increase was detected when bone plugs were infected with $3x10^7$ CFU/ml at 4 hours post-infection. The expression declined however 24 hours post-infection to levels similar to uninfected plugs (Figure 5-6).

We also assessed the impact of *S. aureus* infection on the expression of *ACP5* (TRAP) and CSTK (Cathepsins K), both are markers of osteoclastic activity (Figure 5-7). CSTK expression at 1 hour and 4 hours post-infection showed little change compared to control. However, 24 hours post-infection, CSTK expression was significantly upregulated compared to the uninfected control. The upregulation was statistically significant across *S. aureus* concentration: 4- fold (p=0.0498), 30- fold (p= 0.0016) and 10- fold (p= 0.0251) at $3x10^6$,$1x10^7$ and $3x10^7$ CFU/ml, respectively. Similarly, there was significant increase in *ACP5* expression when bone was infected at the higher concentrations of $1x10^7$ (100- fold; p=0.0002) and $3x10^7$ CFU/ml (21- fold; p= 0.0016) for 24 hours. At the lowest concentration of *S. aureus* infection ($3x10^6$ CFU/ml), the expression of *ACP5* was similar to that of uninfected bone at all three-time points (Figure 5-7).

The effect of *S. aureus* infection on the expression of MMP-1 and MMP-13 was investigated. MMPs are enzymes responsible for the degradation of collagens in the

bone matrix. The mRNA level of *MMP-1* showed no detectable change compared to uninfected bone at any concentration of *S. aureus* at 1- or 4-hour incubation (Figure 5-8). At 24 hours post-infection the higher concentrations of $1x10^7$ and $3x10^7$ CFU/ml, there was a statistically significant increase in *MMP-1* expression (7 and 2-fold, respectively). MMP-13 expression showed no detectable change compared to uninfected bone at any concentration of *S. aureus* at 1 incubation (10-fold). There was statistically significant change at 24 hours with the $1x10^7$ CFU/ml concentration and at 4 hours with the $3x10^7$ CFU/ml concentration.

The inflammatory cytokine response represented by IL-6 and *IL-8* to *S. aureus* infection in the human bone explants was investigated (Figure 5-9). Stimulation of human bone samples with *S. aureus* resulted in no change in *IL-8* mRNA levels at any concentration or incubation period. *IL-6* showed no detectable change compared to controls at 1- or 4-hour incubation. At 24-hour incubation, there was significant upregulation at the higher two concentrations of $1x10^7$ and $3x10^7$ CFU/ml at 6 and 4.5-fold, respectively.

Table 5-1 summarises gene expression collectively as a heatmap. The table boxes were shaded with light green indicating fold change increase of more than 1 relative to control. Red shading indicated CT values below 1-fold change which represents downregulation relative to the control. ANOVA was used to analyse the significance of the fold change in gene expression. The boxes that display darker/dimmer green or darker/dimmer red indicate a fold-change with statistical significance.

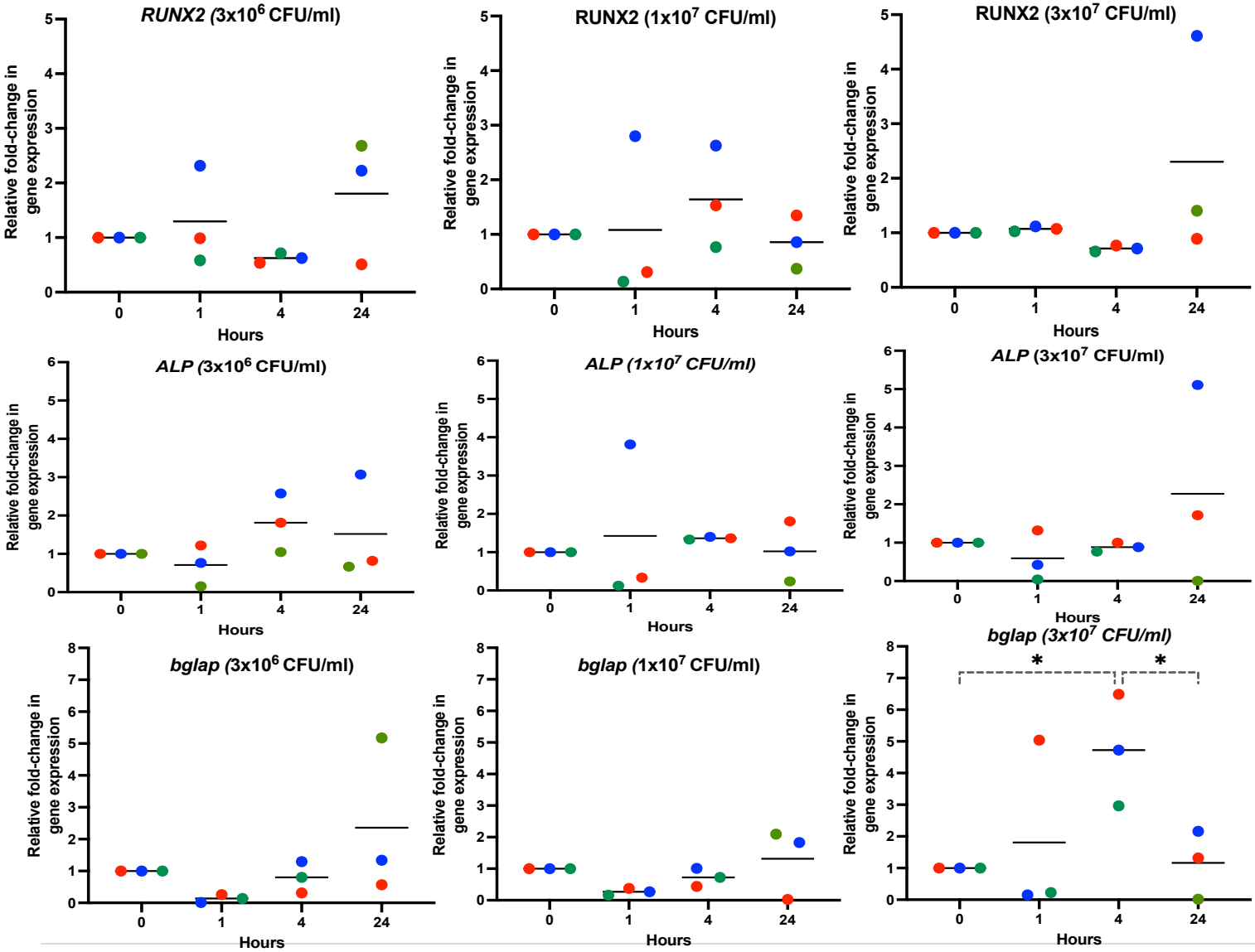

Figure 5-6 The stimulatory effect by *S. aureus* on osteogenic genes. Human bone plugs were infected with *S. aureus* at $3x10^6$, $1x10^7$ and $3x10^7$ CFU/ml and incubated for 1, 4 and 24 hours. At the end of each incubation, RNA was isolated, and cDNA synthesized. qPCR was conducted using TaqMan assays for *RUNX2, ALP* and *bglap*. All values are normalised to B2m expression CT values. *** = $p \leq 0.001$, ** = $p \leq 0.01$, * = $p \leq 0.05$. n=3.

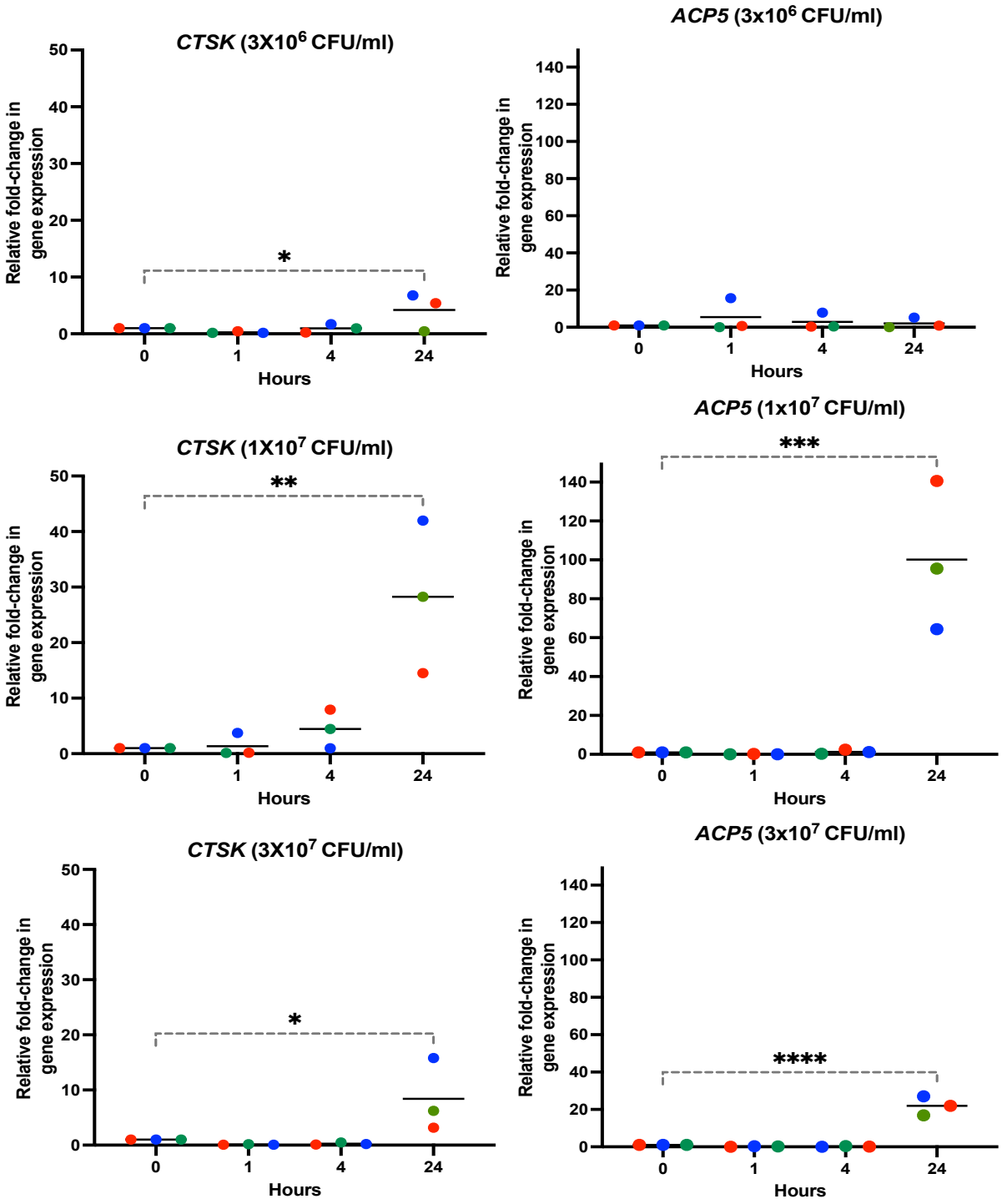

Figure 5-7 The stimulatory effect with *S. aureus* on osteoclastic genes. Human bone plugs were infected by *S. aureus* at 3x10^6, 1x10^7 and 3x10^7 CFU/ml and incubated for 1, 4 and 24 hours. At the end of each incubation, RNA was isolated and quantified using qPCR. TaqMan assays were used for *ACP5* and *CTSK*. All values are normalised to B2m expression. *** = p ≤ 0.001, ** = p ≤ 0.01, * = p ≤ 0.05. n=3.

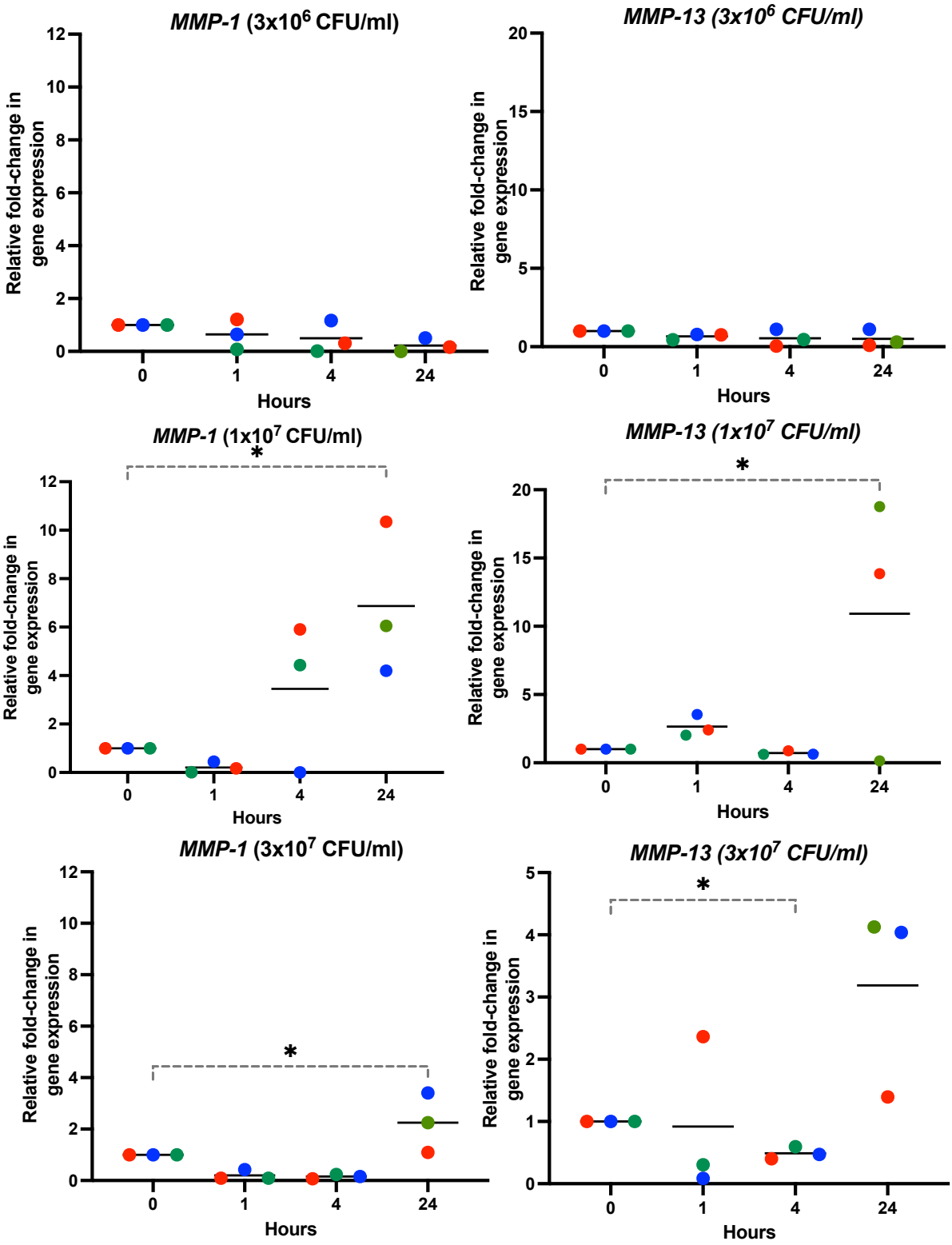

Figure 5- 5-8 The stimulatory effect by *S. aureus* on matrix degradation enzymes. Human bone plugs were infected with *S. aureus* at 3x10^6, 1x10^7 and 3x10^7 CFU/ml and incubated for 1, 4 and 24 hours. At the end of each incubation, RNA from bone plugs was isolated and transcribed into cDNA. TaqMan qPCR assays for *MMP-1* and *MMP-1*3 were conducted. All values are normalised to B2m expression CT values. *** = p ≤ 0.001, ** = p ≤ 0.01, * = p ≤ 0.05. n=3.

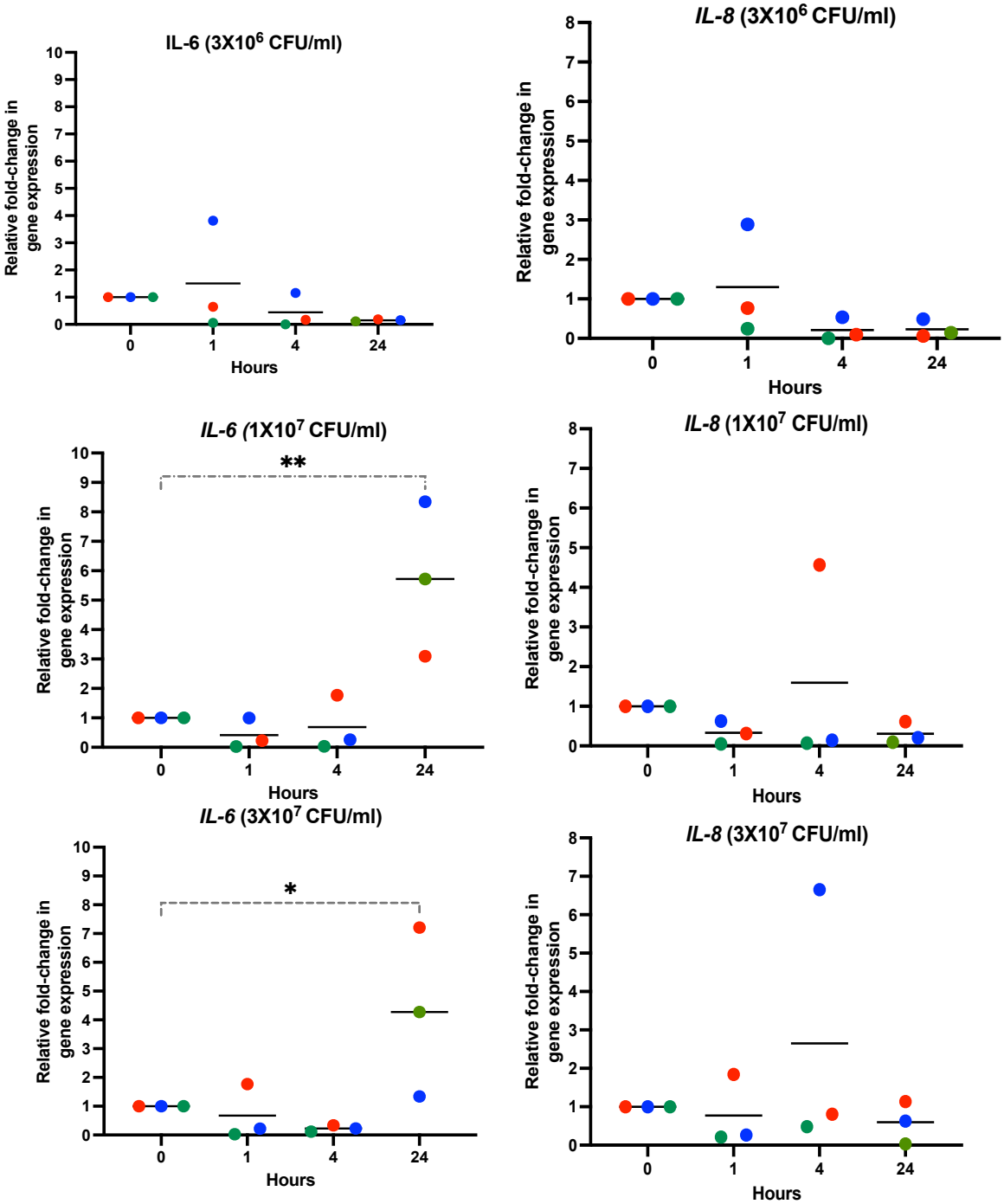

Figure 5-9 The stimulatory effect by *S. aureus* on cytokine genes. Human bone plugs were infected with *S. aureus* at 3x10^6, 1x10^7 and 3x10^7 CFU/ml and incubated for 1, 4 and 24 hours. At the end of each incubation, RNA was isolated and analysed using TaqMan qPCR assay for the expression of IL-6 and IL-8. All values are normalised to B2m expression CT values. *** = p ≤ 0.001, ** = p ≤ 0.01, * = p ≤ 0.05. n = 3.

Table 5-1 Gene expression heatmap of the genes investigated in human infected bone explant.

CFU/ml	Time (h)	Bone formation			Matrix degradation		Bone resorption		Cytokines	
		RUNX2	***ALP***	***bglap***	***MMP-1***	***MMP-13***	***ACP5***	***CTSK***	***IL_6***	***IL_8***
$3x10^6$	**0**	1	1	1	1	1	1	1	1	1
	1	1.295	1.071	0.1376	0.6434	0.6573	5.441	0.2643	1.507	1.299
	4	0.6253	0.7125	0.8021	0.4963	0.5337	2.849	0.9702	0.4421	0.2108
	24	1.806	2.302	2.361	0.2252	0.5009	2.028	4.213	0.151	0.2297
$1x10^7$	**0**	1	1	1	1	1	1	1	1	1
	1	1.082	1.425	0.2699	0.209	2.659	0.07809	1.353	0.4149	0.3306
	4	1.642	1.364	0.7263	3.448	0.7128	1.309	4.447	0.686	1.593
	24	0.859	1.022	1.316	6.868	10.92	100.2	28.25	5.72	0.305
$3x10^7$	**0**	1	1	1	1	1	1	1	1	1
	1	1.071	0.5953	1.806	0.2008	0.9177	0.1902	0.1044	0.6734	0.7722
	4	0.7125	0.8828	4.726	0.1541	0.49	0.212	0.2682	0.2284	2.648
	24	2.302	2.275	1.164	2.25	3.187	21.92	8.395	4.274	0.5992

5.5.6. Western blot assay of osteocalcin and MMP-1 in the bone supernatant

The expression of osteocalcin and MMP-1 was evaluated in the supernatant of the cultured infected bone to determine the effect of *S. aureus* infection on bone synthesis and resorption, respectively. There was an increase in MMP-1 expression compared to untreated bone. Osteocalcin expression showed time dependant decrease and almost abolished by 24-hour incubation with *S. aureus* infection (Figure 5-10).

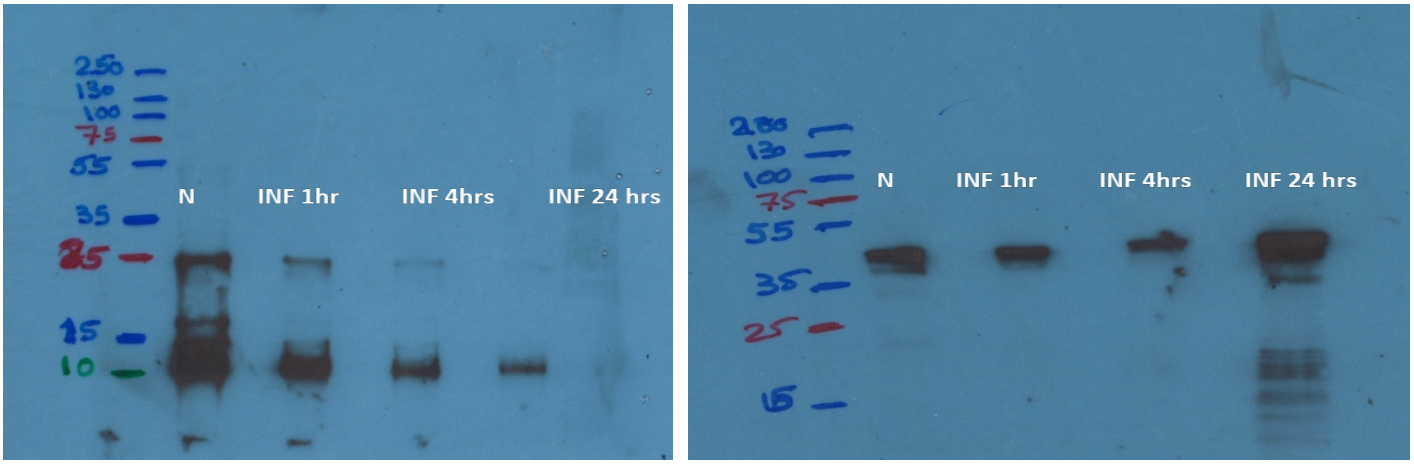

Figure 5-10 Western blot analysis of MMP-1 and osteocalcin protein in the supernatant. Human bone plugs were infected with *S. aureus* at $3x10^7$ CFU/ml and incubated for 1, 4 and 24 hours. At the end of each incubation, supernatant was collected. Western blot was performed, and protein probed with monoclonal antibodies against MMP-1 (50 KDa, right panel) and osteocalcin (5 KDa, left panel). Protein bands were visualised with an anti-mouse secondary antibody conjugated to horseradish peroxidase and developed with a chemiluminescence reagent. INF= infected bone. N= normal osteoblasts. n=1

5.5.7. Gene expression of osteogenic/osteoclastic, inflammatory and bone resorption enzymes in infected bone plugs exposed to MSC-CM

We investigated the effect of MSC-CM on osteogenic/osteoclastogenic markers, inflammatory cytokines, and matrix metalloproteinases enzymes in infected bone plugs after being treated with MSC-CM (Figure 5-11). The osteogenic marker, *bglap* expression increased significantly when infected bone was cultured with MSC-CM at 0 hours ($p=0.0027$). However, there was significant downregulation after MSC-CM

was added 24 hours post-infection (p= 0.0065) (Figure 5-11). This suggested a protective effect by MSC-CM that was less impactful once bacterial infection was established by 24 hours. The analysis of bone resorption markers ACP5 and CSTK revealed that there was significant upregulation of ACP5 expression in infected plugs control group, with an estimated change of 30-fold. MSC-CM treatment was found to downregulate ACP5 expression significantly at 0 and 24 hours to levels similar to uninfected controls (P <0.0001). There was 1.6 and 1.3 - fold change over uninfected control at 0 and 24 hours, respectively. *CTSK* expression was inhibited upon infection compared to uninfected control, albeit without statistical significance. The addition of MSC-CM at 0 or 24 hours appears to protect the plugs by maintaining levels of *CTSK* expression similar to uninfected control. The difference between infected control group and MSC-CM treated infected group was not statistically significant, however.

The expression of the inflammatory cytokines, IL-6 and IL-8, in response to adding MSC-CM onto *S. aureus* infected bone was measured. Significant upregulation in *IL-6* expression of approximately 600-fold was found upon infecting the bone plugs. The addition of MSC-CM resulted in significant downregulation reaching 10- fold change and 5- fold change at 0 and 24 hours, respectively, compared to uninfected control (p=<0.0001). There was no detectable change in *IL-8* expression in any of the studied groups compared to uninfected control.

The effect of MSC-CM cultured with infected bone explants on the expression of *MMP-1* and *MMP-13* was investigated. Similar to *ACP5* and *IL-6,* there was significant increase in *MMP-1* expression (8-fold) in infected bone plugs compared to uninfected control (p= 0.0002). This expression was downregulated significantly upon culture with MSC-CM at 0 and 24 hours, reaching levels similar to uninfected control ($p \leq 0.001$).

Unlike *MMP-1, MMP-13* expression was not affected by infecting the bone plugs. The addition of MSC-CM to infected plugs has however led to statistically significant increase in *MMP-13* expression at 0 hours ($p= 0.0003$) that appears to diminish by 24 hours to levels similar controls.

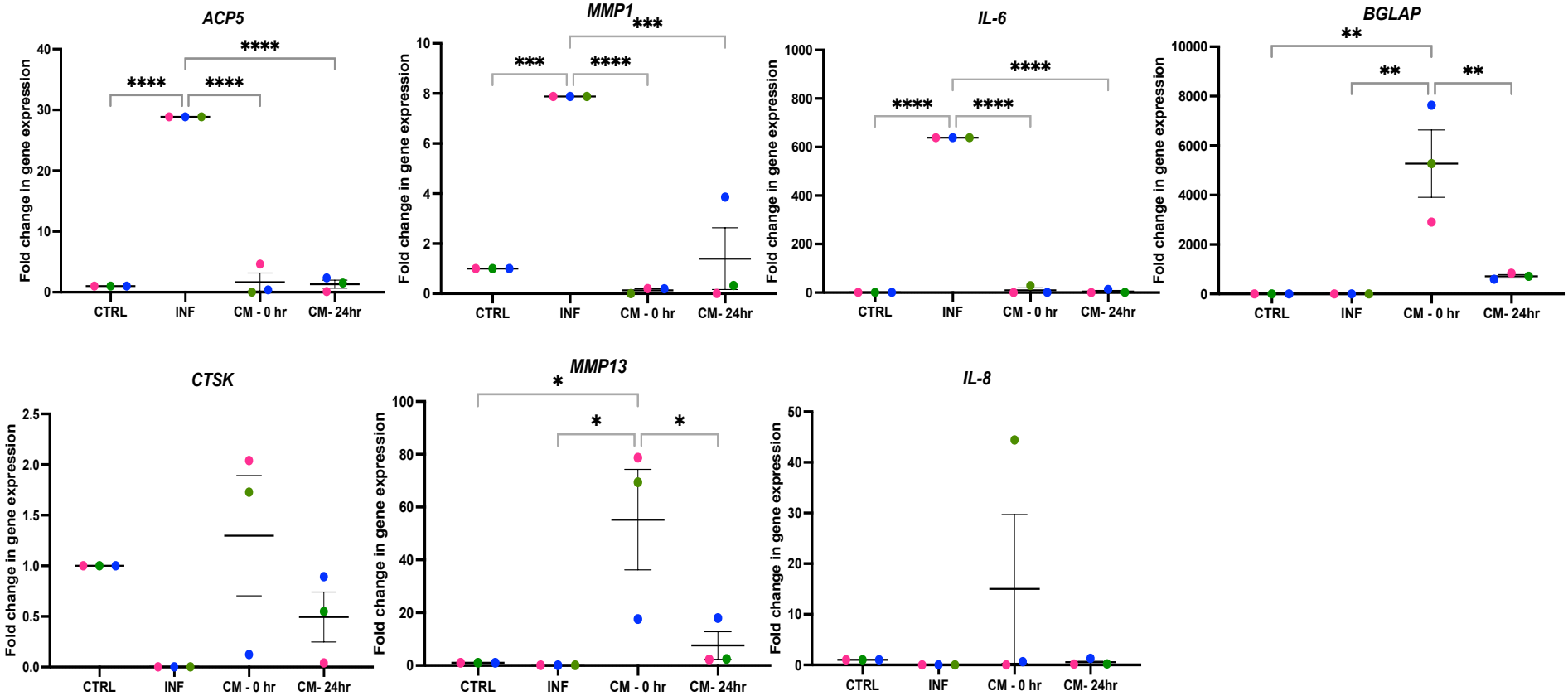

Figure 5-11The stimulatory effect of MSC-CM on the expression of osteogenic markers, osteoclastic markers and ant-inflammatory cytokines. Human bone plugs were infected with *S. aureus* at 3x107 CFU/ml and incubated for 24 hours. MSC-CM from 3 cell lines was added to infected bone and incubated for 24 hours. RNA was isolated and analysed by qPCR using TaqMan assay for *bglap*, *ACP5*, *CTSK*, *MMP-1*, *MMP-13*, *IL-6* and *IL-8.* The data represents 1 experiment with 1 bone sample and MSC-CM from 3 patients. All values are normalised to B2m expression CT values. CTRL= normal bone, INF= infected bone, CM-0hr= MSC-CM added at the time of *S. aureus* infection, CM-24hr= MSC CM added at 24 hours post *S. aureus* infection. *** = $p \leq 0.001$, ** = $p \leq 0.01$, * = $p \leq 0.05$.

5.6. Discussion

This study of an *ex vivo* model of bone infection explored clear molecular interaction between bone cells, their surrounding ECM, and infectious bacteria such as *S. aureus.* Three-dimensional bone models of OM have been proposed to aid in bridging the gap between 2D *in vitro* models and *in vivo* models (264) and to overcome the limitations using cell culture models and animal models (265) .The former lacks 3D complexity of bone architecture, and the latter do not provide a well-controlled experimental condition. The *ex vivo* models of OM preserve their complex *in vivo* 3D morphology and intercellular connections between osseous cells and maintain them surrounded by their native ECM environment. Hence, studies using such models provide a novel understanding of disease progression and drug responses which then can help develop novel therapeutics to treat this challenging disease.

Chapter 5 developed a novel human *ex vivo* model of OM using human bone explants challenged with *S. aureus.* The effects of *S. aureus* infection on bone explant were evaluated through assessing histological changes, bacterial burden, and gene and protein expression studies that reflected the response of bone cells during *S. aureus* infection.

Human bone was chosen because of our interest in investigating the impact of *S. aureus* on human model rather than an animal model. To the best of our knowledge, this is the first study to establish a 3D infected bone model using human femoral bone explants. Previously, Kassim *et al.* explored the mechanism of *S. aureus* infection by using a mouse bone explant (266). In contrast, Yang *et al.* studied *S. aureus* response in an_*ex vivo* human iliac bone model (14), and Marriott *et al.* investigated *IL-6*

expression in bone explants obtained from patients. However, these bone explant models were obtained from prosthetic joint infection or OM patients (267, 268).

The bacterial concentration of $3x10^6$ CFU/ml used in this chapter represented an optimum condition to induce an *in vitro* or *ex vivo* OM-like infection. Employing higher concentrations of *S. aureus* was hypothesised to induce a greater response in infected cells, which could mimic the microenvironment of chronic OM. A range of bacterial doses of *S. aureus* that has not been tested before in a human *ex vivo* infection model and culture durations (1, 4 and 24 hours) were assessed in the study. In our study, the ability of *S. aureus* to adhere to and colonise bone was demonstrated. This colonisation was found to result in increased osteoclastic markers gene expression specifically, TRAP and cathepsin K. Whether this expression translates to physiological activity at protein level remains to be investigated.

Initially, the study attempted to construct an infection model using human bone explants based on $1x10^6$ CFU/ml concentration of *S. aureus* to examine if this dose would impact the bone explants. The purpose of conducting histological analysis was to assess the level of bone tissue damage induced by the bacteria and signs of bacterial adherence to the bone tissues. To this end, haematoxylin and eosin stain were applied to the bone model infected with *S. aureus.* Figures can be found in Appendix 7.1. It was not possible to detect signs of inflammatory polymorphonuclear cells (PMNs), necrotic cells or abscess formation. Moreover, it was not possible to determine a particular pattern for mRNA expressions (Appendix Figure 7-1). Based on these inadequate clear findings, it was hypothesised the concentration of bacteria is

ineffective for the timescale of the study. This led to redesigning the infection strategy by using higher infection concentrations and extended infection periods.

A wide range of *S. aureus* concentrations and multiple infection time points were applied to construct the *ex vivo* infection bone model. Kassim *et al.* explored mechanisms of *S. aureus* infection using mouse explant bone (266). In this chapter, three *S. aureus* MOI's based on infection parameters used in their model were chosen. Due to limited access to clinical bone samples, only three time points (1,4 and 24 hours) and 3 concentrations of *S. aureus* were pursued (266).

The study started with evaluating the metabolic activity of bone cells during *S. aureus* infection, as a measure of bone-cell viability. Alamar Blue assay was used to measure the metabolic activity, showing the rate of resazurin reduction to resorufin (that generates a fluorescence signal), which is indicative of active/viable cells. There was an initial increase in metabolic activity at the beginning of the infection with live *S. aureus* (1 to 4 hours), followed by a sharp drop after 24 hours post-infection (4 to 24 hours). Despite multiple control wells (normal uninfected bone or *S. aureus*) employed, it was not possible to distinguish between the viability of specific cells (osteoblast, osteoclasts, or osteocytes). Moreover, since Alamar Blue dye could also interact with bacteria, we utilised PFA-fixed *S. aureus* to reveal the influence of live bacteria on the assay. Fixed *S. aureus* depressed the metabolic activity of bone cells suggesting that viable bacteria were contributing directly to bone viability assay reading.

It was not possible to find a comparable study that measured bone cell viability during infection; a previous study in a 2D model of osteoblast infection has shown that

metabolic activity increased at 24-, 48-, and 72-hours post-infection using Alamar Blue assay (253). Another study using a 3D model demonstrated that *S. aureus* did not influence the metabolic activity of MC3T3- E1 cells (osteoblast-like cells) seeded within scaffolds (253). To conclude, comparing the explant culture system used in this chapter with other studies that utilised Alamar blue in the presence of *S. aureus*, is challenging. The finding casts doubt on the accuracy of these studies. An alternative method to assess cell viability in such system should be sought.

The bacterial load in the infected bone was estimated by examining the presence *S. aureus* in pulverised fragments of infected bone on MHA plates. There was an initial small increase in *S. aureus* count (between 1 and 4 hours of infection) followed by a decline at 24 hours post-infection. Three different concentrations of *S. aureus* were used to assess the impact of bacterial burden on explant biology. It was assumed that higher concentrations would increase the bacterial burden in bone tissues; however, this was not case. There was no significant difference in CFU count of *S. aureus* retrieved from the bone plugs among different concentrations or time points. This does not preclude the possibility that *S. aureus* can multiply within cells; an element that may not have been captured by the recovery method.

In the experiment, a mortar was used to homogenise bone tissues since it was proved that bacterial recovery from homogenised human tissues is significantly higher than any other bacterial recovery method, such as bead beating and vortexing (269). However, this technique might cause bone tissue destruction and damage to bacterial cells, which may contribute to the imprecise bacterial count. A more accurate approach might consider counting *S. aureus in situ*. Electron microscopy has been previously

used to demonstrate the presence of bacteria within osteoblasts and osteocytes of embryonic chicks following injection with *S. aureus (270).* It can be recommended as a much more precise technique to study the bacterial distribution within bone tissue explant.

It is well known that *S. aureus* infection can cause local and systemic bone destruction by encouraging bone resorption (271). Bone resorption was evaluated by measuring C-terminal telopeptide of type 1 collagen (CTX) secreted in the cultured media as a result of osteoclast activity in the infected bone plugs. Serum CTX assays measure a fragment of the C-terminal telopeptide of type 1 collagen released during the resorption of mature bone. In this investigation, an ELISA assay measured CTX in the supernatant collected from infected bone explant cultures. The results have shown that *S. aureus* infection at concentration of $3x10^7$ CFU/ml could induce CTX release from the explants. Similar findings were reported in mouse parietal bone, which indicates that enhanced release of bone matrix degradation fragments (CTX) from the plugs is dependent on high dose of *S. aureus* (266).

To analyse the impact of *S. aureus* infection on human explant biology, mRNA analysis of various important markers associated with osteogenesis, osteoclastogenesis, anti-inflammatory cytokines, and matrix-resorption enzymes was conducted. Several concentrations and exposure time of S. aureus were applied. The analysis revealed that most of the markers were differentially expressed during infection. There was significant upregulation of *MMP-1* and *MMP-1*3 (enzymes associated with ECM degradation), *CTSK* and *ACP5* (markers related to osteoclastic

differentiation), *IL-6* (an inflammatory cytokine) and *bglap* (an osteogenic marker) in response to *S. aureus* infection.

Given the established impact of infection on bone synthesis in OM pathology, the impact of *S. aureus* infection on the expression of osteogenic genes in the human bone explant was investigated. Osteogenic differentiation is characterised by the expression of the transcription factor, RUNX2, and the sequential expression of a series of bone formation markers such as *ALP and bglap*. There was a slight change in *RUNX2* and *ALP* expression after *S. aureus* infection, but these changes were statistically not significant. On the other hand, here was significant upregulation of *bglap* at a high concentration of *S. aureus* infection at 4 hours post-infection followed by significant downregulation of the gene at 24 hours post infection. To confirm the actual behaviour of *bglap* in the system studied, its protein level was assessed using western blot assay. *bglap* was strongly detectable up to 4 hours post infection, then it showed weaker band at 24 hours post- infection compared to normal uninfected bone. The results suggested that *S. aureus* might negatively impact *bglap* in a time dependent manner at both gene and protein level.

It should be noted that findings from gene analysis of *bglap* and *ALP* have revealed large variations between donor samples in gene expression when bone was infected (Figure 5- 6 and 5-11). This may be due to differences in donor samples including age, gender, underlying health, and the contributing of the well-established phenomenon of heterogeneity found in MSC populations.

The effect of *S. aureus* on osteogenic activity has been investigated before, using a mouse 3D model of bone (266). The authors found that *bglap and ALP* expression

decreased substantially in *S. aureus*-infected mouse parietal bones. The decrease in osteogenic markers expression might be due to some factors released from bone cells that inhibit osteogenesis. Tumour necrosis factor alpha (TNF alpha, TNF-α) is an inflammatory cytokine that has been found to decrease the production of type I collagen, osteocalcin, and alkaline phosphatase in a variety of osteoblast cell culture and bone tissue explant models, thereby reducing matrix deposition and mineralisation (272). A future study investigating TNF-α expression using the explant bone model in the current study could help with understanding OM pathogenesis.

The mRNA expressions of *IL-6* and *IL-8*, the major inflammatory cytokines, were investigated in this chapter. *S. aureus* infection exhibited strong induction of *IL-6* mRNA expression in the explant model. Release of IL-6 triggers osteoclastogenesis, which causes excessive osteoclastic activity and osteolysis (273). Like other inflammatory cytokines, IL-6 acts on osteoblasts to increase RANKL production (274). IL-6 is produced by osteoblasts in response to *S. aureus* infection and has been shown to stimulate osteoclastic bone resorption (275).

Examining the differential expression of MMPs could be important in mediating *S. aureus* infection outcomes on human bone. MMPs are enzymes associated with extracellular matrix remodelling and are expressed in osteoblasts and osteoclasts (276). MMPs act as signals to prepare the initiation sites for bone resorption by osteoclasts at the onset of the remodelling cycle. Gene expression of *MMP-1* was found to be upregulated in infectious conditions such as HIV, hepatitis B and *Mycobacterium tuberculosis* infection. It was also found that functional *MMP-1*

polymorphism is associated with OM disease (277) and this upregulation might result in OM development.

MMP-1 mRNA expression was significantly upregulated at the higher dose of *S. aureus* at $1x10^7$ and $3x10^7$ CFU/ml after 24 hours post-infection, indicating that *MMP-1* expression is infection dose-dependent and time-dependent. Furthermore, MMP-1 protein was evaluated using western blot assays to investigate mechanism in actual levels of MMP-1 during *S. aureus* bone infection. It has shown that *S. aureus* infection at higher concentration $3x10^7$ CFU/ml derived bone cells stimulated *MMP-1* expression to a greater degree than uninfected bone. The results suggest *S. aureus* upregulates *MMP-1* in a concentration dependent manner at gene and protein level. These results suggest a role in tissue degradation and remodelling of the bone matrix in the system.

Unlike with *MMP-1*, there was slight change in the mRNA expression of *MMP-1*3 during *S. aureus* infection of the bone explant. However, there was a significant upregulation at 24 hours post-infection with the higher concentration of $1x10^7$ CFU/ml *S. aureus*, suggesting that *S. aureus* infection associated ECM degradation is dependant in good part on MMP-1 with potential secondary contribution by MMP-13.

Upon successfully establishing the 3D infection model that partially mimics an OM model, the therapeutic effect of the MSC-CM was investigated in the model. MSC-CM is known to have an active secretome, which holds great potential for repairing damaged tissue and preventing infection.

In the current study, the higher concentration of *S. aureus* ($3x10^7$ CFU/ml) and the infection period of 24 hours produced a potential outcome in the bone explant. Then,

MSC-CM was added to the bone simultaneously with *S. aureus* inoculation and incubated for 24 hours. This was to study the protective effects of MSC-CM on human bone during infection, particularly with osteogenic and osteoclastic activities and inflammatory response. The results showed significant downregulation of *IL-6, MMP-1* and *ACP5* and a significant upregulation of *bglap* and *MMP-13* mRNA expression. This suggested that a single injection of MSC-CM could play a protective role by decreasing the pathological effects of *S. aureus* infection and interfering with pathogenic virulence elements of *S. aureus* that cause bone damage.

In another set of experiments, MSC-CM was added to the bone at 24 hours post *S. aureus* infection and incubated for 24 hours. The results showed that MSC-CM attenuated the effect of bone resorption and inflammatory response and prevented matrix degradation judged by the downregulation of *ACP5*, *IL-6,* and *MMP-1* and maintaining stable expression of *CTSK.* The outcome of this experiment suggests that administration of MSCs-CM may have advantageous effects during *S. aureus* infection by preventing bone demineralisation and reducing resorption activity.

The plan of work in this chapter faced lots of challenges that restricts the conclusions of the study. This includes the fact that one bone sample and three MSC lines to generate CM were used. Obtaining primary tissue such bone and MSCs was dependant on good access to clinical samples. There was significant restriction on reaching such samples during the pandemic and this has been explained in the COVID statement of the thesis. Technically, generating pure-quality RNA from bone tissues was one of this study challenges as bone plugs contain a high proportion of mineralised ECM and a small number of cells.

In conclusion, findings in this study demonstrated the possibility of infecting a human, bone explant with *S. aureus* to act as a potential model *ex vivo* of OM. Gene expression and protein analysis of markers relevant to bone biology demonstrated the responsive of the explant model to infection by differential expression of the markers. It was possible to challenge the model and modify its response to infection through exposure to MSC-CM. This exposure has dampened the pathological response due to infection, proposing future studies to elucidate the active component(s) secreted by MSCs towards finding a biological therapeutic approach based on such component(s).

6. General Discussion

OM is an infectious disease of the bone caused predominantly by *S. aureus*. The administration of local/systemic antibiotics is one of the favourable strategies among the current treatment modalities, used to address such orthopaedic infections. However, antibiotics treatment can develop antibiotic-drug resistance and may adversely affect bone regeneration or differentiation. Booysen *et al.* has demonstrated that vancomycin, an antibiotic used to treat methicillin-resistant *Staphylococcus aureus* (MRSA) infection, had a negative impact on osteogenic differentiation (278). Therefore, there is a crucial demand to develop an advanced alternative therapeutic strategy which can effectively address OM infection.

Recent studies have demonstrated that MSCs possess potent immunomodulatory properties including antimicrobial and anti-inflammatory activity that provide protection against microbial attack (279). MSCs have been the subject of many research experiments investigating its advantageous therapeutic outcome in the context of numerous human disorders (228). It is argued that MSCs hold an excellent potential for the cell therapy and regenerative medicine (280).

In chapter three of the thesis, our results showed that bmMSCs stimulated with TLR-2 synthetic agonists; Pam3CSK4, and PGN-SA resulted in significant growth inhibition of *S. aureus* compared to unstimulated control. Based on these results, it was hypothesised that upon stimulation of bmMSCs with TLR-2 and *S. aureus*, bmMSCs respond by increasing the production of antimicrobial proteins. The data presented in section 3.5.5 did not support such hypothesis directly (i.e., bacterial growth inhibition was there but couldn't be attributed to antibacterial peptides). Several studies

investigated TLRs mediating antimicrobial peptides overexpression in different cell types that participate in the innate immune system like keratinocytes, corneal epithelial cells, and epithelial cells (132, 208, 281, 282). However, none of the studies have explored the TLR mediated antimicrobial potential of bmMSCs in a cellular model of OM. The source of the observed inhibition in the model used remains unknown. Future studies could consider a proteomic or an RNAseq approach with bioinformatics analysis to aid in narrowing down candidate target.

In chapter 4, the results showed the ability of human MSC-CM to kill or inhibit the growth of *S. aureus* in infected osteoblasts using three different settings of MSC-CM (harvested from different cell densities). Whilst MSC-CM could inhibit bacterial growth, the data showed in addition that MSC-CM has profitable impact on osteoblast differentiation. One limitation of the experimental methods used is the limited MSC-CM incubation time in order to measure the effect of MSC-CM on osteogenic capacity during infection. To the best of our knowledge, there are no published reports to date that evaluated the MSC-CM cultured with *S. aureus*-infected osteoblasts and its impact on osteogenic state.

Previous studies using rat MSCs reported that MSC-CM enhanced osteoblast migration and proliferation *in vitro*, and increased the expression of osteogenic markers (*bglap* and *RUNX2*) over 8 weeks (241). Moreover, it was shown that MSC-CM (isolated from human maxilla) promoted osteogenesis of human periodontal ligament stem cells over 15 days suggesting that it could drive osteoblastic/odontoblastic differentiation (283). However, Jing Sun *et al.* showed that osteocalcin and OPN expression were downregulated following MSC-CM culture by

day 3, lowering the levels of alkaline phosphatase activity and inhibiting *RUNX2* expression (247).

This study utilised for the first time a human bone explant culture system as an *ex vivo* model of OM infection. Whilst the model provided good insight into the pathology of OM and the potential application of MSC-CM, it came with some with some limitations. First, only the cancellous bone segment was extracted from the femoral head. Different calvaria bones, frontal, parietal and interparietal, that contain different bone microenvironments (e.g. parietal vs frontal calvaria bone) have shown varied gene expression profiles (284). Second, there was large variation in response from the MSC samples obtained from patients for the study. This may be predictable, given differences in donors' age, gender, and health condition, and the known heterogeneity associated with MSC populations. Time and resource permitted, the study would have mitigated this limitation by increasing the (n) number of the samples in excess of n=5. The data presented in this thesis is a stepping stone towards deeper analysis of the impact of MSC and MSC-CM on infected bone. The use of a human bone explant culture system would accelerate the translation of any key therapeutic findings. Future work should consider standardising this system by making sure plugs are taken from the same site, with cortical bone and from healthy patients. This may require access to cadaveric tissue or liaison with an orthopaedic trauma centre. Studies of MSC-CM should develop to define the content of CM as much as possible and isolate components with suspected active antimicrobial/regenerative potential. Learning from work on TLR-2 stimulation, more advanced and sensitive proteomics techniques to broad screen secreted bactericidal protein profiles in MSC-CM after TLR-2 stimulation

should be considered. This can be followed by a multiplexing quantitative assay or ELISA to validate and find novel proteins released in the MSC-CM. Further elucidation of TLR-2 impact on MSCs could come from studies that involve knocking down a specific receptor and chasing the downstream events, ideally in an *ex vivo* model such as one reported here. Moreover, TLR-2 agonists beneficial impact reported in patients in other clinical settings may support administering these agonists in cases of OM to enhance body's own response against infection for example in situations when antibiotics are less effective or faced with resistance. Such combination therapy would be easy to test and establish in humans given the published safety of those agonists in other clinical settings. Finally, finding other MSC stimulatory mechanisms that could further ameliorate the antibacterial/regenerative capacity and enrich MSC-CM with potent effectors should be sought.

7. Appendix

An aim of this work was to establish a profound picture of the infection *ex vivo* human bone model. Different parameters were selected (bacterial concentration and infection time) to create the model in line with previous clinical studies in animal models (285). This appendix includes result of qPCR and histology staining experiments of bone tissue infected with *S. aureus* in order to investigate the molecular and morphological changes during infection with or without MSC-CM.

7.1. qPCR gene expression of osteogenic markers, osteoclastic markers, and inflammatory cytokine

Bone plugs were infected with $3X10^6$ CFU/ml prepared in DMEM media (no antibiotics/no FBS). A 3 ml of *S. aureus* suspension was added into each well. Control bone plugs were incubated with DMEM only. The plate was incubated for 1 hour or 2 hours with bacteria. At the end of incubation, bone plugs were washed and incubated in DMEM for 7 or 14 days. At the end of culture, bone plugs were washed and pulverised in preparation for RNA extraction, cDNA transcription, and qPCR gene analysis (Figure 7-1).

Real-time qPCR experiments were performed to investigate if *S. aureus* infection of human bone explants caused changes in the expression of osteogenic/osteoclastogenic activity markers (i.e., *ALP, bglap, RUNX2* and *ACP5*), as well as *MMP-1* in explant cells. *S. aureus* impact on bone formation in the human bone explant was assessed by evaluating the osteogenic markers ALP, bglap and RUNX2. There was significant increase in *RUNX2, ALP, bglap* and *MMP-1* expression compared to control group when explants were infected with *S. aureus* for one hour

and incubated for 7 and 14 days. However, when bone cells were infected for 2 hours and incubated for 7 and 14 days, the significant upregulation was limited to *bglap* and *ACP5* mRNA level.

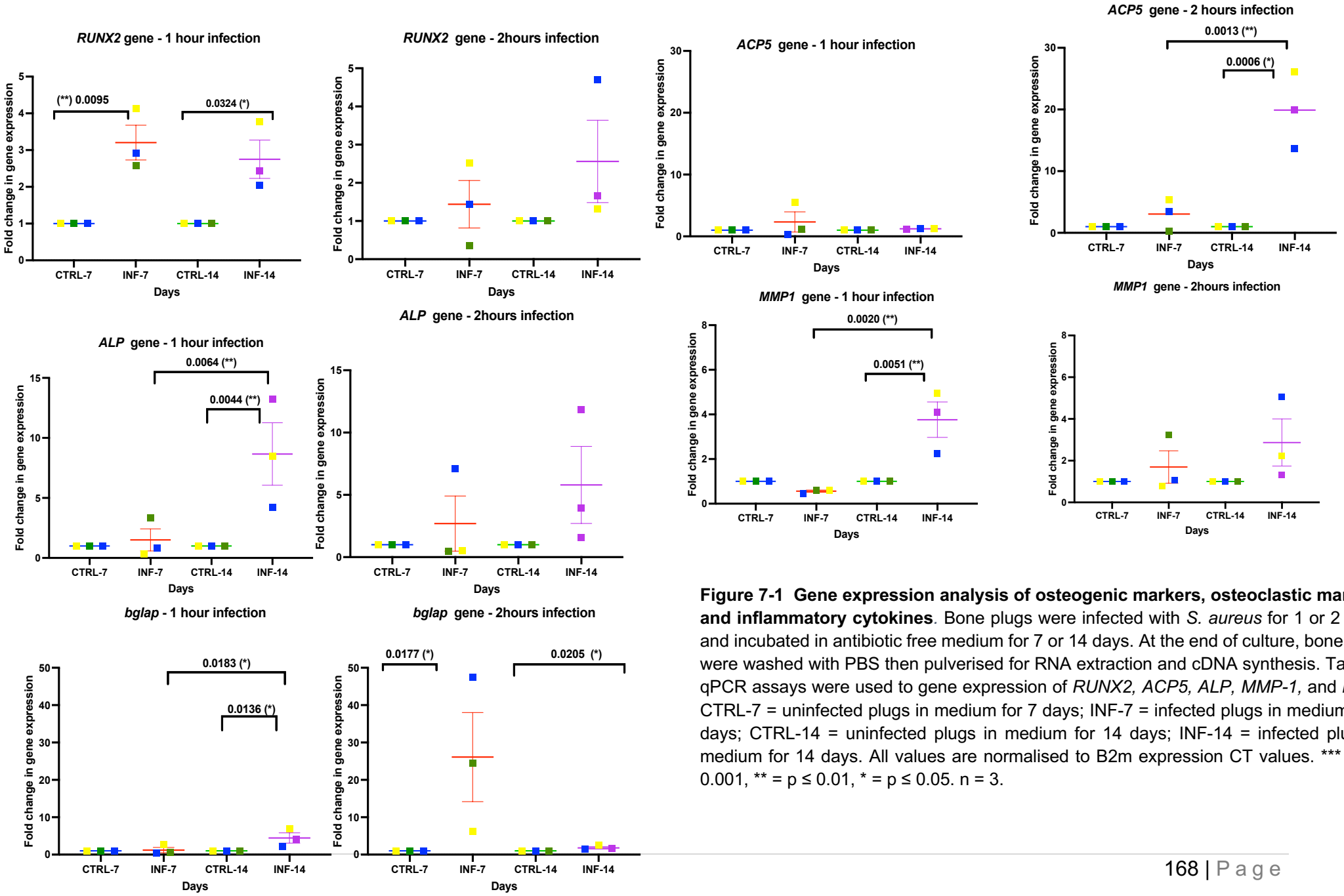

Figure 7-1 Gene expression analysis of osteogenic markers, osteoclastic markers, and inflammatory cytokines. Bone plugs were infected with *S. aureus* for 1 or 2 hours and incubated in antibiotic free medium for 7 or 14 days. At the end of culture, bone plugs were washed with PBS then pulverised for RNA extraction and cDNA synthesis. TaqMan qPCR assays were used to gene expression of *RUNX2, ACP5, ALP, MMP-1,* and *bglap*. CTRL-7 = uninfected plugs in medium for 7 days; INF-7 = infected plugs in medium for 7 days; CTRL-14 = uninfected plugs in medium for 14 days; INF-14 = infected plugs in medium for 14 days. All values are normalised to B2m expression CT values. *** = $p \leq 0.001$, ** = $p \leq 0.01$, * = $p \leq 0.05$. n = 3.

7.2. Histological changes of infected bone

Histological changes in bone tissue are critical characteristics of OM diagnosis. An aim of this work was to establish a profound picture of an infection *ex vivo* human bone model. Different parameters were selected (bacterial concentration and infection time) to create the model in line with previous clinical studies in animal models. *S. aureus* was loaded at a concentration of $1x10^6$ CFU/ml and incubated with the bone plugs for 1 hour or 2 hours. The plugs were incubated in normal media for additional 7 or 14 days. At the end of the culture, the plugs were fixed, decalcified, paraffin-embedded, and histological sections were obtained and stained with H&E. The stained sections were evaluated by light microscopy (Figure 7-2).

The histology showed the cancellous compartment of bone. Control tissue appeared continuous showing typical woven structure that is staining intensely (Figure 7-2A). There was evidence of deteriorating ECM structure associated with increased exposure to bacteria and extended incubation period after infection (Figure 7-2 B-E). The normal woven structure of cancellous bone was lost, and the ECM appears resorbed. There were solid deposits in the infected bone tissue that are suspected to be bacterial aggregates (Figure 7-2 C-E), however, the identity of these aggregate was not confirmed. Other evidence of infection such as neutrophil infiltration was not detectable due to lack of blood supply in the model.

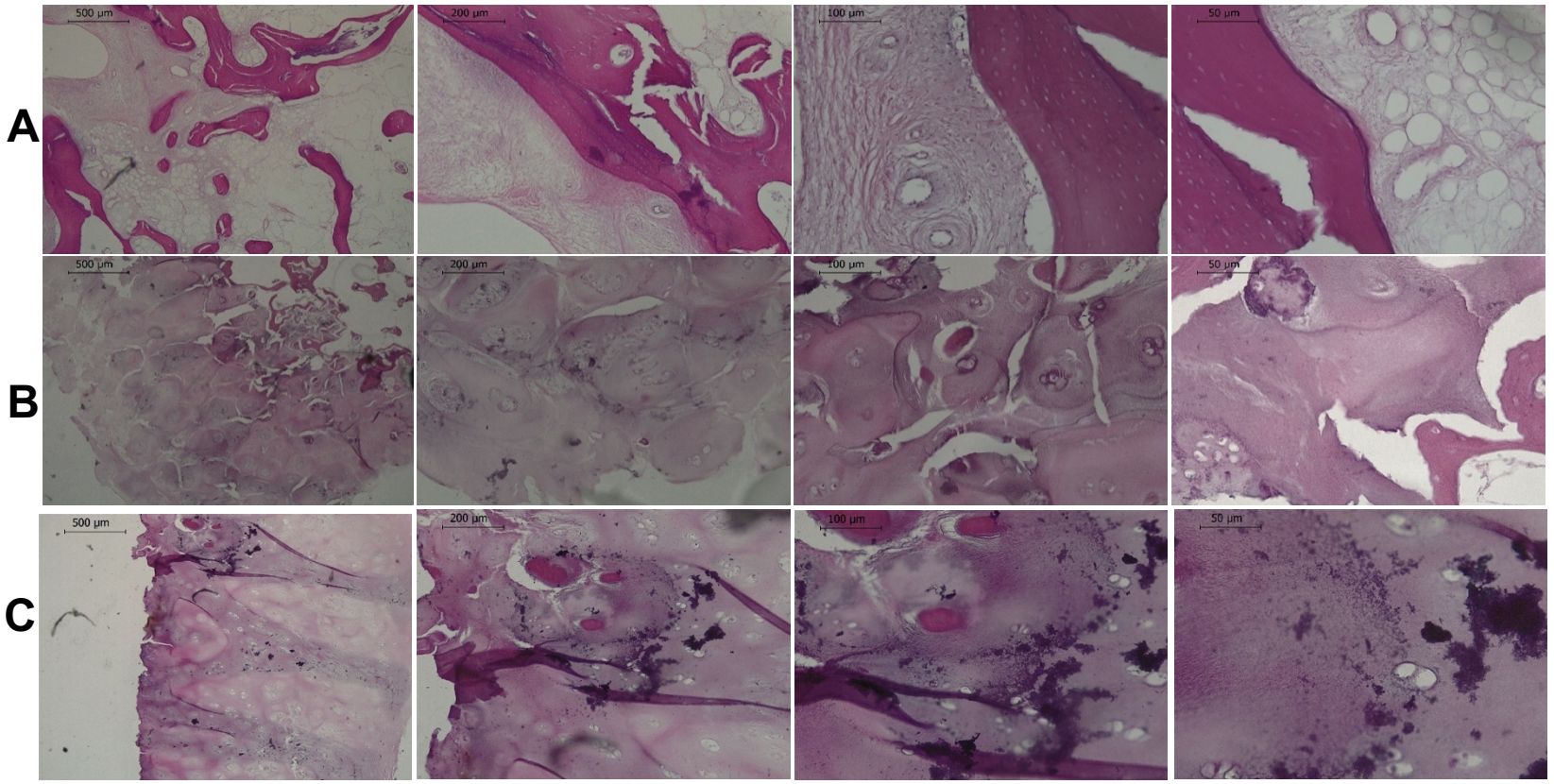
A
B
C
500 µm
200 µm
100 µm
50 µm

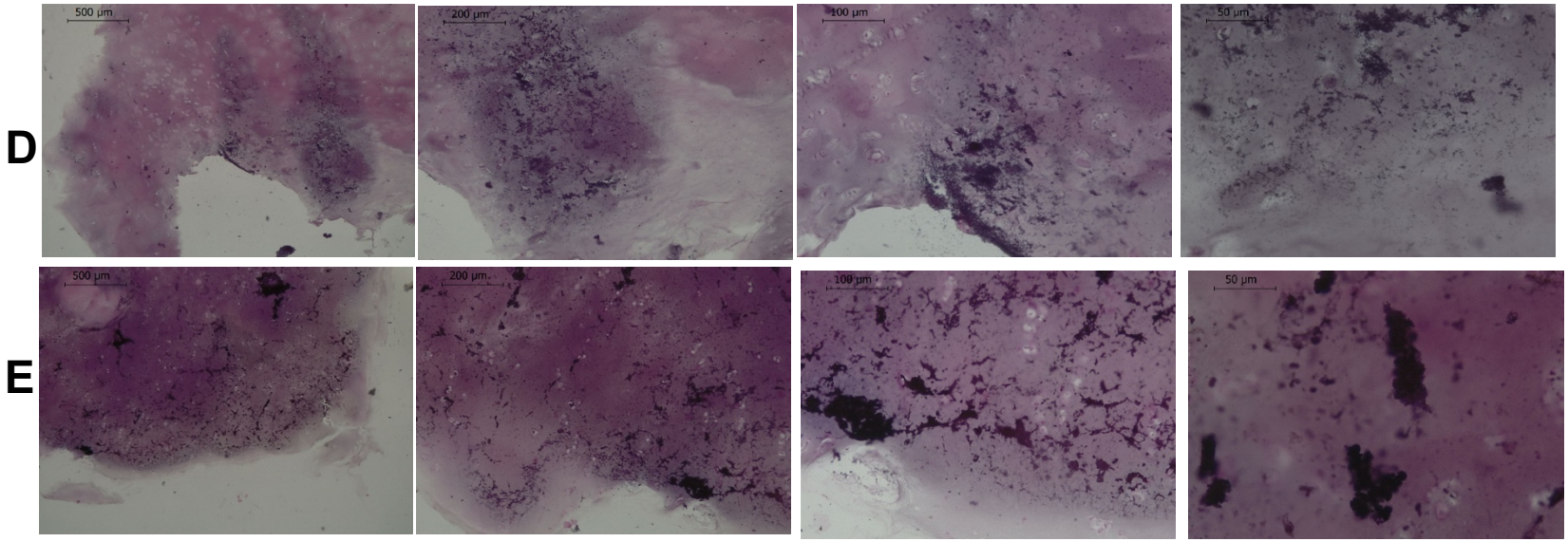

Figure 7-2 Microscopic histological evaluation of formalin-fixed, H&E-stained paraffin sections of infected bone tissue.
Bone plugs taken from human femoral heads were infected with *S. aureus* for 1 or 2 hours and incubated in antibiotic-free media for 7 and 14 days. After the end of culture, the tissues were washed with PBS and fixed in 4% PFA for 48 hours and then processed for decalcification in ETDA. 7µm bone section were cut using microtome and the tissues was stained using H&E. (A) Control, (B) Infected 1hr for 7 days, (C) Infected 2hrs for 7 days (D) Infected 1hr for 7 for 14 days. (E) Infected 1hr for 14 days. Samples photographed at 100, 200 and 500 µm scale.

7.3. Histological changes of infected bone cultured with MSC-CM

An aim of this work was to investigate the effect of MSC-CM on the human infected bone *ex vivo* model. *S. aureus* at a concentration of $1x10^6$ CFU/ml was added to bone plugs and incubated for 2 hours. The plugs were incubated in normal medium for additional 7 days. MSC-CM was added to the infected bone plugs and incubated for further 7 days. At the end of the culture, the plugs were fixed, decalcified, paraffin-embedded, and histological sections were obtained and stained with H&E. The stained sections were evaluated by light microscopy (Figure 7-3).

The histology showed the cancellous compartment of bone. Control bone tissue appeared solid and continuous (Figure 7-3A). There was evidence of changing ECM appearance associated with infection including detectable deposits of suspected bacterial aggregates (Figure 7-3B). The identity of these aggregate was not confirmed however. The addition of MSC-CM appears to revert the appearance of ECM to what is seen in uninfected control (Figure 7-3C). There was detectable reduction in bacterial aggregates in this group.

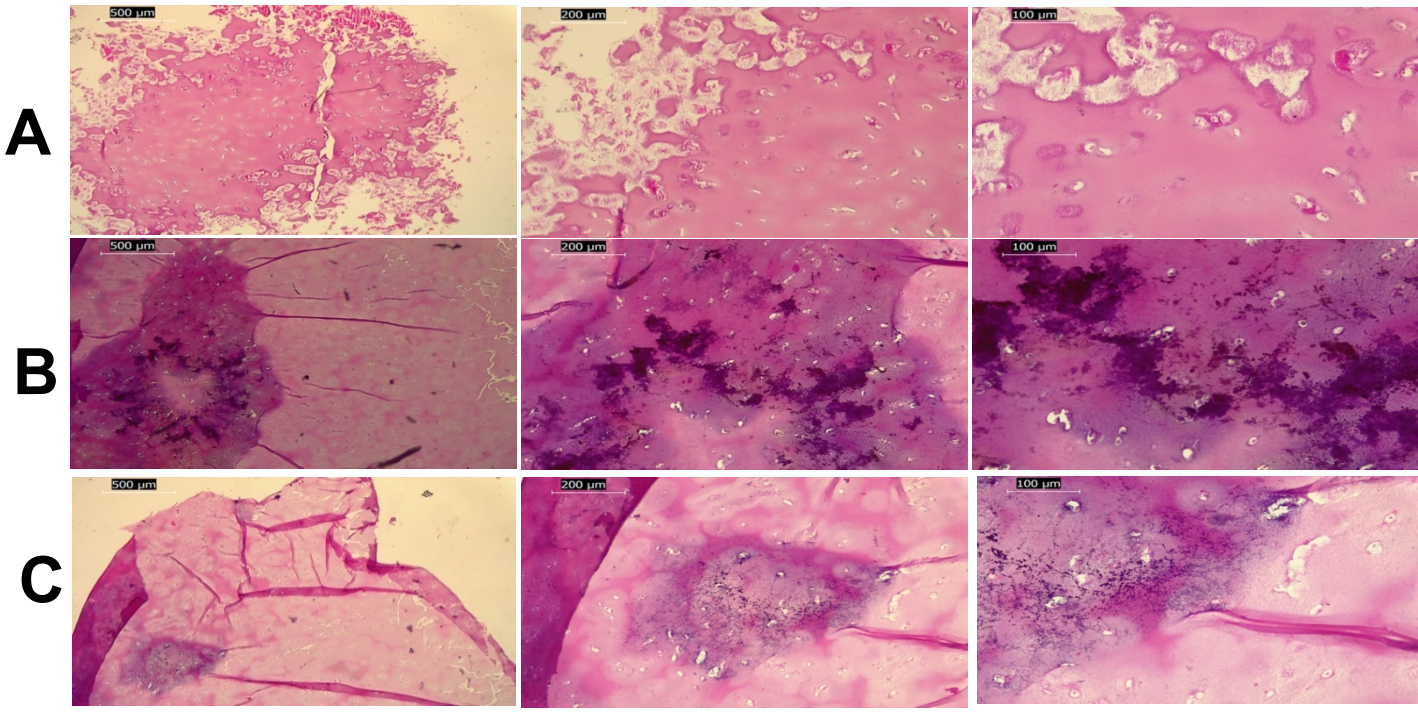

Figure 7-3 Histological evaluation of infected bone tissue cultured with MSC-CM. Bone plugs taken from human femoral heads were infected with *S. aureus* for 2 hours and incubated in antibiotic-free medium for 7 days. The medium was replaced with MSC-CM and incubated for further 7 days with the infected bone plugs. At the end of *culture*, *the* tissues *were* washed with PBS and fixed in 4% PFA for 48 hours and processed for decalcification in ETDA. 7µm bone section were cut using microtome and the tissues was stained using H&E. (A) Normal, (B) infected bone for 7 days, (C) infected bone cultured with MSC-CM. Samples photographed at 100, 200 and 500 µm scale.

8. References

1. Quizlet. Osteomyelitis [Available from: https://quizlet.com/584088374/osteomyelitis-flash-cards/.

2. Kini U, Nandeesh B. Physiology of bone formation, remodeling, and metabolism. Radionuclide and hybrid bone imaging: Springer; 2012. p. 29-57.

3. Buck DW, Dumanian GA. Bone biology and physiology: part I. the fundamentals. Plastic and Reconstructive Surgery. 2012;129(6):1314-20.

4. Walsh JS. Normal bone physiology, remodelling and its hormonal regulation. Surgery (Oxford). 2015;33(1):1-6.

5. Morrison SJ, Scadden DT. The bone marrow niche for haematopoietic stem cells. Nature. 2014;505(7483):327-34.

6. Maheshwari AV, Jelinek JS, Song AJ, Nelson KJ, Murphey MD, Henshaw RM. Metaphyseal and diaphyseal chondroblastomas. Skeletal Radiology. 2011;40(12):1563-73.

7. Parkinson IH, Fazzalari NL. Characterisation of trabecular bone structure. Skeletal aging and osteoporosis: Springer; 2013. p. 31-51.

8. Dwek JR. The periosteum: what is it, where is it, and what mimics it in its absence? Skeletal Radiology. 2010;39(4):319-23.

9. Locke M. Structure of long bones in mammals. Journal of Morphology. 2004;262(2):546-65.

10. QUizlet. Anatomy Quiz : Types of fractures, Anatomy of the Long bone, Functions of the Skeletal System, Types of ossification and disorders/diseases of the bones [Available from: https://quizlet.com/264612857/anatomy-quiz-types-of-fractures-anatomy-of-the-long-bone-functions-of-the-skeletal-system-types-of-ossification-and-disordersdiseases-of-the-bones-diagram/.

11. Ascenzi M-G, Roe AK. The osteon: the micromechanical unit of compact bone. Frontiers in Bioscience-Landmark. 2012;17(4):1551-81.

12. Currey JD. The structure and mechanics of bone. Journal of Materials Science. 2012;47(1):41-54.

13. Karpiński R, Jaworski Ł, Czubacka P. The structural and mechanical properties of the bone. Journal of Technology and Exploitation in mechanical Engineering. 2017;3(1).

14. Florencio-Silva R, Sasso GRD, Sasso-Cerri E, Simoes MJ, Cerri PS. Biology of bone tissue: structure, function, and factors that influence bone cells. Biomed Research International. 2015;2015.

15. Heino TJ, Hentunen TA. Differentiation of Osteoblasts and Osteocytes from Mesenchymal Stem Cells. Current Stem Cell Research & Therapy. 2008;3(2):131-45.

16. Birmingham E, Niebur G, McHugh PE. Osteogenic differentiation of mesenchymal stem cells is regulated by osteocyte and osteoblast cells in a simplified bone niche. European Cells and Materials. 2012;23:13-27.

17. Arvidson K, Abdallah BM, Applegate LA, Baldini N, Cenni E, Gomez-Barrena E, et al. Bone regeneration and stem cells. Journal of Cellular and Molecular Medicine. 2011;15(4):718-46.

18. Gasser JA, Kneissel M. Bone physiology and biology. Bone toxicology: Springer; 2017. p. 27-94.

19. Arvidson K, Abdallah B, Applegate L, Baldini N, Cenni E, Gomez-Barrena E, et al. Bone regeneration and stem cells. Journal of cellular and molecular medicine. 2011;15(4):718-46.

20. Schaffler MB, Cheung WY, Majeska R, Kennedy O. Osteocytes: master orchestrators of bone. Calcified Tissue International. 2014;94(1):5-24.

21. Kannan S, Ghosh J, Dhara SK. Osteogenic differentiation potential of porcine bone marrow mesenchymal stem cell subpopulations selected in different basal media. Biology open. 2020;9(10):bio053280.

22. Komori T. Regulation of bone development and extracellular matrix protein genes by RUNX2. Cell and Tissue Research. 2010;339(1):189-95.

23. Miron RJ, Zohdi H, Fujioka-Kobayashi M, Bosshardt DD. Giant cells around bone biomaterials: Osteoclasts or multi-nucleated giant cells? Acta Biomaterialia. 2016;46:15-28.

24. Lee-Thedieck C, Schertl P, Klein G. The extracellular matrix of hematopoietic stem cell niches. Advanced Drug Delivery Reviews. 2021:114069.

25. Ansari S, Ito K, Hofmann S. Cell sources for human in vitro bone models. Current Osteoporosis Reports. 2021;19(1):88-100.

26. Ikeda K, Takeshita S. The role of osteoclast differentiation and function in skeletal homeostasis. The Journal of Biochemistry. 2016;159(1):1-8.

27. Mun SH, Park PSU, Park-Min KH. The M-CSF receptor in osteoclasts and beyond. Experimental and Molecular Medicine. 2020;52(8):1239-54.

28. Tanaka H, Tanabe N, Kawato T, Nakai K, Kariya T, Matsumoto S, et al. Nicotine affects bone resorption and suppresses the expression of cathepsin K, MMP-9 and vacuolar-type H+-ATPase d2 and actin organization in osteoclasts. PloS one. 2013;8(3):e59402.

29. Arnett TR. Osteoclast biology. Marcus and Feldman's Osteoporosis: Elsevier; 2021. p. 99-110.

30. Long CL, Humphrey MB. Osteoimmunology: the expanding role of immunoreceptors in osteoclasts and bone remodeling. BoneKEy reports. 2012;1.

31. Xu F, Teitelbaum SL. Osteoclasts: new insights. Bone research. 2013;1(1):11-26.

32. Zhao Y, Wang H-L, Li T-T, Yang F, Tzeng C-M. Baicalin ameliorates dexamethasone-induced osteoporosis by regulation of the RANK/RANKL/OPG signaling pathway. Drug Design, Development and Therapy. 2020;14:195.

33. Takayanagi H. New developments in osteoimmunology. Nature Reviews Rheumatology. 2012;8(11):684-9.

34. Crotti TN, Flannery M, Walsh NC, Fleming JD, Goldring SR, McHugh KP. NFATc1 regulation of the human beta(3) integrin promoter in osteoclast differentiation. Gene. 2006;372:92-102.

35. Lin X, Patil S, Gao YG, Qian AR. The bone extracellular matrix in bone formation and regeneration. Frontiers in Pharmacology. 2020;11.

36. Kuropka P, Kuryszko J, Mazurkiewicz-Lyczewska S. Bone mineralization. Medycyna Weterynaryjna-Veterinary Medicine-Science and Practice. 2006;62(5):557-9.

37. Fuchs RK, Thompson WR, Warden SJ. Bone biology. Bone repair biomaterials: Elsevier; 2019. p. 15-52.

38. Kenkre JS, Bassett JHD. The bone remodelling cycle. Annals of Clinical Biochemistry. 2018;55(3):308-27.

39. Del Fattore A, Teti A, Rucci N. Bone cells and the mechanisms of bone remodelling. Frontiers in Bioscience-Elite. 2012;4(6):2302-21.

40. Nandiraju D, Ahmed I. Human skeletal physiology and factors affecting its modeling and remodeling. Fertility and Sterility. 2019;112(5):775-81.

41. Katsimbri P. The biology of normal bone remodelling. European Journal of Cancer Care. 2017;26(6).

42. Kular J, Tickner J, Chim SM, Xu JK. An overview of the regulation of bone remodelling at the cellular level. Clinical Biochemistry. 2012;45(12):863-73.

43. Brunetti G, Benedetto AD, Mori G. Bone remodeling. Imaging of Prosthetic Joints: Springer; 2014. p. 27-37.

44. Quizlet. Skeletal system: Bone remodelling [Available from: https://quizlet.com/ca/263592950/skeletal-system-bone-remodelling-diagram/.

45. Cheng C-C, Chung C-A, Chang C-J, Cheng Y-C, Huang C-J, Chien C-C, et al. Hydrostatic pressure facilitates calcium deposition and osteogenic gene expression in the osteoblastic differentiation of placenta-derived multipotent cells. Taiwanese Journal of Obstetrics and Gynecology. 2022;61(2):270-6.

46. Liu TM, Lee EH. Transcriptional regulatory cascades in Runx2-dependent bone development. Tissue Engineering Part B: Reviews. 2013;19(3):254-63.

47. Rutkovskiy A, Stenslokken KO, Vaage IJ. Osteoblast differentiation at a glance. Medical Science Monitor Basic Research. 2016;22:95-106.

48. Bruderer M, Richards R, Alini M, Stoddart MJ. Role and regulation of RUNX2 in osteogenesis. Eur Cell Mater. 2014;28(28):269-86.

49. Komori T. Whole aspect of Runx2 functions in skeletal development. International Journal of Molecular Sciences. 2022;23(10).

50. Turgeon B, Meloche S. Interpreting neonatal lethal phenotypes in mouse mutants: insights into gene function and human diseases. Physiological reviews. 2009;89(1):1-26.

51. Liao F, Hu X, Chen R. The effects of Omarigliptin on promoting osteoblastic differentiation. Bioengineered. 2021;12(2):11837-46.

52. Paludo E, Ibelli A, Peixoto J, Tavernari F, Lima-Rosa C, Pandolfi J, et al. The involvement of RUNX2 and SPARC genes in the bacterial chondronecrosis with osteomyelitis in broilers. Animal. 2017;11(6):1063-70.

53. Edin ML, Miclau T, Lester GE, Lindsey RW, Dahners LE. Effect of cefazolin and vancomycin on osteoblasts in vitro. Clinical Orthopaedics and Related Research. 1996(333):245-51.

54. Corathers SD. The alkaline phosphatase level: nuances of a familiar test. Pediatr Rev. 2006;27:382.

55. Sama AJ, Schiller NC, Ramirez CM, Yong TM, Donnally CJ, Spielman AF, et al. Leadership trends among orthopaedic trauma surgery fellowship directors: a cross-sectional demographic review. Current Orthopaedic Practice. 2021;32(2):107-11.

56. Jaiswal N, Haynesworth SE, Caplan AI, Bruder SP. Osteogenic differentiation of purified, culture-expanded human mesenchymal stem cells in vitro. Journal of Cellular Biochemistry. 1997;64(2):295-312.

57. Weinreb M, Shinar D, Rodan GA. Di fferent pattern of alkaline-phosphatase, osteopontin, and osteocalcin expression in developing rat bone visualized by insitu hybridization. Journal of Bone and Mineral Research. 1990;5(8):831-42.

58. Komori T. What is the function of osteocalcin? Journal of Oral Biosciences. 2020;62(3):223-7.

59. Moser SC, van der Eerden BCJ. Osteocalcin- a versatile bone-derived hormone. Frontiers in Endocrinology. 2019;9.

60. Ducy P, Desbois C, Boyce B, Pinero G, Story B, Dunstan C, et al. Increased bone formation in osteocalcin-deficient mice. Nature. 1996;382(6590):448-52.

61. Reithmeier A, Panizza E, Krumpel M, Orre LM, Branca RM, Lehtiö J, et al. Tartrate-resistant acid phosphatase (TRAP/ACP5) promotes metastasis-related properties via TGFβ2/TβR and CD44 in MDA-MB-231 breast cancer cells. BMC cancer. 2017;17(1):1-19.

62. AlQranei MS, Senbanjo LT, Aljohani H, Hamza T, Chellaiah MA. Lipopolysaccharide- TLR-4 axis regulates osteoclastogenesis independent of RANKL/RANK signaling. BMC Immunology. 2021;22(1).

63. Singh A, Gill G, Kaur H, Amhmed M, Jakhu H. Role of osteopontin in bone remodeling and orthodontic tooth movement: a review. Progress in Orthodontics. 2018;19.

64. Luukkonen J, Hilli M, Nakamura M, Ritamo I, Valmu L, Kauppinen K, et al. Osteoclasts secrete osteopontin into resorption lacunae during bone resorption. Histochemistry and Cell Biology. 2019;151(6):475-87.

65. Ek-Rylander B, Andersson G. Osteoclast migration on phosphorylated osteopontin is regulated by endogenous tartrate-resistant acid phosphatase. Experimental Cell Research. 2010;316(3):443-51.

66. Bader-Meunier B, Van Nieuwenhove E, Breton S, Wouters C. Bone involvement in monogenic autoinflammatory syndromes. Rheumatology. 2018;57(4):606-18.

67. Lipowsky HH. Protease activity and the role of the endothelial glycocalyx in inflammation. Drug Discovery Today: Disease Models. 2011;8(1):57-62.

68. Singh D, Srivastava SK, Chaudhuri TK, Upadhyay G. Multifaceted role of matrix metalloproteinases (MMPs). Frontiers in Molecular Biosciences. 2015;2.

69. Shlopov BV, Gumanovskaya ML, Hasty KA. Autocrine regulation of collagenase 3 (matrix metalloproteinase 13) during osteoarthritis. Arthritis & Rheumatism: Official Journal of the American College of Rheumatology. 2000;43(1):195-205.

70. Stickens D, Behonick DJ, Ortega N, Heyer B, Hartenstein B, Yu Y, et al. Altered endochondral bone development in matrix metalloproteinase 13-deficient mice. Development. 2004;131(23):5883-95.

71. Zhang YH, Huang HG, Zhao GX, Yokoyama T, Vega H, Huang Y, et al. ATP6V1H Deficiency Impairs Bone Development through Activation of MMP9 and MMP13. Plos Genetics. 2017;13(2).

72. Schmitt SK. Osteomyelitis. Infectious Disease Clinics. 2017;31(2):325-38.

73. Kavanagh N, Ryan EJ, Widaa A, Sexton G, Fennell J, O'Rourke S, et al. *Staphylococcal* osteomyelitis: disease progression, treatment challenges, and future directions. Clinical Microbiology Reviews. 2018;31(2).

74. Mandell JC, Khurana B, Smith JT, Czuczman GJ, Ghazikhanian V, Smith SE. Osteomyelitis of the lower extremity: pathophysiology, imaging, and classification, with an emphasis on diabetic foot infection. Emergency radiology. 2018;25(2):175-88.

75. Mustafa M, Yusof SM, Iftikhar M. Osteomyelitis: pathogenesis, clinical and therapeutic challenge. International Journal of Medicine and Pharmaceutical Sciences. 2014;4:9-18.

76. Zimmerli W. Osteomyelitis: classification. Bone and Joint Infections: From Microbiology to Diagnostics and Treatment. 2021:265-72.

77. Waldvogel FA, Medoff G, Swartz MN. Osteomyelitis: A review of clinical features, therapeutic considerations and unusual aspects .3. New England Journal of Medicine. 1970;282(6):316-+.

78. Geurts J, Hohnen A, Vranken T, Moh P. Treatment strategies for chronic osteomyelitis in low-and middle-income countries: systematic review. Tropical Medicine & International Health. 2017;22(9):1054-62.

79. Birt MC, Anderson DW, Toby EB, Wang JX. Osteomyelitis: Recent advances in pathophysiology and therapeutic strategies. Journal of Orthopaedics. 2017;14(1):45-52.

80. Jarocki VM, Tacchi JL, Djordjevic SP. Non-proteolytic functions of microbial proteases increase pathological complexity. Proteomics. 2015;15(5-6):1075-88.

81. Herman-Bausier P, Valotteau C, Pietrocola G, Rindi S, Alsteens D, Foster TJ, et al. Mechanical strength and inhibition of the *Staphylococcus aureus* collagen-binding protein Cna MBio. 2016;7(5):01529-16.

82. Tong SYC, Davis JS, Eichenberger E, Holland TL, Fowler VG. *Staphylococcus aureus* Infections: epidemiology, pathophysiology, clinical manifestations, and management. Clinical Microbiology Reviews. 2015;28(3):603-61.

83. Kitaura H, Kimura K, Ishida M, Kohara H, Yoshimatsu M, Takano-Yamamoto T. Immunological reaction in TNF-α-mediated osteoclast formation and bone resorption in vitro and in vivo. Clinical and Developmental Immunology. 2013;2013.

84. Roper PM, Shao C, Veis DJ. Multitasking by the OC lineage during bone infection: bone resorption, immune modulation, and microbial niche. Cells. 2020;9(10):2157.

85. Roy M, Somerson JS, Kerr KG, Conroy JL. Pathophysiology and pathogenesis of osteomyelitis. INTECH Open Access Publisher. 2012:1-26.

86. Marais L, Ferreira N, Aldous C, Le Roux T. The pathophysiology of chronic osteomyelitis. SA Orthopaedic Journal. 2013;12(4):14-8.

87. Idrees M, Sawant S, Karodia N, Rahman A. *Staphylococcus aureus* biofilm: morphology, genetics, pathogenesis and treatment strategies. International Journal of Environmental Research and Public Health. 2021;18(14).

88. Rasigade J-P, OanaLina, Gérard. New epidemiology of S*taphylococcus aureus* infections. . Clinical Microbiology and Infection. 2014;20 (7):587-8.

89. Iwamoto M, YiLynfield, RuthBulens, Sandra NNadle, JoelleAragon, DeborahPetit, SusanRay, Susan MHarrison, Lee HDumyati, Ghinwa. Trends in invasive methicillin-resistant *Staphylococcus aureus* infections. Pediatrics. 2013;132(4):e817-e24.

90. Looney WJ. Small-colony variants of *Staphylococcus aureus*. British Journal of Biomedical Science. 2000;57(4):317-22.

91. Seligman SJ. Small-colony variants of *Staphylococcus aureus*. Clinical Infectious Diseases. 2006;42(1):155-6.

92. Perez K. *Staphylococcus epidermidis* interactions with the human host that permit evasion of immune killing: College of Medicine-Mayo Clinic; 2018.

93. Makarewicz O, Klinger-Strobel M, Ehricht R, Kresken M, Pletz MW. Antibiotic resistance in pulmonary infections: mechanisms and epidemiology. Anti-infectives and the Lung: ERS Monograph. 2017;75:21.

94. Nourbakhsh F, Namvar AE. Detection of genes involved in biofilm formation in *Staphylococcus aureus* isolates. Gms Hygiene and Infection Control. 2016;11.

95. Mah TF. Biofilm-specific antibiotic resistance. Future Microbiology. 2012;7(9):1061-72.

96. Berry KA, Verhoef MT, Leonard AC, Cox G. *Staphylococcus aureus* adhesion to the host. Annals of the New York Academy of Sciences. 2022.

97. Birt MC, Anderson DW, Toby EB, Wang J. Osteomyelitis: recent advances in pathophysiology and therapeutic strategies. Journal of orthopaedics. 2017;14(1):45-52.

98. Josse J, Velard F, Gangloff SC. *Staphylococcus aureus* vs. osteoblast: relationship and consequences in osteomyelitis. Frontiers in Cellular and Infection Microbiology. 2015;5.

99. Wen Q, Gu F, Sui Z, Su Z, Yu T. The process of osteoblastic infection by *Staphylococcus aureus*. International Journal of Medical Sciences. 2020; 17(10):1327.

100. Shi SF, Zhang XL. Interaction of *Staphylococcus aureus* with osteoblasts (Review). Experimental and Therapeutic Medicine. 2012;3(3):367-70.

101. Stracquadanio S, Musso N, Costantino A, Lazzaro LM, Stefani S, Bongiorno D. *Staphylococcus aureus* internalization in osteoblast cells: mechanisms, interactions and biochemical processes. What did we learn from experimental models? Pathogens. 2021;10(2):239.

102. Vandenesch F, Lina G, Henry T. *Staphylococcus aureus* hemolysins, bi-component leukocidins, and cytolytic peptides: a redundant arsenal of membrane-damaging virulence factors? Frontiers in Cellular and Infection Microbiology. 2012;2.

103. Brandt SL, Putnam NE, Cassat JE, Serezani CH. I nnate immunity to *Staphylococcus aureus*: evolving paradigms in soft tissue and invasive infections. The Journal of Immunology. 2018;200(12):3871-80.

104. Bianco P. "Mesenchymal" stem cells. Annual Review of Cell and Developmental Biology, Vol 30. 2014;30:677-704.

105. Lavoie JR, Rosu-Myles M. Uncovering the secretes of mesenchymal stem cells. Biochimie. 2013;95(12):2212-21.

106. Sousa BR, Parreira RC, Fonseca EA, Amaya MJ, Tonelli FM, Lacerda SM, et al. Human adult stem cells from diverse origins: an overview from multiparametric immunophenotyping to clinical applications. Cytometry Part A. 2014;85(1):43-77.

107. Calloni R, Cordero EAA, Henriques JAP, Bonatto D. Reviewing and updating the major molecular markers for stem c ells. Stem Cells and Development. 2013;22(9):1455-76.

108. Keramaris NC, Kaptanis S, Moss HL, Loppini M, Pneumaticos S, Maffulli N. Endothelial progenitor cells (EPCs) and mesenchymal stem cells (MSCs) in bone healing. Current Stem Cell Research & Therapy. 2012;7(4):293-301.

109. Bieback K, Schallmoser K, Klutera H, Strunk D. Clinical protocols for the isolation and expansion of mesenchymal stromal cells. Transfusion Medicine and Hemotherapy. 2008;35(4):286-94.

110. Ikebe C, Suzuki K. Mesenchymal stem cells for regenerative therapy: Optimization of cell preparation protocols. Biomed research international. 2014;2014.

111. Cong Q, Xu Y, Wang YH, Jiang W, Wang YS, Li B, et al. Isolation and characterization of mesenchymal stem cells from human bone marrow. International Journal of Clinical and Experimental Medicine. 2016;9(7):12904-10.

112. Bahar AA, Ren D. Antimicrobial peptides. Pharmaceuticals. 2013;6(12):1543-75.

113. Haney EF, Mansour SC, Hancock RE. Antimicrobial peptides: an introduction. Antimicrobial Peptides. 2017:3-22.

114. Kang HK, Kim C, Seo CH, Park Y. The therapeutic applications of antimicrobial peptides (AMPs): a patent review. Journal of Microbiology. 2017;55(1):1-12.

115. Seyfi R, Kahaki FA, Ebrahimi T, Montazersaheb S, Eyvazi S, Babaeipour V, et al. Antimicrobial peptides (AMPs): roles, functions and mechanism of action. International Journal of Peptide Research and Therapeutics. 2020;26(3):1451-63.

116. Divyashree M, Mani MK, Reddy D, Kumavath R, Ghosh P, Azevedo V, et al. Clinical applications of antimicrobial peptides (AMPs): where do we stand now? Protein and peptide letters. 2020;27(2):120-34.

117. Brender JR, McHenry AJ, Ramamoorthy A. Does cholesterol play a role in the bacterial selectivity of antimicrobial peptides? Frontiers in Immunology. 2012;3.

118. McHenry AJ, Sciacca MFM, Brender JR, Ramamoorthy A. Does cholesterol suppress the antimicrobial peptide induced disruption of lipid raft containing membranes? Biochimica Et Biophysica Acta-Biomembranes. 2012;1818(12):3019-24.

119. Alcayaga-Miranda F, Cuenca J, Khoury M. Antimicrobial activity of mesenchymal stem cells: current status and new perspectives of antimicrobial peptide-based therapies. Frontiers in Immunology. 2017;8.

120. Noore J, Noore A, Li BY. Cationic antimicrobial peptide LL-37 is effective against both extra- and entracellular *Staphylococcus aureus*. Antimicrobial Agents and Chemotherapy. 2013;57(3):1283-90.

121. Choi H, Yang Z, Weisshaar JC. Oxidative stress induced in E. coli by the human antimicrobial peptide LL-37. PLOS pathogens. 2017;13(6):e1006481.

122. Krasnodembskaya A, Samarani G, Song YL, Zhuo HJ, Su X, Lee JW, et al. Human mesenchymal stem cells reduce mortality and bacteremia in gram-negative sepsis in mice in part by enhancing the phagocytic activity of blood monocytes. American Journal of Physiology-Lung Cellular and Molecular Physiology. 2012;302(10):L1003-L13.

123. Putnam NE. Innate Immunity and Bone Remodeling during *Staphylococcus aureus* Osteomyelitis: Vanderbilt University; 2018.

124. Yagi H, Chen AF, Hirsch D, Rothenberg AC, Tan J, Alexander PG, et al. Antimicrobial activity of mesenchymal stem cells against *Staphylococcus aureus*. Stem Cell Research & Therapy. 2020;11(1).

125. Verjans E-T, Zels S, Luyten W, Landuyt B, Schoofs L. Molecular mechanisms of LL-37-induced receptor activation: An overview. Peptides. 2016;85:16-26.

126. Conibear AC, Craik DJ. The chemistry and biology of theta defensins. Angewandte Chemie International Edition. 2014;53(40):10612-23.

127. Shah R, Chang TL. Defensins in viral infection. Small wonders: peptides for disease control: ACS Publications; 2012. p. 137-71.

128. da Silva FP, Machado MCC. Antimicrobial peptides: clinical relevance and therapeutic implications. Peptides. 2012;36(2):308-14.

129. Garcia JRC, Krause A, Schulz S, Rodriguez-Jimenez FJ, Kluver E, Adermann K, et al. Human beta-defensin 4: a novel inducible peptide with a specific salt-sensitive spectrum of antimicrobial activity. Faseb Journal. 2001;15(8):1819-+.

130. Harder J, Bartels J, Christophers E, Schroder JM. Isolation and characterization of human beta-defensin-3, a novel human inducible peptide antibiotic. Journal of Biological Chemistry. 2001;276(8):5707-13.

131. Duits LA, Nibbering PH, van Strijen E, Vos JB, Mannesse-Lazeroms SPG, van Sterkenburg M, et al. Rhinovirus increases human beta-defensin-2 and -3 mRNA expression in cultured bronchial epithelial cells. Fems Immunology and Medical Microbiology. 2003;38(1):59-64.

132. Sumikawa Y, Asada H, Hoshino K, Azukizawa H, Katayama I, Akira S, et al. Induction of beta-defensin 3 in keratinocytes stimulated by bacterial lipopeptides through toll-like receptor 2. Microbes and Infection. 2006;8(6):1513-21.

133. Harder J, Meyer-Hoffert U, Wehkamp K, Schwichtenberg L, Schroder JM. Differential gene induction of human beta-defensins (hBD-1, -2, -3, and -4) in keratinocytes is inhibited by retinoic acid. Journal of Investigative Dermatology. 2004;123(3):522-9.

134. Harder J, Bartels J, Christophers E, Schroder JM. A peptide antibiotic from human skin. Nature. 1997;387(6636):861-.

135. Bolatchiev A. Antibacterial activity of human defensins against *Staphylococcus aureus* and *Escherichia coli*. PeerJ. 2020;8:e10455.

136. Midorikawa K, Ouhara K, Komatsuzawa H, Kawai T, Yamada S, Fujiwara T, et al. *Staphylococcus aureus* susceptibility to innate antimicrobial peptides, beta-defensins and CAP18, expressed by human keratinocytes. Infection and Immunity. 2003;71(7):3730-9.

137. Koprivnjak T, Weidenmaier C, Peschel A, Weiss JP. Wall teichoic acid deficiency in *Staphylococcus aureus* confers selective resistance to mammalian group IIA phospholipase A(2) and human p-defensin 3. Infection and Immunity. 2008;76(5):2169-76.

138. King NJC, Thomas SR. Molecules in focus: Indoleamine 2,3-dioxygenase. International Journal of Biochemistry & Cell Biology. 2007;39(12):2167-72.

139. Bilir C, Sarisozen C. Indoleamine 2, 3-dioxygenase (IDO): only an enzyme or a checkpoint controller? Journal of Oncological Sciences. 2017;3(2):52-6.

140. Schmidt SK, Siepmann S, Kuhlmann K, Meyer HE, Metzger S, Pudelko S, et al. Influence of tryptophan contained in 1-methyl-tryptophan on antimicrobial and immunoregulatory functions of indoleamine 2,3-dioxygenase. Plos One. 2012;7(9).

141. Beekhuizen H, De Gevel JSV. Gamma interferon confers resistance to infection with *Staphylococcus aureus* in human vascular endothelial cells by cooperative proinflammatory and enhanced intrinsic antibacterial activities. Infection and Immunity. 2007;75(12):5615-26.

142. Schroten H, Spors B, Hucke C, Stins M, Kim KS, Adam R, et al. Potential role of human brain microvascular endothelial cells in the pathogenesis of brain abscess: Inhibition of *Staphylococcus aureus* by activation of indoleamine 2,3-dioxygenase. Neuropediatrics. 2001;32(4):206-10.

143. Nizet V, Ohtake T, Lauth X, Trowbridge J, Rudisill J, Dorschner RA, et al. Innate antimicrobial peptide protects the skin from invasive bacterial infection. Nature. 2001;414(6862):454-7.

144. Parisien A, Allain B, Zhang J, Mandeville R, Lan C. Novel alternatives to antibiotics: bacteriophages, bacterial cell wall hydrolases, and antimicrobial peptides. Journal of applied microbiology. 2008;104(1):1-13.

145. Lopez-Garcia L, Castro-Manrreza ME. TNF-alpha and INF- gamma participate in improving the immunoregulatory capacity of mesenchymal stem stromal cells: importance of cell-cell contact and extracellular vesicles. International Journal of Molecular Sciences. 2021;22(17).

146. Wang YF, Tian MY, Wang F, Heng BC, Zhou J, Cai ZJ, et al. Understanding the immunological mechanisms of mesenchymal stem cells in allogeneic transplantation: from the aspect of major histocompatibility complex class I. Stem Cells and Development. 2019;28(17):1141-50.

147. Newman MA, Sundelin T, Nielsen JT, Erbs G. MAMP (microbe-associated molecular pattern) triggered immunity in plants. Frontiers in Plant Science. 2013;4.

148. Kwon Y, Park C, Lee J, Park DH, Jeong S, Yun CH, et al. Regulation of bone cell differentiation and activation by microbe-associated molecular patterns. International Journal of Molecular Sciences. 2021;22(11).

149. Michaelis LJ. The immunological mechanisms underlying the development of immune tolerance in childhood: Universty of Southampton; 2018.

150. Kawasaki T, Kawai T. Toll-like receptor signaling pathways. Frontiers in Immunology. 2014;5.

151. Pandey S, Kawai T, Akira S. Microbial sensing by Toll-like receptors and intracellular nucleic acid sensors. Cold Spring Harbor Perspectives in Biology. 2015;7(1).

152. Takeda K, Akira S. Toll-like receptors. Current protocols in immunology. 2015;109(1):14.2. 1-.2. 0.

153. Kim C. Toll-Like Receptors (TLRs). In: Glycobiology of Innate Immunology. . Springer, editor. Singapore: Springer; 2002 2022.

154. Kang JY, Lee JO. Structural biology of the Toll-like receptor family. Annual Review of Biochemistry, Vol 80. 2011;80:917-41.

155. Botos I, Segal DM, Davies DR. The structural biology of Toll-like receptors. Structure. 2011;19(4):447-59.

156. Moresco EMY, LaVine D, Beutler B. Toll-like receptors. Current Biology. 2011;21(13):R488-R93.

157. Fitzgerald KA, Kagan JC. Toll-like receptors and the control of immunity. Cell. 2020;180(6):1044-66.

158. Kawasaki T, Kawai T. Toll-like receptor signaling pathways. Frontiers in immunology. 2014:461.

159. Nasi S, Ea H-K, Chobaz V, van Lent P, Lioté F, So A, et al. Dispensable role of myeloid differentiation primary response gene 88 (MyD88) and MyD88-dependent toll-like receptors (TLRs) in a murine model of osteoarthritis. Joint Bone Spine. 2014;81(4):320-4.

160. Zhu S, Xiang XJ, Xu X, Gao SN, Mai KS, Ai QH. TIR domain-containing adaptor-inducing interferon-beta (TRIF) participates in antiviral immune responses and hepatic lipogenesis of large yellow croaker (Larimichthys crocea). Frontiers in Immunology. 2019;10.

161. Kawai T, Akira S. Toll-like receptors and their crosstalk with other innate receptors in infection and immunity. Immunity. 2011;34(5):637-50.

162. Aliprantis AO, Yang R-B, Mark MR, Suggett S, Devaux B, Radolf JD, et al. Cell activation and apoptosis by bacterial lipoproteins through toll-like receptor-2. Science. 1999;285(5428):736-9.

163. Hashimoto M, Tawaratsumida K, Kariya H, Kiyohara A, Suda Y, Krikae F, et al. Not lipoteichoic acid but lipoproteins appear to be the dominant immunobiologically active compounds in *Staphylococcus aureus*. The Journal of Immunology. 2006;177(5):3162-9.

164. Takeuchi O, Hoshino K, Kawai T, Sanjo H, Takada H, Ogawa T, et al. Differential roles of TLR2 and TLR4 in recognition of gram-negative and gram-positive bacterial cell wall components. Immunity. 1999;11(4):443-51.

165. Takeuchi O, Hoshino K, Akira S. Cutting edge: TLR2-deficient and MyD88-deficient mice are highly susceptible to *Staphylococcus aureus* infection. The Journal of Immunology. 2000;165(10):5392-6.

166. Fournier B. The function of TLR2 during S*taphylococcal* diseases. Frontiers in Cellular and Infection Microbiology. 2013;3.

167. Mele T, Madrenas J. TLR2 signalling: At the crossroads of commensalism, invasive infections and toxic shock syndrome by *Staphylococcus aureus*. International Journal of Biochemistry & Cell Biology. 2010;42(7):1066-71.

168. Muller-Anstett MA, Muller P, Albrecht T, Nega M, Wagener J, Gao Q, et al. *Staphylococcal* peptidoglycan co-localizes with NOD2 and TLR2 and activates innate immune response via both receptors in primary murine keratinocytes. Plos One. 2010;5(10).

169. Su LJ, Wang Y, Wang JM, Mifune Y, Morin MD, Jones BT, et al. Structural basis of TLR2/TLR1 activation by the s ynthetic agonist diprovocim. Journal of Medicinal Chemistry. 2019;62(6):2938-49.

170. Lee CC, Avalos AM, Ploegh HL. Accessory molecules for Toll-like receptors and their function. Nature Reviews Immunology. 2012;12(3):168-79.

171. DelaRosa O, Dalemans W, Lombardo E. Toll-like receptors as modulators of mesenchymal stem cells. Frontiers in Immunology. 2012;3.

172. van den Akker F, de Jager SCA, Sluijter JPG. Mesenchymal stem cell therapy for cardiac inflammation: immunomodulatory properties and the influence of toll-like receptors. Mediators of Inflammation. 2013;2013.

173. Opitz CA, Litzenburger UM, Lutz C, Lanz TV, Tritschler I, Koppel A, et al. Toll-like receptor engagement enhances the immunosuppressive properties of human bone marrow-derived mesenchymal stem cells by inducing indoleamine-2,3-dioxygenase-1 via interferon-beta and protein kinase R. Stem Cells. 2009;27(4):909-19.

174. DelaRosa O, Lombardo E. Modulation of adult mesenchymal stem cells activity by toll-like receptors: implications on therapeutic potential. Mediators of Inflammation. 2010;2010.

175. Wang Y, Chen XD, Cao W, Shi YF. Plasticity of mesenchymal stem cells in immunomodulation: pathological and therapeutic implications. Nature Immunology. 2014;15(11):1009-16.

176. Najar M, Krayem M, Meuleman N, Bron D, Lagneaux L. Mesenchymal stromal cells and toll-like receptor priming: A critical review. Immune Network. 2017;17(2):89-102.

177. Cho HH, Shin KK, Kim YJ, Song JS, Kim JM, Bae YC, et al. NF-kappa B activation stimulates osteogenic differentiation of mesenchymal stem cells derived from human adipose tissue by increasing TAZ expression. Journal of Cellular Physiology. 2010;223(1):168-77.

178. Shirjang S, Mansoori B, Solali S, Hagh MF, Shamsasenjan K. Toll-like receptors as a key regulator of mesenchymal stem cell function: an up-to-date review. Cellular Immunology. 2017;315:1-10.

179. Cho HH, Bae YC, Jung JS. Role of toll-like receptors on human adipose-derived stromal cells. Stem Cells. 2006;24(12):2744-52.

180. Pond CM, Mattacks CA. In vivo evidence for the involvement of the adipose tissue surrounding lymph nodes in immune responses. Immunology letters. 1998;63(3):159-67.

181. Fritz JM, McDonald JR. Osteomyelitis: approach to diagnosis and treatment. Physician and Sportsmedicine. 2008;36(1):50-4.

182. Hatzenbuehler J, Pulling TJ. Diagnosis and management of osteomyelitis. American Family Physician. 2011;84(9):1027-33.

183. Chen XJ, Niyonsaba F, Ushio H, Okuda D, Nagaoka I, Ikeda S, et al. Synergistic effect of antibacterial agents human beta-defensins, cathelicidin LL-37 and lysozyme against *Staphylococcus aureus* and *Escherichia coli*. Journal of Dermatological Science. 2005;40(2):123-32.

184. Edwards AM, Potts JR, Josefsson E, Massey RC. *Staphylococcus aureus* host cell invasion and virulence in sepsis is facilitated by the multiple repeats within FnBPA. Plos Pathogens. 2010;6(6).

185. Nordstrom K, Forsgren A. Effect of protein - A on adsorption of bacteriophages to *Staphylococcus aureus* Journal of Virology. 1974;14(2):198-202.

186. Dayan GH, Mohamed N, Scully IL, Cooper D, Begier E, Eiden J, et al. *Staphylococcus aureus:* the current state of disease, pathophysiology and strategies for prevention. Expert Review of Vaccines. 2016;15(11):1373-92.

187. Lima ALL, Oliveira PR, Carvalho VC, Cimerman S, Savio E. Recommendations for the treatment of osteomyelitis. Brazilian Journal of Infectious Diseases. 2014;18:526-34.

188. Nauta AJ, Fibbe WE. Immunomodulatory properties of mesenchymal stromal cells. Blood, The Journal of the American Society of Hematology. 2007;110(10):3499-506.

189. Weiss ARR, Dahlke MH. Immunomodulation by mesenchymal stem cells (MSCs): mechanisms of action of living, apoptotic, and dead MSCs. Frontiers in Immunology. 2019;10.

190. Gebler A, Zabel O, Seliger B. The immunomodulatory capacity of mesenchymal stem cells. Trends in Molecular Medicine. 2012;18(2):128-34.

191. Fontaine MJ, Shih H, Schafer R, Pittenger MF. Unraveling the mesenchymal stromal cells' paracrine immunomodulatory effects. Transfusion Medicine Reviews. 2016;30(1):37-43.

192. Murphy MB, Moncivais K, Caplan AI. Mesenchymal stem cells: environmentally responsive therapeutics for regenerative medicine. Experimental & molecular medicine. 2013;45(11):e54-e.

193. Abnave P, Ghigo E, editors. Role of the immune system in regeneration and its dynamic interplay with adult stem cells. Seminars in cell & developmental biology; 2019: Elsevier.

194. Sallustio F, Curci C, Stasi A, De Palma G, Divella C, Gramignoli R, et al. Role of toll-like receptors in actuating stem/progenitor cell repair mechanisms: different functions in different cells. Stem Cells International. 2019;2019.

195. Johnson V, Webb T, Dow S. Activated mesenchymal stem cells amplify antibiotic activity against chronic *Staphylococcus aureus* infection. Journal of Immunology. 2013;190.

196. Johnson V, Webb T, Norman A, Coy J, Kurihara J, Regan D, et al. Activated mesenchymal stem cells interact with antibiotics and host innate immune responses to control chronic bacterial infections. Scientific Reports. 2017;7.

197. Dietrich L, Lucius R, Roider J, Klettner A. Interaction of inflammatorily activated retinal pigment epithelium with retinal microglia and neuronal cells. Experimental Eye Research. 2020;199.

198. Alcayaga-Miranda F, Cuenca J, Khoury M. Antimicrobial activity of mesenchymal stem cells: current status and new perspectives of antimicrobial peptide-based therapies. Frontiers in immunology. 2017;8:339.

199. Wang XR, Zhang Z, Louboutin JP, Moser C, Weiner DJ, Wilson JM. Airway epithelia regulate expression of human beta-defensin 2 through toll-like receptor 2. Faseb Journal. 2003;17(10):1727-+.

200. Birchler T, Seibl R, Buchner K, Loeliger S, Seger R, Hossle JP, et al. Human Toll-like receptor 2 mediates induction of the antimicrobial peptide human beta-defensin 2 in response to bacterial lipoprotein. European Journal of Immunology. 2001;31(11):3131-7.

201. Liu PT, Stenger S, Li HY, Wenzel L, Tan BH, Krutzik SR, et al. Toll-like receptor triggering of a vitamin D-mediated human antimicrobial response. Science. 2006;311(5768):1770-3.

202. Hertz CJ, Wu Q, Porter EM, Zhang YJ, Weismüller K-H, Godowski PJ, et al. Activation of Toll-like receptor 2 on human tracheobronchial epithelial cells induces the antimicrobial peptide human β defensin-2. The Journal of Immunology. 2003;171(12):6820-6.

203. Pezzanite LM, Chow L, Johnson V, Griffenhagen GM, Goodrich L, Dow S. Toll-like receptor activation of equine mesenchymal stromal cells to enhance antibacterial activity and immunomodulatory cytokine secretion. Veterinary Surgery. 2021;50(4):858-71.

204. Abe Y, Akiyama H, Arata J. Production of experimental S*taphylococc*al impetigo in mice. Journal of Dermatological Science. 1992;4(1):42-8.

205. Yu Y, Yip KH, Tam IYS, Sam SW, Ng CW, Zhang W, et al. Differential effects of the Toll-like receptor 2 agonists, PGN and Pam3CSK4 on anti-IgE induced human mast cell activation. PLoS One. 2014;9(11):e112989.

206. Funderburg NT, Jadlowsky JK, Lederman MM, Feng ZM, Weinberg A, Sieg SF. The Toll-like receptor 1/2 agonists Pam(3)CSK(4) and human beta-defensin-3 differentially induce interleukin-10 and nuclear factor-kappa B signalling patterns in human monocytes. Immunology. 2011;134(2):151-60.

207. Nguyen DT, de Witte L, Ludlow M, Yuksel S, Wiesmuller KH, Geijtenbeek TBH, et al. The synthetic bacterial lipopeptide Pam3CSK4 modulates respiratory syncytial virus infection independent of TLR activation. Plos Pathogens. 2010;6(8).

208. Hertz CJ, Wu Q, Porter EM, Zhang YJ, Weismuller KH, Godowski PJ, et al. Activation of toll-like receptor 2 on human tracheobronchial epithelial cells induces the antimicrobial peptide human beta defensin-2. Journal of Immunology. 2003;171(12):6820-6.

209. Cahuascanco B, Bahamonde J, Huaman O, Jervis M, Cortez J, Palomino J, et al. Bovine fetal mesenchymal stem cells exert antiproliferative effect against mastitis causing pathogen *Staphylococcus aureus*. Veterinary Research. 2019;50.

210. Harman RM, Yang S, He MK, Van de Walle GR. Antimicrobial peptides secreted by equine mesenchymal stromal cells inhibit the growth of bacteria commonly found in skin wounds. Stem Cell Research & Therapy. 2017;8(1):1-14.

211. MacKenzie CR, Worku D, Daubener W. Regulation of IDO-mediated bacteriostasis in macrophages: Role of antibiotics and anti-inflammatory agents. Developments in Tryptophan and Serotonin Metabolism. 2003;527:67-76.

212. Furset G, Floisand Y, Sioud M. Impaired expression of indoleamine 2, 3-dioxygenase in monocyte-derived dendritic cells in response to Toll-like receptor-7/8 ligands. Immunology. 2008;123(2):263-71.

213. Godin-Ethier J, Hanafi LA, Duvignaud JB, Leclerc D, Lapointe R. IDO expression by human B lymphocytes in response to T lymphocyte stimuli and TLR engagement is biologically inactive. Molecular Immunology. 2011;49(1-2):253-9.

214. Salazar F, Awuah D, Negm OH, Shakib F, Ghaemmaghami AM. The role of indoleamine 2,3-dioxygenase-aryl hydrocarbon receptor pathway in the TLR4-induced tolerogenic phenotype in human DCs. Scientific Reports. 2017;7.

215. Oliveira JA, Gandini M, Sales JS, Fujimori SK, Barbosa MG, Frutuoso VS, et al. Mycobacterium leprae induces a tolerogenic profile in monocyte-derived dendritic cells via TLR2 induction of IDO. Journal of Leukocyte Biology. 2021;110(1):167-76.

216. Burd RS, Furrer JL, Sullivan J, Smith AL. Murine β-defensin-3 is an inducible peptide with limited tissue expression and broad-spectrum antimicrobial activity. Shock. 2002;18(5):461-4.

217. Xuan JQ, Feng WG, Wang JY, Wang RC, Zhang BW, Bo LT, et al. Antimicrobial peptides for combating drug-resistant bacterial infections. Drug Resistance Updates. 2023;68.

218. Carratelli CR, Mazzola N, Paolillo R, Sorrentino S, Rizzo A. Toll-like receptor-4 (TLR4) mediates human beta-defensin-2 (HBD-2) induction in response to Chlamydia pneumoniae in mononuclear cells. Fems Immunology and Medical Microbiology. 2009;57(2):116-24.

219. Lai Y, Cogen AL, Radek KA, Park HJ, MacLeod DT, Leichtle A, et al. Activation of TLR2 by a small molecule produced by *Staphylococcus epidermidis* increases antimicrobial defense against bacterial skin infections. Journal of Investigative Dermatology. 2010;130(9):2211-21.

220. Krasnodembskaya A, Song Y, Fang X, Gupta N, Serikov V, Lee J-W, et al. Antibacterial effect of human mesenchymal stem cells is mediated in part from secretion of the antimicrobial peptide LL-37. Stem cells. 2010;28(12):2229-38.

221. Huh J-E, Lee SY. IL-6 is produced by adipose-derived stromal cells and promotes osteogenesis. Biochimica et Biophysica Acta (BBA)-Molecular Cell Research. 2013;1833(12):2608-16.

222. Wu W, Dietze KK, Gibbert K, Lang KS, Trilling M, Yan H, et al. TLR ligand induced IL-6 counter-regulates the anti-viral CD8+ T cell response during an acute retrovirus infection. Scientific reports. 2015;5(1):1-14.

223. Pevsner-Fischer M, Morad V, Cohen-Sfady M, Rousso-Noori L, Zanin-Zhorov A, Cohen S, et al. Toll-like receptors and their ligands control mesenchymal stem cell functions. Blood. 2007;109(4):1422-32.

224. Lopes D, Martins-Cruz C, Oliveira MB, Mano JF. Bone physiology as inspiration for tissue regenerative therapies. Biomaterials. 2018;185:240-75.

225. Neve A, Corrado A, Cantatore FP. Osteoblast physiology in normal and pathological conditions. Cell and Tissue Research. 2011;343(2):289-302.

226. Gunawardena TNA, Rahman MT, Abdullah BJJ, Abu Kasim NH. Conditioned media derived from mesenchymal stem cell cultures: The next generation for regenerative medicine. Journal of Tissue Engineering and Regenerative Medicine. 2019;13(4):569-86.

227. Merimi M, El-Majzoub R, Lagneaux L, Agha DM, Bouhtit F, Meuleman N, et al. The therapeutic potential of mesenchymal stromal cells for regenerative medicine: current knowledge and future understandings. Frontiers in Cell and Developmental Biology. 2021;9.

228. Wei X, Yang X, Han ZP, Qu FF, Shao L, Shi YF. Mesenchymal stem cells: a new trend for cell therapy. Acta Pharmacologica Sinica. 2013;34(6):747-54.

229. Izumoto-Akita T, Tsunekawa S, Yamamoto A, Uenishi E, Ishikawa K, Ogata H, et al. Secreted factors from dental pulp stem cells improve glucose intolerance in streptozotocin-induced diabetic mice by increasing pancreatic β-cell function. BMJ Open Diabetes Research and Care. 2015;3(1):e000128.

230. Benavides-Castellanos MP, Garzón-Orjuela N, Linero I. Effectiveness of mesenchymal stem cell-conditioned medium in bone regeneration in animal and human models: a systematic review and meta-analysis. Cell Regeneration. 2020;9(1):1-22.

231. Otsuru S, Desbourdes L, Guess AJ, Hofmann TJ, Relation T, Kaito T, et al. Extracellular vesicles released from mesenchymal stromal cells stimulate bone growth in osteogenesis imperfecta. Cytotherapy. 2018;20(1):62-73.

232. Porzionato A, Zaramella P, Dedja A, Guidolin D, Van Wemmel K, Macchi V, et al. Intratracheal administration of clinical-grade mesenchymal stem cell-derived extracellular vesicles reduces lung injury in a rat model of bronchopulmonary dysplasia. American Journal of Physiology-Lung Cellular and Molecular Physiology. 2019;316(1):L6-L19.

233. Linero I, Chaparro O. Paracrine effect of mesenchymal stem cells derived from human adipose tissue in bone regeneration. Plos One. 2014;9(9).

234. Katagiri W, Osugi M, Kawai T, Hibi H. First-in-human study and clinical case reports of the alveolar bone regeneration with the secretome from human mesenchymal stem cells. Head & Face Medicine. 2016;12.

235. Furuta T, Miyaki S, Ishitobi H, Ogura T, Kato Y, Kamei N, et al. Mesenchymal stem cell-derived exosomes promote fracture healing in a mouse model. Stem Cells Translational Medicine. 2016;5(12):1620-30.

236. Chang W, Kim R, Park SI, Jung YJ, Ham O, Lee J, et al. Enhanced healing of rat calvarial bone defects with hypoxic conditioned medium from mesenchymal stem

cells through increased endogenous stem cell migration via regulation of ICAM-1 Targeted-microRNA-221. Molecules and Cells. 2015;38(7):643-50.

237. Nakamura Y, Miyaki S, Ishitobi H, Matsuyama S, Nakasa T, Kamei N, et al. Mesenchymal-stem-cell-derived exosomes accelerate skeletal muscle regeneration. FEBS letters. 2015;589(11):1257-65.

238. Zhang S, Chu WC, Lai RC, Lim SK, Hui JHP, Toh WS. Exosomes derived from human embryonic mesenchymal stem cells promote osteochondral regeneration. Osteoarthritis and Cartilage. 2016;24(12):2135-40.

239. Kawai T, Katagiri W, Osugi M, Sugimura Y, Hibi H, Ueda M. Secretomes from bone marrow–derived mesenchymal stromal cells enhance periodontal tissue regeneration. Cytotherapy. 2015;17(4):369-81.

240. Garg P, Mazur MM, Buck AC, Wandtke ME, Liu JY, Ebraheim NA. Prospective Review of Mesenchymal Stem Cells Differentiation into Osteoblasts. Orthopaedic Surgery. 2017;9(1):13-9.

241. Osugi M, Katagiri W, Yoshimi R, Inukai T, Kawai T, Hibi H, et al. Conditioned media from bone marrow derived mesenchymal stem cells and adipose derived stem cells enhanced bone regeneration in rat calvarial bone defects. Journal of Tissue Engineering and Regenerative Medicine. 2012;6:283-.

242. Lange-Consiglio A, Gusmara C, Manfredi E, Idda A, Soggiu A, Greco V, et al. Antimicrobial effects of conditioned medium from amniotic progenitor cells in vitro and in vivo: toward tissue regenerative therapies for bovine mastitis. Frontiers in Veterinary Science. 2019;6:443.

243. Sung DK, Chang YS, Sung SI, Yoo HS, Ahn SY, Park WS. Antibacterial effect of mesenchymal stem cells against *Escherichia coli* is mediated by secretion of beta-defensin-2 via toll-like receptor 4 signalling. Cellular Microbiology. 2016;18(3):424-36.

244. Cortes-Araya Y, Amilon K, Rink BE, Black G, Lisowski Z, Donadeu FX, et al. Comparison of Antibacterial and Immunological Properties of Mesenchymal Stem/Stromal Cells from Equine Bone Marrow, Endometrium, and Adipose Tissue. Stem Cells and Development. 2018;27(21):1518-25.

245. Park J, Kim S, Lim H, Liu A, Hu S, Lee J, et al. Therapeutic effects of human mesenchymal stem cell microvesicles in an ex vivo perfused human lung injured with severe E. coli pneumonia. Thorax. 2019;74(1):43-50.

246. Cequier A, Vazquez FJ, Fuente S, Vitoria A, Romero A, Rodellar C, et al. Immunomodulatory capacity of equine mesenchymal stem cells (MSCs) is influenced by inflammation, differentiation and compatibility for the major histocompatibility complex (MHC). Human Gene Therapy. 2021;32(19-20):A146-A.

247. Sun J, Zhou H, Deng Y, Zhang Y, Gu P, Ge S, et al. Conditioned medium from bone marrow mesenchymal stem cells transiently retards osteoblast differentiation by downregulating runx2. Cells Tissues Organs. 2012;196(6):510-22.

248. Elkington P, Shiomi T, Breen R, Nuttall RK, Ugarte-Gil CA, Walker NF, et al. MMP-1 drives immunopathology in human tuberculosis and transgenic mice. The Journal of Clinical Investigation. 2011;121(5):1827-33.

249. Hu QC, Ecker M. Overview of MMP-13 as a promising target for the treatment of osteoarthritis. International Journal of Molecular Sciences. 2021;22(4).

250. Leeman MF, Curran S, Murray GI. The structure, regulation, and function of human matrix metalloproteinase-13. Critical Reviews in Biochemistry and Molecular Biology. 2002;37(3):149-66.

251. Ortega N, Behonick DJ, Werb Z. Matrix remodeling during endochondral ossification. Trends in Cell Biology. 2004;14(2):86-93.

252. Lew DP, Waldvogel FA. Osteomyelitis. Lancet. 2004;364(9431):369-79.

253. Parente R, Possetti V, Schiavone ML, Campodoni E, Menale C, Loppini M, et al. 3D cocultures of osteoblasts and s*taphylococcus aureus* on biomimetic bone scaffolds as a tool to investigate the host-pathogen interface in osteomyelitis. Pathogens. 2021;10(7).

254. Tuchscherr L, Medina E, Hussain M, Volker W, Heitmann V, Niemann S, et al. *Staphylococcus aureus* phenotype switching: an effective bacterial strategy to escape host immune response and establish a chronic infection. Embo Molecular Medicine. 2011;3(3):129-41.

255. de Mesy Bentley KL, Trombetta R, Nishitani K, Bello-Irizarry SN, Ninomiya M, Zhang L, et al. Evidence of *Staphylococcus aureus* deformation, proliferation, and migration in canaliculi of live cortical bone in murine models of osteomyelitis Journal of Bone and Mineral Research. 2017;32(5): 985-90.

256. Craig MR, Poelstra KA, Sherrell JC, Kwon MS, Belzile EL, Brown TE. A novel total knee arthroplasty infection model in rabbits. Journal of Orthopaedic Research. 2005;23(5):1100-4.

257. Yuste I, Luciano FC, Gonzalez-Burgos E, Lalatsa A, Serrano DR. Mimicking bone microenvironment: 2D and 3D in vitro models of human osteoblasts. Pharmacological Research. 2021;169.

258. Cramer E, Ito K, Hofmann S. Ex vivo bone models and their potential in preclinical evaluation. Current Osteoporosis Reports. 2021;19(1):75-87.

259. Owen R, Reilly GC. In vitro models of bone remodelling and associated disorders. Frontiers in Bioengineering and Biotechnology. 2018;6.

260. Khan J. Developing ex vivo models for understanding microbial infection associated with hip and knee implants: Cardiff University; 2022.

261. Bellido T, Delgado-Calle J. Ex Vivo Organ Cultures as Models to Study Bone Biology. Jbmr Plus. 2020;4(3).

262. Prescott MJ, Lidster K. Improving quality of science through better animal welfare: the NC3Rs strategy. Lab Animal. 2017;46(4):152-6.

263. Marino S, Staines KA, Brown G, Howard-Jones RA, Adamczyk M. Models of ex vivo explant cultures: applications in bone research. Bonekey Reports. 2016;5.

264. Kwakwa KA, Vanderburgh JP, Guelcher SA, Sterling JA. Engineering 3D models of tumors and bone to understand tumor-induced bone disease and improve treatments. Current Osteoporosis Reports. 2017;15(4):247-54.

265. Hofstee MI, Muthukrishnan G, Atkins GJ, Riool M, Thompson K, Morgenstern M, et al. Current concepts of osteomyelitis from pathologic mechanisms to advanced research methods. American Journal of Pathology. 2020;190(6):1151-63.

266. Kassem A, Lindholm C, Lerner UH. Toll-like receptor 2 stimulation of osteoblasts mediates *Staphylococcus aureus* induced bone resorption and osteoclastogenesis through enhanced RANKL. Plos One. 2016;11(6).

267. Marriott I, Gray DL, Tranguch SL, Fowler VG, Stryjewski M, Levin LS, et al. Osteoblasts express the inflammatory cytokine interleukin-6 in a murine model of

S*taphylococcus aureus* osteomyelitis and infected human bone tissue. American Journal of Pathology. 2004;164(4):1399-406.

268. Yang DQ, Wijenayaka AR, Solomon LB, Pederson SM, Findlay DM, Kidd SP, et al. Novel insights into *Staphylococcus aureus* deep bone infections: the involvement of osteocytes. Mbio. 2018;9(2).

269. Askar M, Ashraf W, Scammell B, Bayston R. Comparison of different human tissue processing methods for maximization of bacterial recovery. European Journal of Clinical Microbiology & Infectious Diseases. 2019;38(1):149-55.

270. Reilly SS, Hudson MC, Kellam JF, Ramp WK. In vivo internalization of *Staphylococcus aureus* by embryonic chick osteoblasts. Bone. 2000;26(1):63-70.

271. Widaa A, Claro T, Foster TJ, O'Brien FJ, Kerrigan SW. *Staphylococcus aureus* protein A plays a critical role in mediating bone destruction and bone loss in osteomyelitis. Plos One. 2012;7(7).

272. Wright JA, Nair SP. Interaction of *Staphylococci* with bone. International Journal of Medical Microbiology. 2010;300(2-3):193-204.

273. Harmer D, Falank C, Reagan MR. Interleukin-6 interweaves the bone marrow microenvironment, bone loss, and multiple myeloma. Frontiers in Endocrinology. 2019;9.

274. Wong PKK, Quinn JMW, Sims NA, van Nieuwenhuijze A, Campbell IK, Wicks IP. Interleukin-6 modulates production of T lymphocyte-derived cytokines in antigen-induced arthritis and drives inflammation-induced osteoclastogenesis. Arthritis and Rheumatism. 2006;54(1):158-68.

275. Ishimi Y, Miyaura C, Jin CH, Akatsu T, Abe E, Nakamura Y, et al. IL-6 is produced by osteoblasts and induces bone-resorption. Journal of Immunology. 1990;145(10):3297-303.

276. Varghese S. Matrix metalloproteinases and their inhibitors in bone: an overview of regulation and functions. Frontiers in Bioscience-Landmark. 2006;11:2949-66.

277. Montes AH, Valle-Garay E, Alvarez V, Pevida M, Perez EG, Paz J, et al. A functional polymorphism in MMP1 could influence osteomyelitis development. Journal of Bone and Mineral Research. 2010;25(4):912-9.

278. Booysen E, Sadie-Van Gijsen H, Deane SM, Ferris W, Dicks LMT. The effect of vancomycin on the viability and osteogenic potential of bone-derived mesenchymal stem cells. Probiotics and Antimicrobial Proteins. 2019;11(3):1009-14.

279. Dabrowska S, Andrzejewska A, Janowski M, Lukomska B. Immunomodulatory and regenerative effects of mesenchymal stem cells and extracellular vesicles: therapeutic outlook for inflammatory and degenerative diseases. Frontiers in Immunology. 2021;11.

280. Han Y, Li XZ, Zhang YB, Han YP, Chang F, Ding JX. Mesenchymal stem cells for regenerative medicine. Cells. 2019;8(8).

281. Kumar A, Zhang J, Yu FSX. Toll-like receptor 2-mediated expression of beta-defensin-2 in human corneal epithelial cells. Microbes and Infection. 2006;8(2):380-9.

282. Gao N, Kumar A, Yu F-SX. Matrix metalloproteinase-13 as a target for suppressing corneal ulceration caused by Pseudomonas aeruginosa infection. The Journal of Infectious Diseases. 2015;212(1):116-27.

283. Lin HB, Chen HS, Zhao XT, Chen Z, Zhang PP, Tian Y, et al. Advances in mesenchymal stem cell conditioned medium-mediated periodontal tissue regeneration. Journal of Translational Medicine. 2021;19(1).

284. Al-Amer O. Bone marker gene expression in calvarial bones: different bone microenvironments. Journal of Biological Research-Thessaloniki. 2017;24.

285. Reizner W, Hunter JG, O'Malley NT, Southgate RD, Schwarz EM, Kates SL. A systematic review of animal models for *Staphylococcus aureus* osteomyelitis. European Cells & Materials. 2014;27:196-212.